NATIONAL CENTRE FOR GROUNDWATER RESEARCH AND TRAINING

THE HYDROGEOLOGY OF THE ROCKY HILL REGION, NORTHERN TERRITORY

Flinders UNIVERSITY

NORTHERN TERRITORY GOVERNMENT

PowerWater

CloudGMS

Prepared by: The National Centre for Groundwater Research and Training
C/Flinders University
GPO Box 2100
Adelaide SA 5000
+61 8 8201 2193

ISBN: **978-1-925562-37-8**

DOI: **https://doi.org/10.25957/5ef191fb0f133**

Citation: For bibliographic purposes, this report may be cited as:
Cook PG, Wischusen J. and Knapton A, 2020, *The Hydrogeology of the Rocky Hill Region, Northern Territory.* National Centre for Groundwater Research and Training, Australia, and Department of Environment and Natural Resources, Water Resources Division. WRD Report 13/2020.

THE HYDROGEOLOGY OF THE ROCKY HILL REGION, NORTHERN TERRITORY

Department of Environment and Natural Resources

Water Resources Division

Report 13/2020

P.G. Cook, J. Wischusen and A. Knapton

Executive Summary

The Rocky Hill area has been identified as a potential future bore field for Alice Springs town water supply, and in 1996 NT Portion 4704 was set aside for that purpose. The area has been the focus of several hydrogeological investigations over the past 50 years, most recently in 1998-2000 (Read and Paul, 2000, 2002). The current report updates the hydrogeological characterisation of this area, based on drilling and sampling of new test production bores within NT Portion 4704, and water level, geochemistry and geophysical surveys carried out within the Rocky Hill region within the last 20 years. This data will be used in a groundwater model which will assess the long-term sustainability of Rocky Hill as a future water supply for Alice Springs. The groundwater model will be the focus of a subsequent report.

Based on a review of stratigraphic and hydraulic data, we simplify the stratigraphic interpretation, and consider the Ooraminna Sandstone as part of the Mereenie Sandstone. Within the Rocky Hill area, the Hermannsburg Sandstone is up to 150 m thick and overlain by a thin veneer of Quaternary and Tertiary sediments. The water table mostly occurs within the Hermannsburg Sandstone. The Hermannsburg Sandstone is underlain by the Mereenie Sandstone, which is approximately 200 m thick. The Mereenie Sandstone is underlain by the Pacoota Sandstone and the Goyder and Shannon formations. The thickness of these combined units has not been measured within the Rocky Hill region but has been estimated to be several hundred metres.

Hydraulic conductivity data obtained from core samples shows that the Mereenie Sandstone is significantly more permeable than the underlying Pacoota Sandstone. Hydraulic conductivity values obtained from pumping tests average between 10 and 100 times greater than those obtained from core samples, which suggests that fractures or thin layers of high hydraulic conductivity (which are not represented in the core samples) are important for groundwater flow. The mean hydraulic conductivity from pumping tests in the Rocky Hill region is 4 m/day, which is significantly lower than the mean value of 22 m/day for the Roe Creek area. However, at two sites tested within NT Portion 4704, the mean hydraulic conductivity was estimated to be only 0.3 m/day. Vertical hydraulic conductivity is between 10 and 100 times lower than horizontal hydraulic conductivity. The porosity of the Hermannsburg, Mereenie and Pacoota sandstones is approximately 0.25. The specific yield is 0.15 in the Hermannsburg and Mereenie sandstones, which means that 150 L of water can be extracted from each 1 m^3 of aquifer.

Water level data shows that drawdown associated with pumping from the Roe Creek bore field has reached the edge of the proposed Rocky Hill borefield (NT Portion 4704). Over the last 18 years, water levels near the western boundary of the proposed borefield have been

declining at almost 0.2 m/y. Further east, water levels have been declining at approximately 0.1 m/y for the past 30-40 years. Water level declines in the east of the Rocky Hill area are not attributed to pumping from Roe Creek. The reasons for these declining water levels are not well understood but may be due to a relaxation of water levels following historic periods of higher recharge together with groundwater use by deep-rooted vegetation. Pumping for agricultural activities within the region is not the major cause of this water table decline.

Groundwater salinity within NT Portion 4704 and the surrounding area is low. Total dissolved solids (TDS) is less than 600 mg/L over an area of more than 140 km^2, including the whole of NT Portion 4704 as well as areas to the south and east. An area of high salinity occurs approximately 2.5 km to the southeast of NT Portion 4704, as indicated by analysis of groundwater samples and aerial electromagnetic survey data. While there is some evidence that salinity increases with depth, water chemistry analyses on piezometers installed within NT Portion 4704 indicate that good quality water (TDS < 600 mg/L) occurs to at least 475 m depth, and this is also supported by aerial electromagnetic data.

The extractable volume of good quality groundwater (TDS < 600 mg/L) to 300 m depth in the Mereenie and Hermannsburg aquifers within the Rocky Hill – Ooraminna Management Zone of the Water Allocation Plan is estimated to be 5 200 GL[1]. This increases to 10 700 GL if groundwater with TDS up to 1000 mg/L is considered. Considerable additional volume is contained in the Pacoota and Goyder/Shannon aquifers, although almost most of this is located beyond 400 m depth. This is considerably greater than previous estimates of available groundwater.

Groundwater recharge is believed to occur preferentially through infiltration of flood waters of the Todd River and Roe Creek. Stable isotope data suggests that this usually occurs during months with more than 60 mm of rainfall. The mean recharge rate is estimated to be up to 2000 ML/y based on a chloride mass balance, which is equivalent to up to 40 mm/y over an area of approximately 50 km^2. In comparison, ^{14}C isotope data from piezometers installed in NT Portion 4704 indicates a mean recharge rate of between 4 and 20 mm/y. Much of the groundwater beneath Rocky Hill is several thousands of years old, although active recharge does still occur, as evidenced by rises in water levels associated with flow events in the Todd River.

[1] One gigalitre (GL) is equal to 1000 ML, or 10^6 m^3.

Table of Contents

1. INTRODUCTION

Alice Springs' public water supply is largely sourced from the Roe Creek borefield, located approximately 15 km south-southwest of the town, in the northeastern section of the Amadeus Basin. The borefield was commissioned in 1964, when the supply from the alluvial sediments beneath the town became inadequate. Early reports (Roberts, 1974) believed that maximum yield of the Roe Creek borefield would be reached by the mid-1980s, and that alternative supplies would need to be developed before that time. These early predictions proved to be overly pessimistic. Nevertheless, extensive drilling investigations took place in the Rocky Hill region in the 1970s (Verhoven et al., 1977), and in 1996 NT Portion 4704 was set aside for the future borefield. Further detailed hydrogeological investigations in the area took place in 1998-2000 to define the hydraulic properties of the aquifers and map the extent of low salinity groundwater (Read and Paul, 2000, 2002). The work identified more than 2.5 million ML of water with salinity less than 1000 mg/L in the upper 200 m of the aquifer system in the Rocky Hill region.

In 2016, the NT Government initiated a project to re-assess the potential of the Rocky Hill area for water supply development. This re-assessment was in part prompted by the potential for expansion of irrigated agriculture immediately west of the proposed borefield. A review of previous work conducted in the initial stages of this study identified a number of areas of uncertainty. These included uncertainties associated with the distribution of good quality water, particularly how far this water extends to the southeast and southwest, and a lack of information on the vertical distribution of aquifer hydraulic properties and water quality. It also became apparent that, although there is a large number of wells within the Rocky Hill region, very few of these had been completed according to modern well construction practices. For many bores, the annulus between the well casing and the aquifer material was not filled during well construction, and the casing was simply 'hung' from the surface. This annulus may have partially collapsed, and so the extent to which it provides a pathway for water to move vertically within the well is unclear. For other bores, the annulus between the casing and the aquifer appears to have been simply backfilled with drill cuttings. In a small number of cases, the annulus was backfilled with gravel (e.g., RN 17817). At the time of this review, the only observation well within the region that was constructed using bentonite or cement to isolate a short section of aquifer was RN 18334, which was completed as a set of three nested piezometers within the same borehole. (RN 18334 is in the extreme east of the study area; Figure 1.) Uncertainty in the nature of the connectivity between the casing and the aquifer of the other wells causes uncertainty in interpretation of hydraulic tests (and in attributing pumping test results to different formations, or parts of different formations), and also causes uncertainty in the depth of origin of water samples obtained from these bores.

Following review of previous studies, several new investigations were undertaken to address data gaps, and to enable quantitative predictions to be made of the impacts of pumping the proposed borefield. These studies included:

- An examination of the potential for groundwater contamination due to irrigation activities within the Rocky Hill region (Cook et al., 2017).
- A review of existing salinity data, including an analysis of the reliability of the data used by Read and Paul (2000, 2002) to construct their salinity map (Cozens, 2017).
- A downhole electromagnetic survey of 22 bores to examine possible trends in water quality with depth (Cozens, 2017).
- An aerial electromagnetic survey of the Roe Creek and Rocky Hill region to assist with stratigraphic and salinity mapping (Seiler et al., 2018).
- A review of stratigraphy of the Rocky Hill region, including downhole gamma surveys of several bores to assist with stratigraphic characterisation (Wischusen, 2020).
- Construction of nine new bores within NT Portion 4704, comprising two test production bores and seven observation bores. Two of the observation bores included dual pipes screened at different depths. The installations were designed to provide information on changes in aquifer properties with depth.
- Pumping tests on the two test production bores, and drawdown observations in adjacent piezometers.
- Drilling of five new regional bores to provide additional information on the spatial pattern of salinity surrounding NT Portion 4704.
- Collection of groundwater samples from 45 bores, which were analysed for major ion chemistry.
- Continued monitoring of water levels on 59 observation bores within the Rocky Hill region.
- Development of a groundwater flow and solute transport model to examine potential pumping scenarios from a proposed borefield within NT Portion 4704. The model is scheduled for completion in 2020.

This report summarises the current understanding of the hydrogeology of the region based on previous studies and the 2016 – 2020 investigations.

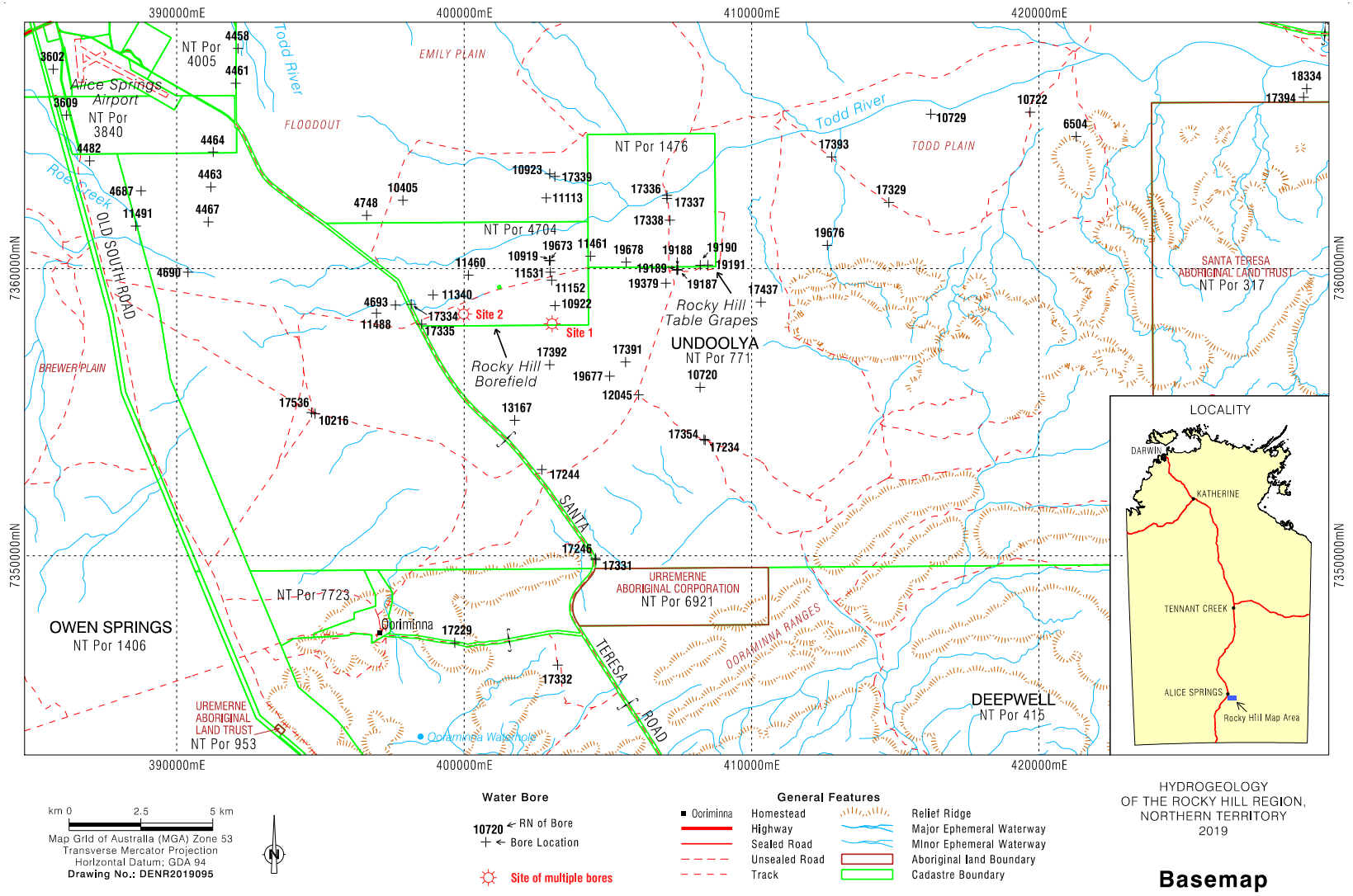

Figure 1. Location map of the Rocky Hill region, showing NT Portion 1476 (Undoolya Rocky Hill Agricultural Block), NT Portion 4704 (the proposed site of the Rocky Hill borefield), and selected observation bores. Sites 1 and 2 were the focus of intense drilling during this study.

2. METHODS

2.1 Drilling

A number of bores were drilled between 2016 and 2018 (i) within and adjacent to the agricultural block to examine potential impacts of agricultural activities on water quality, (ii) within the proposed borefield to better define aquifer hydraulic properties and potential pumping yields, and (iii) surrounding the proposed borefield to better define the regional salinity distribution. Details of all new bores are listed in Table 1. Bores RN 19187 – RN 19379 were drilled as part of an examination of the impacts of agricultural activities on groundwater, and drilling reports logs for these bores are provided in Cook et al. (2017). RN19380 – RN 19388 were drilled at two sites within the proposed borefield (NT Portion 4704), and their configuration is shown schematically in Figure 2. Bores RN 19673 – RN 19678 were drilled to fill gaps in the regional bore network. Bore RN19675

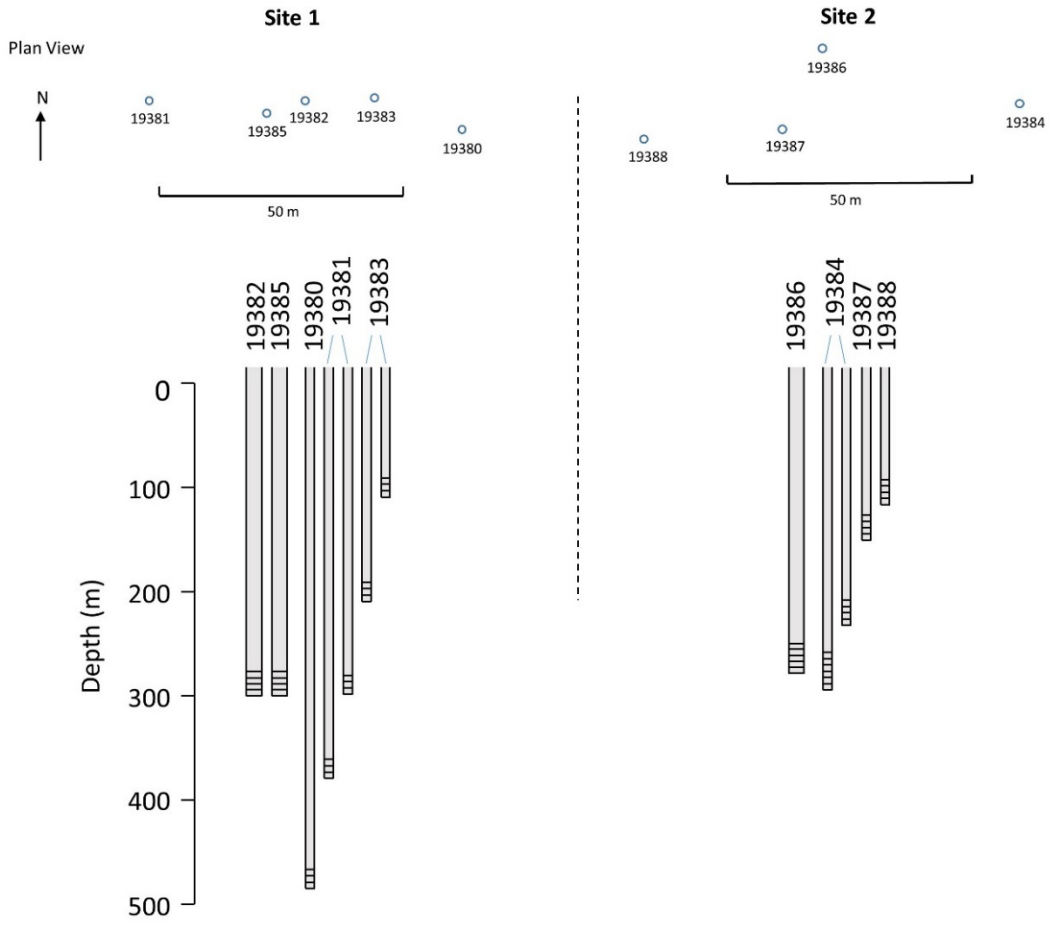

Figure 2. Schematic illustration of locations and construction of new wells drilled within NT Portion 4704. Locations of Site 1 and Site 2 within NT Portion 4704 are shown on Figure 1.

Table 1. Details of bores drilled in 2016 - 2018. Where two screen depths are indicated, nested piezometers have been constructed. In the text, the piezometer with the deeper screen is designated with the suffix '-1', and that with the shallower screen has the suffix '-2'.

Bore	Easting	Northing	Date Drilled	Total Depth (m)	Casing	Screen Depth (m)
RN 19187	407432	7359963	20/7/2016 – 25/7/2016	57.0	NA	NA
RN 19188	407442	7359954	25/7/2016 – 30/7/2016	48.3	NA	NA
RN 19189	407400	7359960	30/7/2016 – 3/8/2016	57.0	100 mm PVC	49.9 – 55.2
RN 19190	408215	7360118	3/8/2016 – 17/8/2016	72.4	100 mm PVC	57.0 – 63.0
RN 19191	408481	7360121	17/8/2016 – 25/8/2016	66.0	100 mm PVC	59.0 – 63.0
RN 19379	407020	7359489	24/8/2016 – 31/8/2016	60.3	100 mm PVC	52.0 – 55.0
RN 19380	403092	7358067	24/3/2017 – 23/5/2017	484.5	50 mm Steel	473.3 – 477.5
RN 19381	403028	7358079	25/3/2017 – 10/6/2017	379.6	50 mm Steel	287.8 – 291.8 373.4 – 377.6
RN 19382	403060	7358079	10/6/2017 – 15/7/2017	300.0	165 mm Steel	273.6 – 298.0
RN 19383	403074	7358080	15/7/2017 – 11/8/2017	211.0	50 mm Steel	106.0 – 110.0 201.0 – 205.0
RN 19384	399925	7358425	12/8/2018 – 6/8/2017	300.0	50 mm Steel	222.0 – 226.0 266.0 – 290.0
RN 19385	403052	7358074	13/9/2017 – 10/10/2017	300.0	168 mm Steel	277.6 – 298.0
RN 19386	399885	7358436	9/4/2018 – 18/5/2018	294.8	152 mm Steel	252.0 – 286.1
RN 19387	399978	7358416	10/4/2018 – 18/4/2018	163.8	100 mm PVC	148.0 – 152.0
RN 19388	399856	7358416	18/4/2018 – 24/4/2018	114.0	100 mm PVC	101.0 – 105.0
RN 19673	402994	7360283	30/4/2018 – 15/5/2018	220.0	100 mm PVC	204.0 – 210.0
RN 19675	412635	7360810	2/7/2018 – 24/7/2018	114.8	NA	NA
RN 19676	412635	7360810	25/7/2018 – 2/8/2018	170.0	100 mm PVC	158.0 – 164.0
RN 19677	405062	7356257	6/8/2018 – 24/8/2018	200.0	NA	NA
RN 19678	405634	7360222	25/8/2018 – 4/9/2018	201.2	100 mm PVC	183.7 – 189.7

was abandoned at 114.8 m depth and replaced by RN19676. RN19677 was abandoned at 200.0 m depth and was not completed, but samples collected during drilling provide information on water quality.

Drilling of wells at for this project was often difficult; the chief problems encountered were the ingress of sand when attempting air drilling and loss of circulation when drilling with mud. In many holes mud losses were significant and injection of drilling mud into aquifers occurred. KCl was added to several bores during drilling to reduce the loss of drilling fluids, and soda ash was also added to condition the mud and raise the pH to improve the efficiency of the bentonite seals. Wells installed within the proposed borefield were mostly constructed using 50 or 100 mm diameter casing with relatively short slotted intervals, so that groundwater samples could be obtained from discrete depths. Although bores were subsequently developed using air, and pumped to remove drilling fluids, the short production zones of most of the wells together with the small casing

diameter of a number of wells meant that development was difficult. Only modest airlift yields were possible and only a small fraction of the sandstone aquifer affected by mud invasion was able to be purged through the screens. Consequently, integrity of subsequent chemical and isotope samples obtained from these piezometers is uncertain, as discussed below.

2.2 Geochemical Sampling and Analysis

Water quality and geochemistry sampling took place on piezometers installed at Site 1 and Site 2 (Table 2), with a focus on understanding trends on water chemistry with depth. Electrical conductivity (EC) at different depths was measured on airlifted samples during drilling of RN 19381, and samples were collected from the completed piezometers on several occasions between August 2017 and October 2019. Sample collection used either air lifting or using a submersible Bennett pump. Ion chemistry data from these repeat samplings show high K/Cl ratios in several piezometers, which is evidence of incomplete purging of drilling fluids (and particularly the added KCl). This is most apparent on RN 19383–2 and RN 19383–1, which show EC, Cl and K concentrations and K/Cl ratios that decrease over time. Molar K/Cl ratios greater than 0.1 are probably indicative of incomplete purging, and so questions remain about the thoroughness of purging at several wells.

The removal of mud products from production bores (RN 19382, RN 19385 and RN 19386) during well development is more likely to be effective due to the greater amount of aquifer open to the bore and higher yields possible. Thus, October 2019 water chemistry results from bore RN 19386, which was subjected to more extensive development by way of airlifting yield and long-term pump testing, show the lowest EC and Cl and K concentrations and are most likely to be representative of native groundwater. However, there is no clear relationship between K/Cl ratios of groundwater samples and whether or not KCl was added during drilling, based on drillers log books. This suggests that the drillers log books are incomplete and/or that KCl has migrated between bores. Thus, for example, drillers log books for RN 19380 and RN 19381 do not record KCl addition, and groundwater from these bores has low K/Cl ratios, whereas for RN 19388 there is no record of KCl addition yet it has a very high K/Cl ratio. Major ion data for wells at Sites 1 and 2 are therefore not considered in this report.

Groundwater samples were collected in October 2019 from several of the Site 1 and Site 2 piezometers for analysis of ^{13}C and ^{14}C in dissolved inorganic carbon, ^{18}O, ^{2}H and $^{36}Cl/Cl$. Although $^{36}Cl/Cl$ data from RN 19383–2 and RN 19383–1 shows obvious signs of contamination from KCl addition, other isotope results are unlikely to be affected by addition of KCl to drilling muds and are considered representative of the ambient groundwater.

Table 2. Details of water chemistry and isotope sampling at Site 1 and Site 2.

Bore	Date Sampled	Method	EC (µS/cm)	Cl (mg/L)	K (mg/L)	K/Cl (moles/moles)
Site 1						
RN 19383-2	10/08/17 24/03/2019 19/10/2019	Air Lift Air Lift Bennett Pump	14000 1500 900	4200 210 130	3500 120 27	0.76 0.52 0.19
RN 19383-1	09/08/17 26/03/2019 22/10/2019	Air Lift Air Lift Bennett Pump	4200 1100 1400	970 160 650	910 68 100	0.85 0.39 0.14
RN 19381-2	09/06/17 05/06/2018 28/03/2019 22/10/2019	Air Lift Bennett Pump Air Lift Bennett Pump	570 570 810 690	100 100 120 150	16 11 8.3 8.1	0.15 0.10 0.06 0.05
RN 19381-1	10/06/17 29/03/2019 23/10/2019	Air Lift Air Lift Bennett Pump	780 780 790	85 91 120	10 6.5 6.6	0.11 0.06 0.05
RN 19380	23/05/17 05/11/2018 20/03/2019 24/10/2019	Air Lift Bennett Air Lift Bennett Pump	830 720 760 740	110 97 110 140	9.1 8.5 8.9 6.6	0.08 0.08 0.07 0.04
RN 19382	15/07/2017	Air Lift	1000	92	92	0.91
Site 2						
RN 19388	23/04/2018	Air Lift	1100	62	32	0.47
RN 19387	18/04/2018 17/10/2019	Air Lift Bennett Pump	960 780	120 99	35 18	0.26 0.17
RN 19384-2	07/06/2018 18/10/2019	Air Lift Bennett Pump	920 810	75 130	6.3 6.1	0.08 0.04
RN 19384-1	07/06/2018 20/10/2019	Air Lift Bennett Pump	870 810	79 110	7.0 6.6	0.08 0.05
RN 19386	18/05/2018 21/10/2019	Air Lift Bennett Pump	900 590	67 54	7.8 6.2	0.11 0.10

Water quality sampling was also carried out between November 2016 and March 2017 on 45 bores within the region. Of these bores, 17 were sampled by bailing, 25 by airlifting, and 3 were actively pumping for pastoral use and sampled from the discharge line. Of the analyses on samples from these 45 bores, 24 had ion balances within 5%, and 33 had ion balances within 10%. For the remainder, total anion and cations differed by more than 20%. Interestingly, of the 17 bailed samples, 10 have ion imbalances greater than 20%, whereas only one of the pumped or airlifted samples had a poor ion balance. Samples with ion imbalances greater than 20% are not considered in this report, and data from other studies with ion balances that are not within 20% have also been excluded from the analysis.

Geochemical data are also presented for radioactive isotope (^{36}Cl, ^{14}C and ^{3}H) and stable isotope (^{2}H, ^{18}O and ^{13}C) analyses on groundwater collected from regional bores between 1975 and 2000. Isotopes are atoms of the same chemical element (i.e., the same number of protons and electrons)

with different numbers of neutrons. Stable isotopes are isotopes that do not undergo radioactive decay, and ratios of different stable isotopes of the same element can provide useful indicators of water sources and chemical reactions. Stable isotope data is expressed either as the ratio of heavy to light isotopes on individual ions of specific molecules (e.g., $^{18}O/^{16}O$ and $^{2}H/^{1}H$ of H_2O) or groups of molecules (e.g., $^{13}C/^{12}C$ of total dissolved inorganic carbon, TDIC), using the delta (δ) notation:

$$\delta = \frac{R_{sample} - R_{std}}{R_{std}} \times 1000\ ‰ \quad (1)$$

where R_{sample} is the isotope ratio in the sample and R_{std} is the ratio in the standard. Here $\delta^{18}O$ and $\delta^{2}H$ values are expressed relative to standard mean ocean water (SMOW) and $\delta^{13}C$ values are expressed relative to the Pee Dee Belemnite (PDB) standard.

Radioactive tracers, which decay at a known rate and which have had relatively constant input concentrations, provide information on groundwater residence time. This can be used to determine recharge rates and groundwater flow velocities. ^{14}C and ^{36}Cl have half-lives of 5730 and 301,000 years, respectively, allowing them to be used to determine groundwater residence times over timescales between approximately 1000 years and more than 1,000,000 years. Concentrations of the radioactive isotope ^{14}C in TDIC is expressed as percent modern carbon (pmC), where 100 pmC represents the concentration in the atmosphere prior to the industrial revolution (when burning of fossil fuels reduced the atmospheric ^{14}C activity). ^{36}Cl is expressed as an atom ratio to stable chloride (^{35}Cl). ^{3}H has low natural concentrations in rainfall but was present in high concentrations in the 1950s and 1960s due to above-ground thermonuclear testing. The half-life of ^{3}H is 12.3 years, and measurable concentrations in groundwater indicate contributions from rainfall since the 1950s. ^{3}H is measured in tritium units (TU), where 1 TU represents one atom of ^{3}H in 10^{18} atoms of hydrogen. ^{14}C, $\delta^{13}C$, $\delta^{2}H$, $\delta^{18}O$ and $^{36}Cl/Cl$ have been measured on groundwater samples from piezometers at Site 1 and 2. Data on these isotopes and ^{3}H is also available from previous studies but was not reported by Read and Paul (2000, 2002).

2.3 Hydraulic Testing

Pumping tests were carried out on RN 19385 (Site 1) and RN 19386 (Site 2) to examine vertical connectivity between aquifer layers. An initial step test was used at each production bore to determine the pumping rate for a subsequent constant rate pumping test. Both constant rate tests were planned to run for a 7-day pumping period, followed by recovery, although technical difficulties limited the constant rate test at Site 2 to 3.5 days. Prior to testing, each of the

production bores were developed by pumping until drilling mud was not visible in the discharge water and the pump rate and drawdown were steady. This was difficult at Site 1 because of the low yield of RN 19385. The erratic electrical conductivity (EC) of discharge water during the step test at this site (Section 4.3) may indicate that the production bore hadn't fully developed until early into the constant rate test. The piezometers at both sites were all developed prior to the pumping tests by airlifting using an air compressor until the discharge water appeared free from drilling mud.

Water levels in the piezometers were recorded manually and using non-vented pressure transducers (Level TROLL 400; In-Situ Inc., USA) that were corrected for barometric pressure changes using a dedicated transducer (BaroTROLL; In-Situ Inc., USA). A measurement frequency of one minute was used for each test. Water quality parameters (temperature, pH and EC) of the discharge water were measured throughout each of the step and constant rate tests using a field meter (TPS WP-81; TPS Pty. Ltd., Australia). It should be noted that the EC of a water sample from RN 19386 (Site 2) was recorded at 715 μS/cm in the DENR laboratory, and the field EC meter (used by the pump test crew) recorded 550 μS/cm. It was later found that the field meter needed calibration. Thus, the EC time series data show incorrect absolute EC values but should still be reliable relative values. The field meter was re-calibrated before the tests at Site 1.

2.4 Geophysical Surveys

Results of a downhole electromagnetic survey of 22 bores is described in Cozens (2017), and results of a downhole gamma survey of 23 bores are described in Wischusen (2020). An aerial electromagnetic survey of the region was carried out in 2017 and is described in Seiler et al. (2018).

3. GEOLOGY AND HYDROSTRATIGRAPHY

The Amadeus Basin is a large (ca 170 000 km^2] intracratonic sedimentary basin in central Australia. It extends for over 800 km east-west and up to 300 km north-south. The basin contains a range of sediments up to 14 km in thickness deposited from the late Proterozoic until the late Devonian. These sediments have undergone significant modification associated with several tectonic events. The area of this study is along the northern part of the eastern flank of the Amadeus Basin and concentrates only on Ordovician and younger sediments from the upper part of the basin. Within these sediments there are three main hydrostratigraphic units. From youngest to oldest these are; the Hermannsburg Sandstone, a red-brown and grey-brown kaolinitic and silty poorly sorted sandstone; the Mereenie Sandstone, a white or pale brown, fine grained, predominantly well rounded and sorted orthoquartzite; the Pacoota Sandstone, a pale orange and brown to light grey, fine to medium-grained quartzose sandstone with thin siltstone interbeds. Some previous studies have postulated that another sandstone, the Ooraminna Sandstone, constitutes a fourth main hydrostratigraphic unit in this area. However, recent analysis of stratigraphic data conducted as part of this project (Wischusen, 2020) concludes that there is currently insufficient evidence to identify the Ooraminna Sandstone within the sedimentary succession in the Roe Creek and Rocky Hill area of the Amadeus Basin. Consequently, the more commonly applied interpretation of stratigraphy from most previous studies is preferred. Thus, where the Ooraminna Sandstone has been previously proposed to exist (in this study area) we now consider these intervals to be a part of the Mereenie Sandstone.

The Goyder and Shannon formations underlie the Pacoota Sandstone in the Rocky Hill region. The Shannon Formation consists of alternating beds of limestone and siltstone, and the Goyder Formation includes limestone, siltstone and sandstone layers. Although no bores within the Rocky Hill area have been drilled into these formations, elsewhere they can provide productive aquifers (Verhoeven and Knott, 1982).

In the Roe Creek borefield, the Mereenie Sandstone has a thickness of approximately 365 m, and is the main aquifer targeted for water supply. This is also considered to be the main aquifer in the Rocky Hill area. The Hermannsburg, Mereenie and Pacoota aquifers outcrop in the south and eastern part of the study area (Figure 3), but in the area of NT Portion 4704, the Hermannsburg Sandstone is overlain by a thin layer of Quaternary alluvium and colluvium. The top of the Mereenie Sandstone occurs at approximately 150 m depth, and the unit is around 200 m thick. The Rocky Hill and Roe Creek areas are both situated along the northern flank of the Amadeus Basin but due to structural variation the Rocky Hill area sediments have a shallower (≈10°) southerly dip than that found at Roe Creek (≈30°). Furthermore, due to uplift and erosion associated with tectonic events it is apparent that the Hermannsburg, Mereenie and Pacoota Sandstones are thinner at Rocky Hill than at Roe Creek. Thus, sandstone units are thinner, occur closer to the surface and dip more gently at Rocky Hill than at Roe Creek.

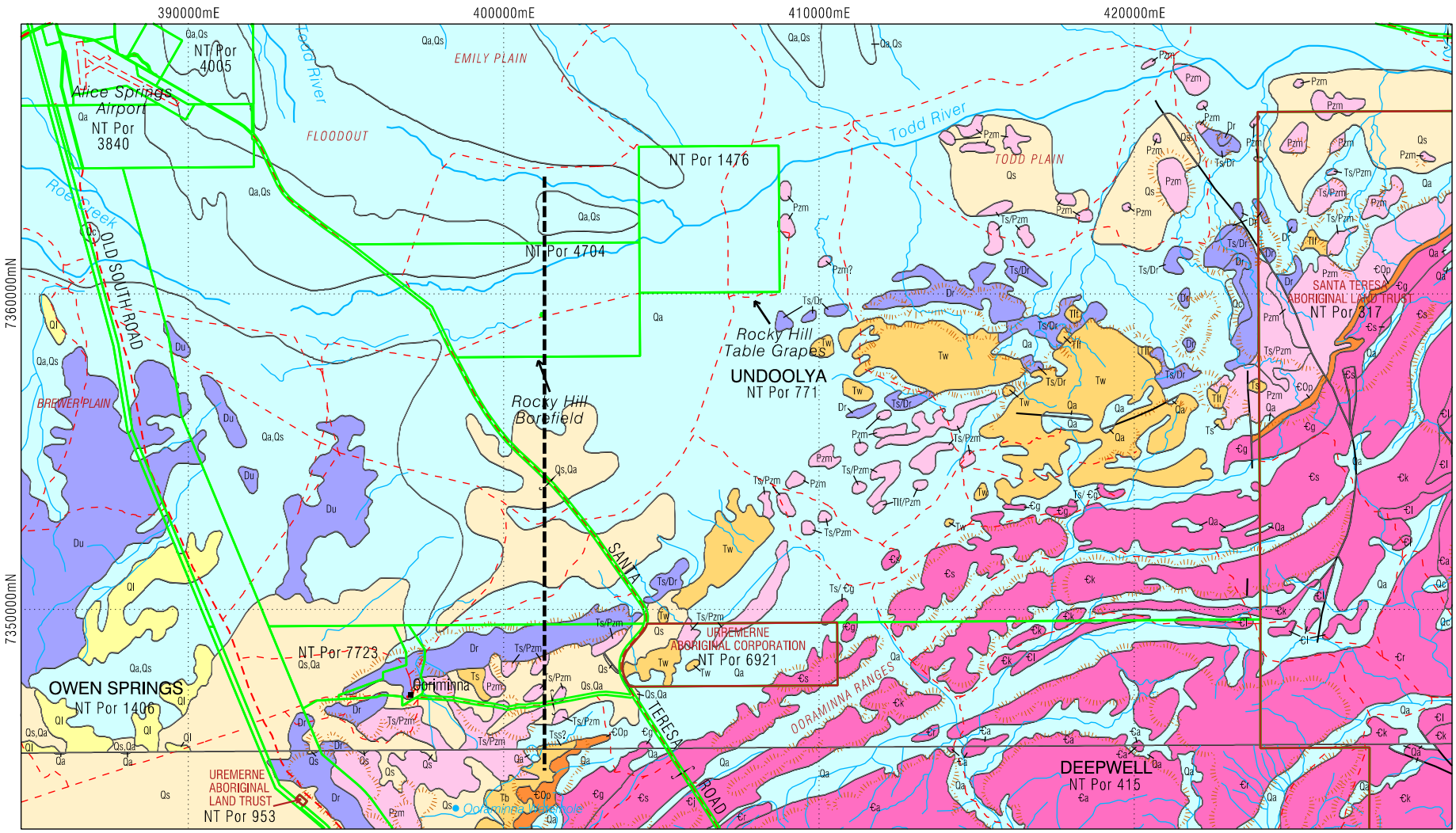
390000mE
400000mE
410000mE
420000mE
7360000mN
7350000mN
NT Por 4005
Alice Springs Airport
NT Por 3840
Todd River
EMILY PLAIN
FLOODOUT
NT Por 1476
NT Por 4704
Todd River
TODD PLAIN
Rocky Hill Table Grapes
UNDOOLYA
NT Por 771
Rocky Hill Borefield
OLD SOUTH ROAD
BREWER PLAIN
SANTA TERESA
ABORIGINAL LAND TRUST
NT Por 317
NT Por 7723
Ooriminna
OWEN SPRINGS
NT Por 1406
UREMERNE
ABORIGINAL CORPORATION
NT Por 6921
OORAMINNA RANGES
UREMERNE
ABORIGINAL
LAND TRUST
NT Por 953
DEEPWELL
NT Por 415
Ooraminna Waterhole
km 0
2.5
5 km
Map Grid of Australia (MGA) Zone 53
Transverse Mercator Projection
Horizontal Datum: GDA 94
Drawing Ref: DENR2019083
Geology
Quaternary
Tertiary
Pertnjara Group
Mereenie Sandstone
Larapinta Group
Pertaoorta Group
Fault
See Geology Reference for full unit descriptions
General Features
Ooriminna
Homestead
Highway
Sealed Road
Unsealed Road
Track
Relief Ridge
Major Ephemeral Waterway
Minor Ephemeral Waterway
Aboriginal land Boundary
Cadastre Boundary
Geology Source: Alice Springs SF5314 (1983) & Rodinga GS5302 (1968)
HYDROGEOLOGY
OF THE ROCKY HILL REGION,
NORTHERN TERRITORY
2019
Geology

Figure 3A (Preceding page). Surface geology. A detailed legend is presented as Figure 3B, below. Note that the Pacoota Sandstone is part of the Larapinta Group and the Hermannsburg Sandstone is part of the Pertnjara Group. The broken black line shows the location of the north-south cross-section shown in Figure 4.

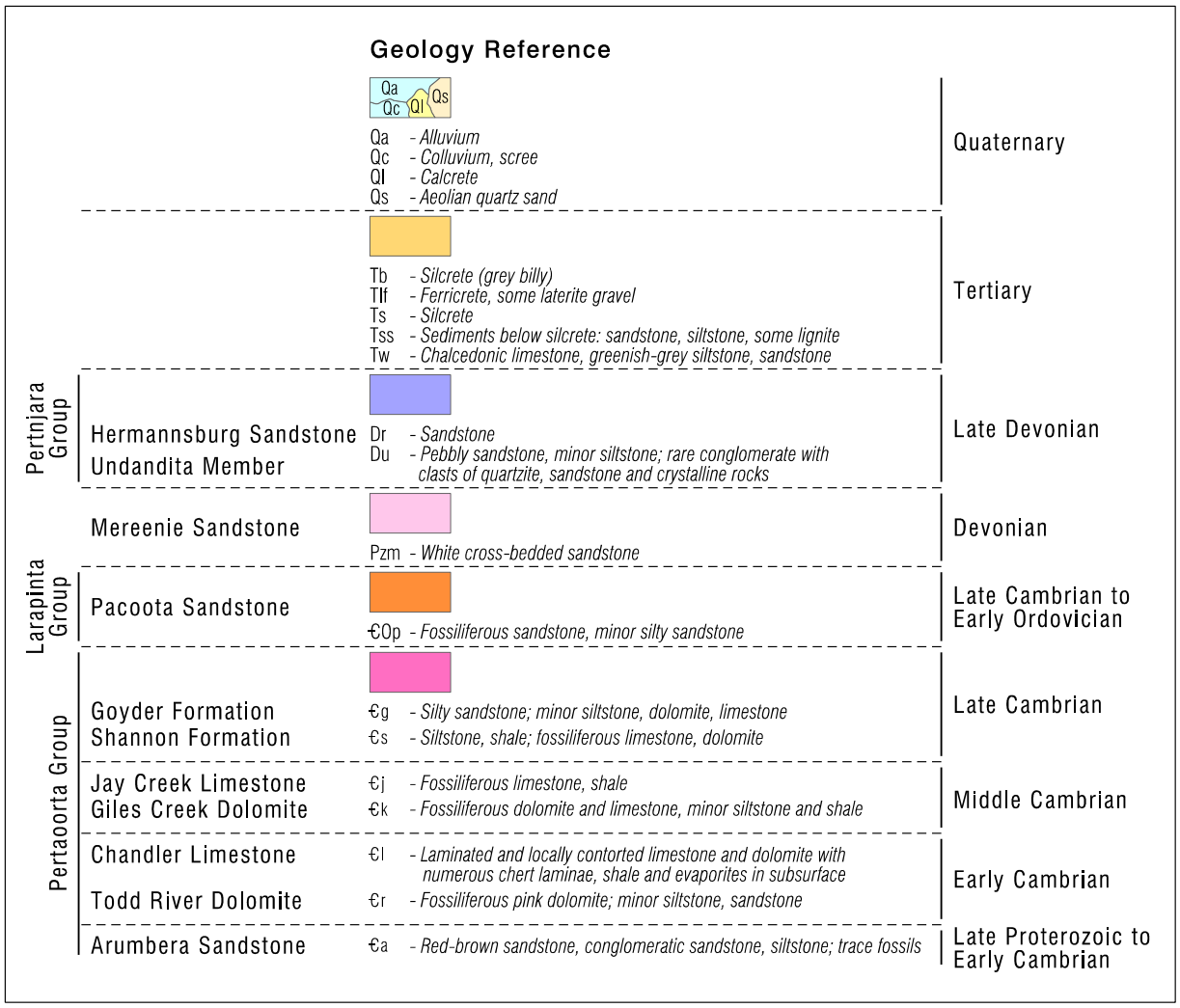

Figure 3B. Legend for geology map in Figure 3A.

A north south orientated cross-section through the proposed Rocky Hill borefield (NT Portion 4704) shows the borefield on the northern limb of a syncline structure (Figure 4). However, it should be noted that the precise layer boundaries are somewhat uncertain, as the different formations are not easily distinguished from geological or geophysical logs. Also, the thickness of sediments above the Pacoota Sandstone in the deepest part of the syncline are defined only by well RN 13167. The thickness of these sediments elsewhere is not well defined as only a small number of bores reach the Pacoota Sandstone in this area. Figure 5 shows the stratigraphic unit which forms the upper aquifer unit across the Rocky Hill area. In the centre of the syncline structure, the water table occurs within the Hermannsburg Sandstone. However, moving north and south, the Mereenie Sandstone, Pacoota Sandstone and finally the Goyder / Shannon Formation are the upper aquifer units, as the overlying units are absent. While outcrops of Pacoota and Goyder/Shannon Formation occur on the southern limb of the syncline, the northern limb is overlain by Cainozoic sediments (Figure 3). The thickness of the entire succession reaches almost 800 m within NT Portion 4704 but is considerably greater to the south and west (Figure 6). Both Figure 5 and Figure 6 have been prepared from available stratigraphic logs, supplemented by measurements of dips of geological strata and areas of surface outcrop.

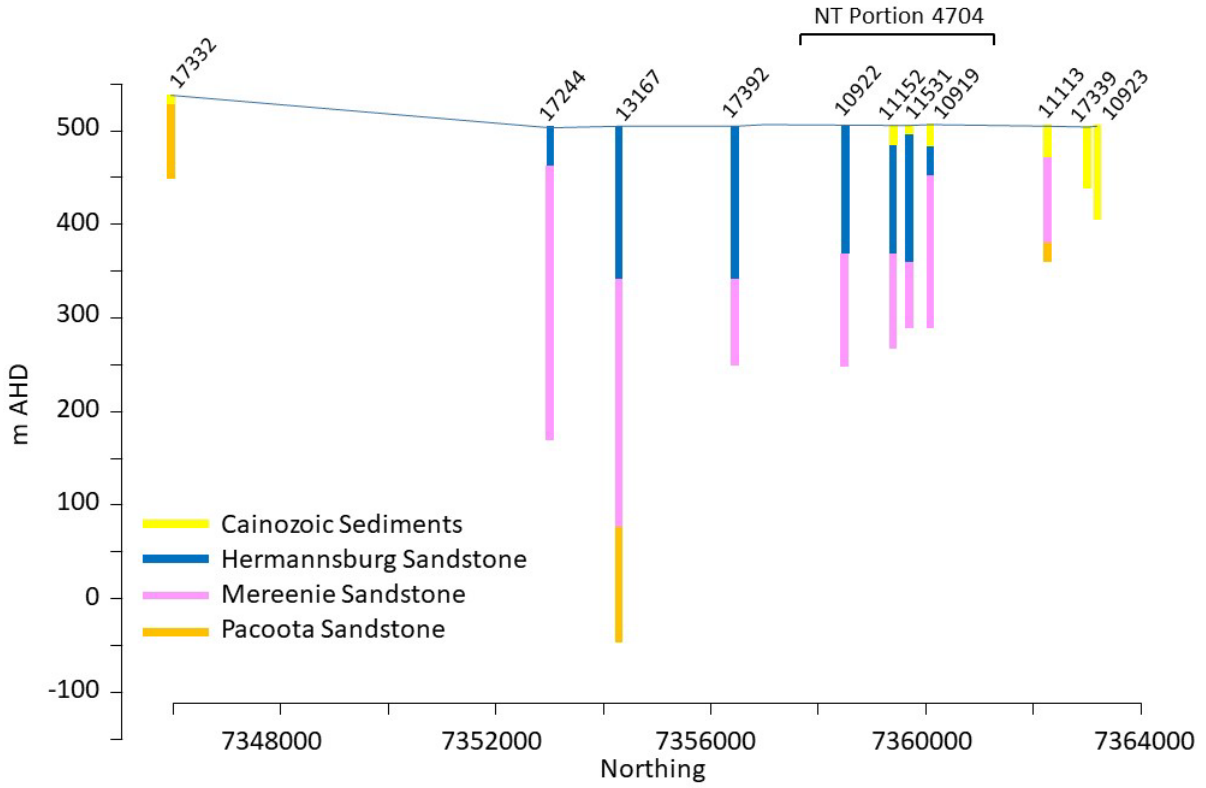

Figure 4. Geological cross-section approximately representing the 402700E survey line, which goes through NT Portion 4704. Stratigraphy is based on Read and Paul (2002), as modified by Wischusen (2020). Bore locations are shown in Figure 1.

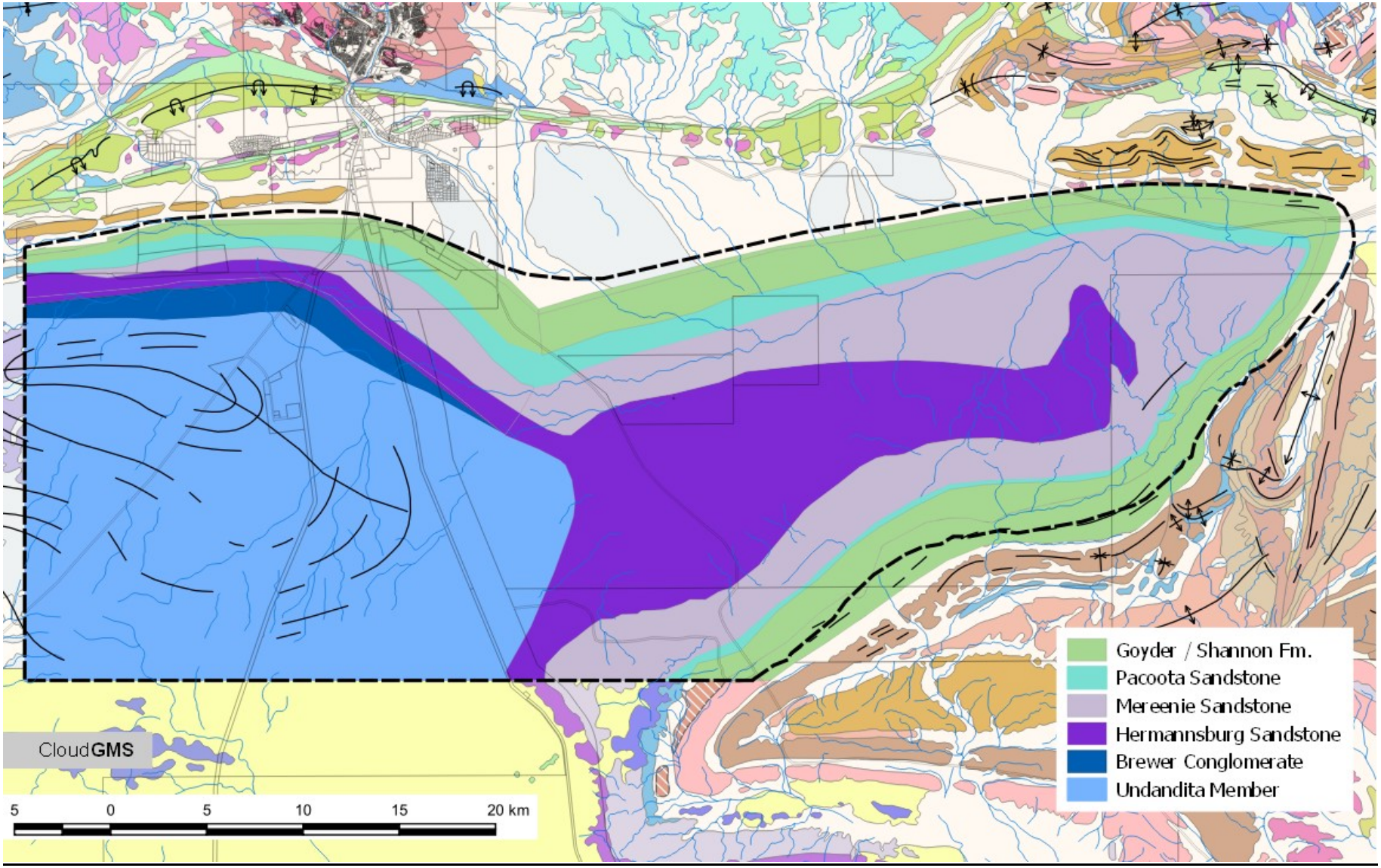

Figure 5. Aquifer structure within the Rocky Hill region. Stratigraphically lower (older) geological units form the upper aquifer towards the edges of the syncline structure.

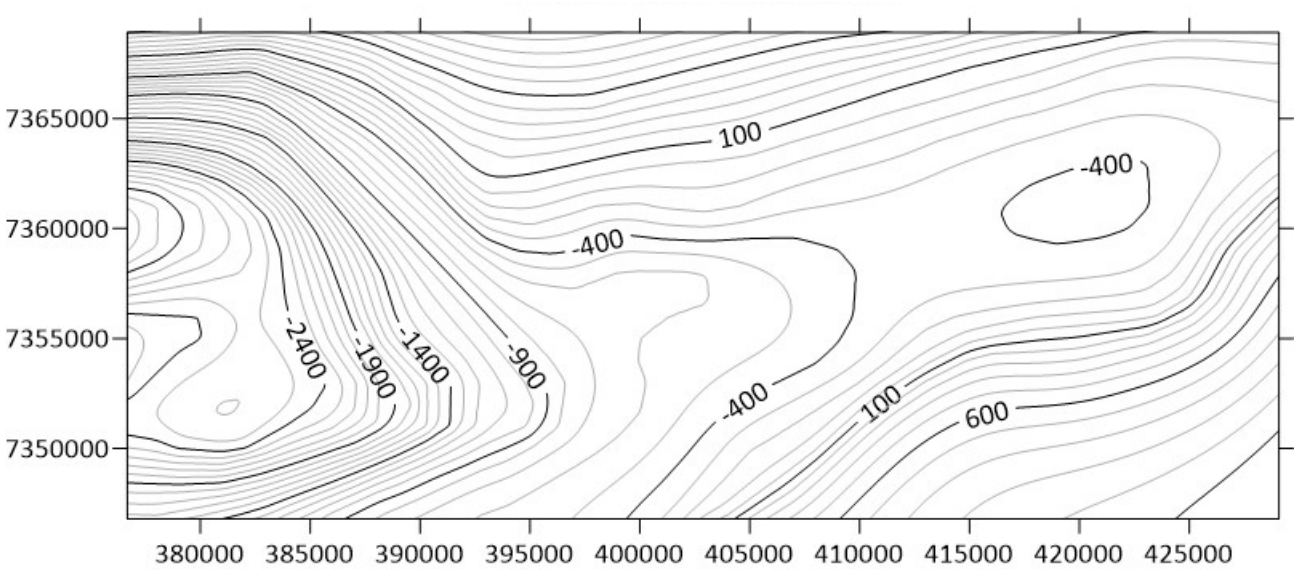

Figure 6. Elevation of the base of the Goyder or Shannon Formation (m AHD), which marks the base of the main aquifer units. The land surface elevation is generally 450 – 550 m AHD.

4. HYDRAULIC CHARACTERISATION

Hydraulic properties of the aquifers within the Rocky Hill area have been determined both from analysis of pumping tests and from laboratory analysis of core samples obtained during drilling.

Between 1973 and 1977, pumping tests were carried out on 20 bores within the Rocky Hill region. Most of these bores were screened within the Mereenie Sandstone, although the nature of well construction means that they may also be open to other formations. Observation bores were only available for two of these tests. Pumping tests were carried out on a further five bores between 1992 and 2002, and two of these tests included observation bores. Pumping tests were conducted in 2019 on two bores, with multiple observation bores for each of these tests. This allowed vertical variations in aquifer hydraulic properties to be determined as well as anisotropy ratios.

Core samples have been obtained from 11 bores, with a total of 28 separate intervals tested for hydraulic conductivity and porosity. This includes samples from the Hermannsburg, Mereenie and Pacoota sandstones.

4.1 Hydraulic Conductivity of Core Samples

Core samples have been obtained from 11 bores, with a total of 28 separate intervals tested for hydraulic conductivity and porosity (Table 3). Measurements were obtained from small cores that were cut from larger diameter drill cores. The earliest measurements include vertical measurements (cores cut down the centre of the drilling cores) and horizontal measurements on cores cut perpendicular to the axis of the original drill core, both in the dip and strike directions (Woolley, 1966). (The average of the dip and strike measurements is included in Table 3.) Subsequent measurements were either on cores cut perpendicular to the axis of the original drill core, but without specifying whether they were in the dip or strike direction, or do not specify any direction (either vertical or horizontal). Porosity data is obtained from either air or helium porosimetry, while permeability data used either air or water as the fluid. In all cases, measured permeabilities have been converted to equivalent hydraulic conductivity for fresh water.

Figure 7 compares hydraulic conductivity data for the different formations. For the purposes of this figure, all available measurements for each core interval were averaged (i.e., vertical and horizontal and along strike or along dip). Too few measurements were made using both air and water permeability to determine a relationship between these measurements, and so they have also both been included. Stratigraphic data has been assigned based on cross-sections in Read and Paul (2002), as reinterpreted by Wischusen (2020). Although the sample set is relatively small, hydraulic conductivity is significantly lower for the Pacoota Sandstone than for the other formations. There

does not appear to be any significant difference between the hydraulic properties of the Mereenie and Hermannsburg formations.

Table 3. Hydraulic properties of aquifers in Rocky Hill area obtained from analysis of core samples. Porosity data is obtained using either air or helium porosimetry. Hydraulic conductivity data has been converted from permeability data obtained either using air or water as the fluid. Values obtained using air are given in parentheses and are usually greater than those obtained using water. Based on Woolley (1966), Read and Paul (2000, 2002) and Wischusen (2020).

Bore	Depth (m)	Stratigraphic Unit	Vertical		Horizontal		Direction Unspecified		
			K (m/day)	Porosity	K (m/day)	Porosity	K (m/day)	Porosity	Specific Yield[a]
3609	194.8	Mereenie	0.011	0.2	0.075	0.21			
10216	436.0	Mereenie			(< 0.004)[b]	0.1			
	537.8	Mereenie			(< 0.004)[b]	0.11			
	342.7	Mereenie			(0.103)	0.22			
	251.9	Hermannsburg			(0.130)	0.24			
	656.6	Pacoota			(0.006)	0.17			
	826.7	Pacoota			(0.028)	0.13			
	907.5	Pacoota			(< 0.004)[b]	0.065			
17334	70.9	Hermannsburg			(0.15)	0.29			
17335	70.07	Hermannsburg			(17.2)	0.25	0.003	0.26	0.098
	71.86	Hermannsburg			(>2.5)	0.26	1.7	0.27	0.232
17336	51.3	Mereenie			(0.84)	0.26			
	51.4	Mereenie			(0.42)	0.26	0.33	0.26	0.187
17337	50.5	Mereenie			(0.6)	0.25			
	52.8	Mereenie			(0.6)	0.25			
17338	51.5	Mereenie			(0.23)	0.24			
17354	101.1	Hermannsburg					0.058	0.21	0.142
	152.4	Hermannsburg					0.029	0.19	0.130
	200.0	Mereenie					0.18	0.23	0.166
	251.8	Mereenie					0.03	0.21	0.114
	302.3	Mereenie					0.86	0.25	0.202
	351.3	Mereenie					0.13	0.22	0.155
	400.4	Mereenie					$<8x10^{-6}$	0.1	0.013
	450.8	Pacoota					0.023	0.08	0.065
	500.7	Pacoota					0.033	0.1	0.078
17392	214.9	Mereenie			(0.23)	0.22	0.16	0.23	0.143
17393	90.8	Mereenie			(0.11)	0.25			
17536	349.4	Mereenie					0.65	0.26	0.221

[a] Estimated from water loss between saturation and 240 kPa.

[b] These values were reported as zero, and a detection limit was not given. However, the lowest value reported for any sample was 0.004 m/day, and so values are assumed to be less than this value.

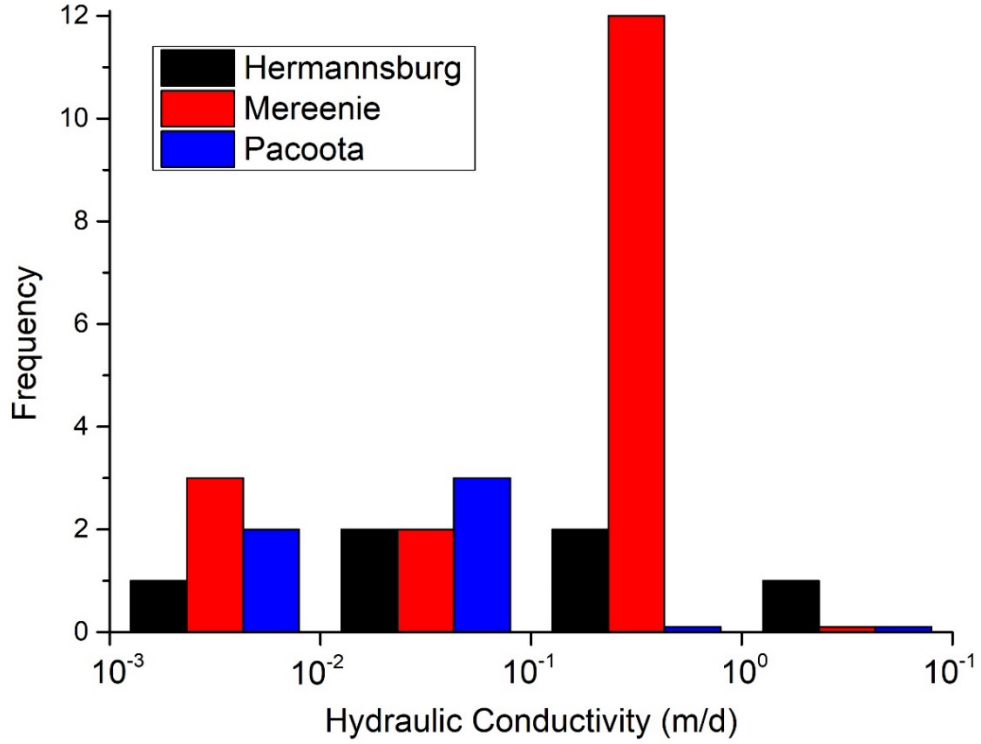

Figure 7. Histogram of hydraulic conductivity data on core samples.

4.2 Pumping Tests

Between 1973 and 1977, pumping tests were carried out on 20 bores within the Rocky Hill region. Read and Paul (2000) reviewed most of this data and obtained estimates of aquifer transmissivity (Table 4). Pumping tests were carried out on a further five bores between 1992 and 2002. The transmissivity estimated from tests on these 25 bores ranges from 6 to 3000 m^2/d, with a mean value of 570 m^2/day. Most of the bores tested are located within or immediately west of the proposed borefield. Only a small number of tests are located elsewhere within the basin, and no clear spatial patterns are apparent in the data (Figure 8). The hydraulic conductivity is estimated based on the total drilled depth of each bore less a nominal 50 m unsaturated zone thickness, and ranges between 0.02 and 17 m/day, with a mean of 4 m/day and median of 1 m/day. Due to issues with well construction discussed above, we have used the total bore depth rather than the screened or slotted interval of the bore in estimating hydraulic conductivity. However, this may slightly under-estimate hydraulic conductivity in some cases. Hydraulic conductivity values derived from these pumping tests average between 10 and 100 times greater than those obtained from core samples (Figure 9). This is commonly attributed to the role of preferential pathways (high hydraulic conductivity layers or fractures) which control pumping test performance but are usually

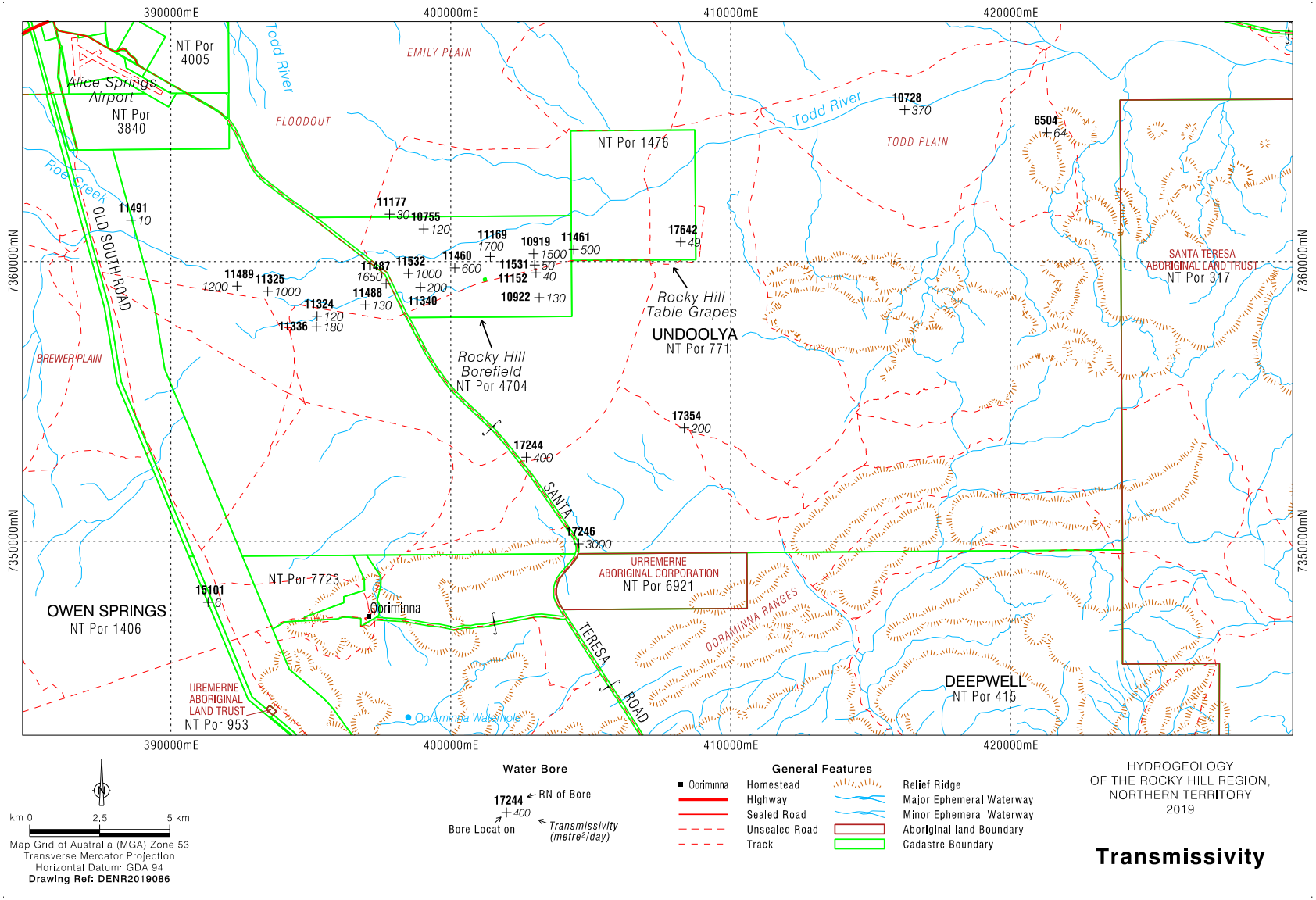

Figure 8. Map showing transmissivity measurements from analysis of pumping tests conducted prior to the current study.

Table 4. Hydraulic properties of aquifers in Rocky Hill area obtained from analysis of pumping test data. The stratigraphic unit denotes the primary unit within the screened interval of each bore. Data is mostly from Read and Paul (2000, 2002). Hydraulic conductivity is calculated from transmissivity by dividing by the bore depth, less a nominal 50 m unsaturated zone thickness.

Pumped Bore	Stratigraphic Unit	Observation Bores	Year Tested	Transmissivity (m^2/d)	Hydraulic Conductivity (m/day)
RN 6504	Mereenie		1973	64	0.21
RN 10728	Mereenie/Pacoota		1974	370	8.0
RN 10755	Mereenie/Pacoota		1974	120	0.67
RN 10919	Mereenie/Pacoota		1975	1500	8.9
RN 10922	Mereenie		1975	130	0.62
RN 11152	Mereenie		1976	40	0.22
RN 11169	Mereenie		1976	1700	13
RN 11177	Pacoota		1976	30	0.26
RN 11324	Mereenie		1976	120	0.67
RN 11325	Mereenie	RN 11408	1977	1000	7.9
RN 11336	Mereenie		1976	180	1.0
RN 11340	Mereenie		1977	200	1.2
RN 11460	Mereenie		1977	600	3.8
RN 11461	Mereenie		1977	500	3.0
RN 11487	Mereenie		1977	1650	17
RN 11488	Mereenie		1977	130	0.57
RN 11489	Mereenie		1977	1200	8.9
RN 11491	Mereenie		1977	10	0.04
RN 11531	Mereenie/Pacoota		1977	50	0.23
RN 11532	Mereenie	RN 11487 RN 11569	1977	1000	5.2
RN 15101	Hermannsburg		1992	6	0.02
RN 17244	Mereenie/Pacoota	RN 17245	1999	400	1.4
RN 17246	Mereenie	RN 17331	1999	3000	15
RN 17354	Mereenie/Pacoota		2000	200	0.44
RN 17642	Mereenie		2002	49	0.42
RN 19385	Mereenie	RN 19381-1,2 RN 19382 RN 19383-1,2	2019	110	0.32
RN 19386	Mereenie	RN 19384-1,2 RN 19387 RN 19388	2019	110	0.24

not represented in core samples. Joints and/or fractures are known to contribute to the high permeability of Mereenie Sandstone bores at Roe Creek (Wooley, 1966; Verhoeven et al., 1979).

Transmissivity and hydraulic conductivity values are also lower than comparative values estimated in the Roe Creek region (Figure 10). The mean transmissivity in the Roe Creek area, based on pumping tests carried out on 30 bores is 3940 m^2/day. The hydraulic conductivity, based on the total drilled depth of each bore less a nominal 50 m unsaturated zone thickness, ranges between 0.7 and 83 m/day, with a mean of 22 m/day and median of 20 m/day. At Rocky Hill, the mean transmissivity based on pumping tests on 25 bores is 570 m^2/day, the mean hydraulic conductivity is 4.0 m/day and median hydraulic conductivity is 1.0 m/day. Based on these pumping test results, the hydraulic conductivity at Rocky Hill is therefore approximately 10 times lower than that at Roe Creek.

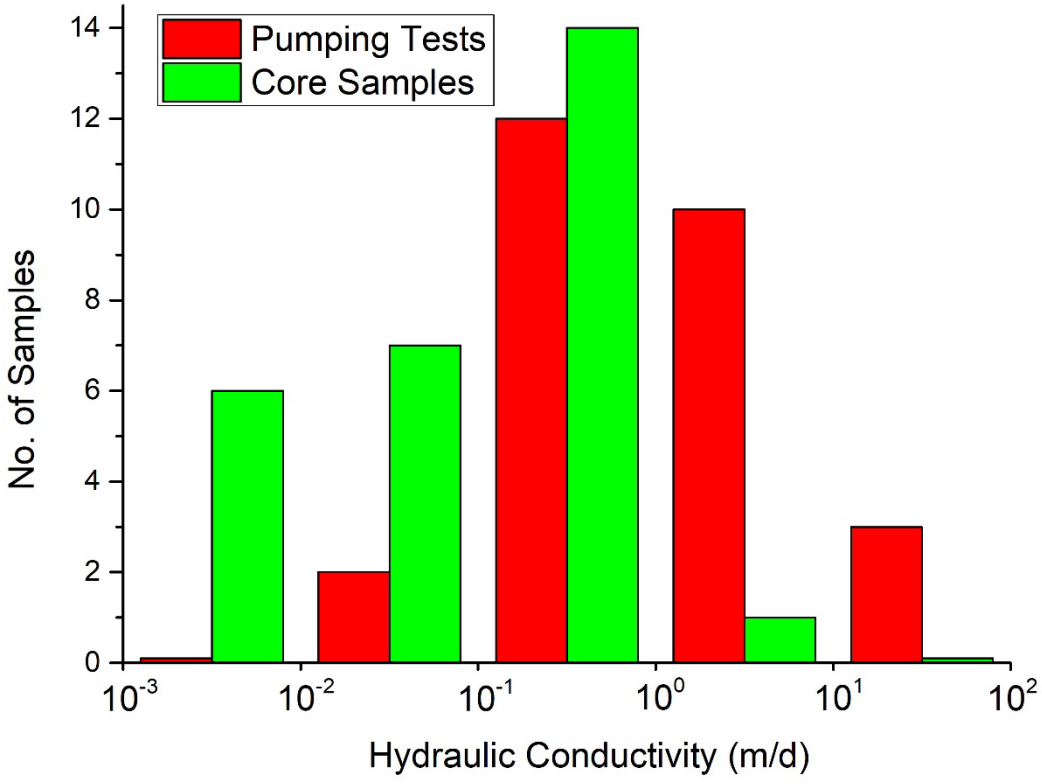

Figure 9. Histogram of hydraulic conductivity data from Rocky Hill area based on pumping test analysis and core samples. For pumping test data, hydraulic conductivity has been estimated by dividing transmissivity by the total drilled depth of the tested bore, minus a nominal unsaturated zone thickness of 50 m. (Pumping test data only contains results on testing prior to 2016.)

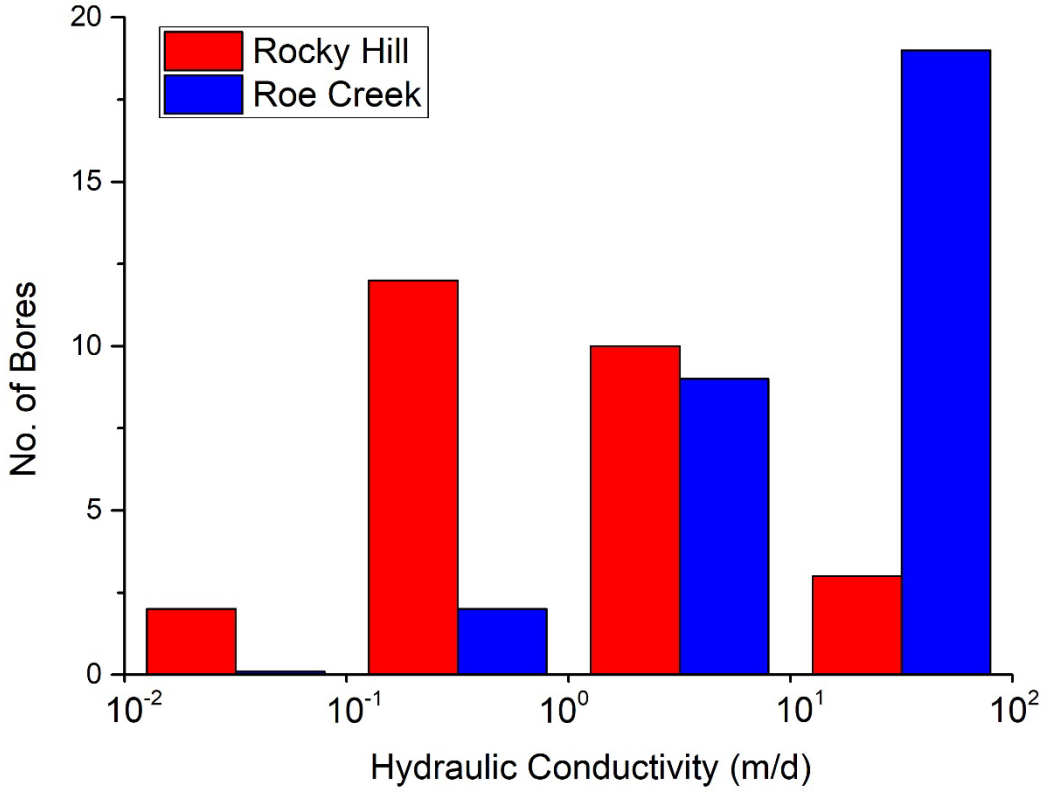

Figure 10. Histogram of hydraulic conductivity data derived from pumping tests carried out at Rocky Hill and Roe Creek. For pumping test data, hydraulic conductivity has been estimated by dividing transmissivity by the total drilled depth of the bore, less a nominal 50 m unsaturated zone thickness. (Pumping test data only contains results on testing prior to 2016.)

4.3 Anisotropy and Vertical Hydraulic Conductivity

Pumping tests with several observation bores were carried out on RN 19385 (Site 1) and RN 19386 (Site 2) to examine vertical connectivity between aquifer layers. At Site 2, a step test was conducted on RN 19386 on 14 May 2019, with pumping rates of 6.2, 10.2 and 15.8 L/s each for 100 minutes, and this induced drawdown of approximately 11, 20 and 41 m, respectively, in the pumping well (Figure 11).

The constant rate test at Site 2 was conducted over a period of 3.5 days (5000 minutes) with a constant pumping rate of 12 L/s. Drawdown during the test was monitored on the pumping bore and four observation piezometers (Figure 12). Recovery was monitored for a further three days.

Approximately 32 m of drawdown was achieved on the pumping bore (screened from 252 – 286 m BGL), with 3.5 m of drawdown observed in RN 19384-1 (screened from 266 – 290 m BGL) and RN

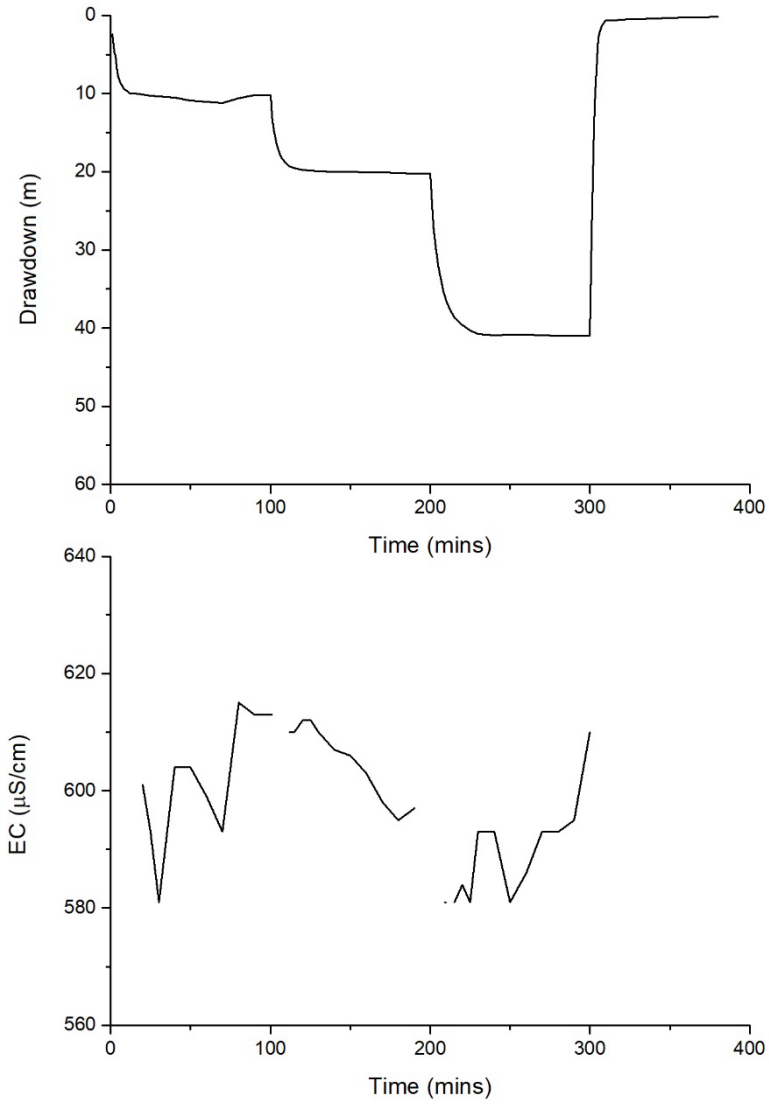

Figure 11. Drawdown in pumping bore and electrical conductivity of pump discharge during step test in RN 19386 (Site 2) conducted using pumping rates of 6.2, 10.2 and 15.8 L/s, each for a period of 100 minutes.

19384-2 (222 – 226 m BGL). Less drawdown is observed in the shallower piezometers, with 1 m drawdown in RN 19387 (148 – 152 m BGL) and 0.25 m in RN 19388 (101 – 105 m BGL).

At Site 1, RN 19385 was initially pumped at 0.8 L/s for a period of 90 minutes (on 23.05.2019) and this produced 40 m of drawdown in the pumping well. Following recovery, a step test was conducted, with pumping rates of 0.5, 0.7, 0.9 and 1.2 L/s, each for a period of 100 minutes, with

drawdown in the pumping well stabilising at approximately 23 m, 32 m, 42 m and 57 m, respectively, at the end of each 100 minute period. The well was then pumped at 0.9 L/s for 7 days (10,000 minutes). Drawdown was monitored in the pumped well, and in five observation wells. Approximately 42 m of drawdown was achieved on the pumping bore (screened from 278 – 298 m BGL), with 2.0 m of drawdown observed in 19382 (screened from 274 – 298 m BGL) and 1.7 m of drawdown in RN 19381-1 (288-292 m BGL). The large difference in drawdown between the pumping well and these two piezometers, which are screened at similar depths and in close proximity, suggests a very low bore efficiency for RN 19385. RN 19383-1 (201 – 205 m BGL), RN 19383-2 (106 – 110 m BGL) and RN 19381-1 (374 – 378 m BGL) produced respectively 0.35 m, 0.12 m and 0.09 m of drawdown after 7 days of pumping. There was no measurable drawdown on RN 19380 (473 – 478 m BGL). The small drawdown in shallow and deep bores suggest low permeability layers above and below the pumping zone.

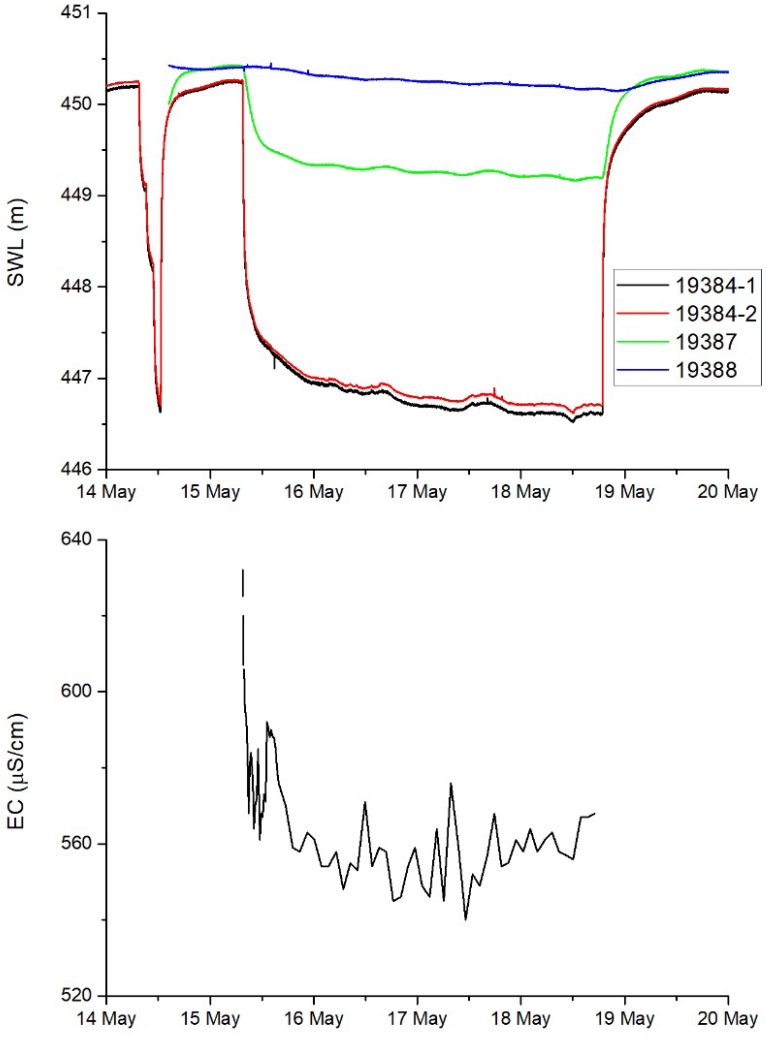

Figure 12. Drawdown in observation bores during pumping of RN 19386 (Site 2) at 12 L/s for 3.5 days, and EC of pump discharge.

Electrical conductivity of pump discharge was monitored throughout the step tests and pumping tests. At Site 2, EC varied between about 540 and 640 μS/cm through the step test and pumping test and did not show any clear trend with time. At Site 1, EC in pump discharge was 815 μS/cm after 30 minutes of the initial 0.8 L/s test, and this dropped to 738 after 80 mins. During the step test, EC was 817 μS/cm after 40 minutes of pumping at 0.5 L/s and dropped to 810 μS/cm after 100 minutes (Figure 13). The increase in pumping rate to 0.7 L/s resulted in a sudden increase in EC to

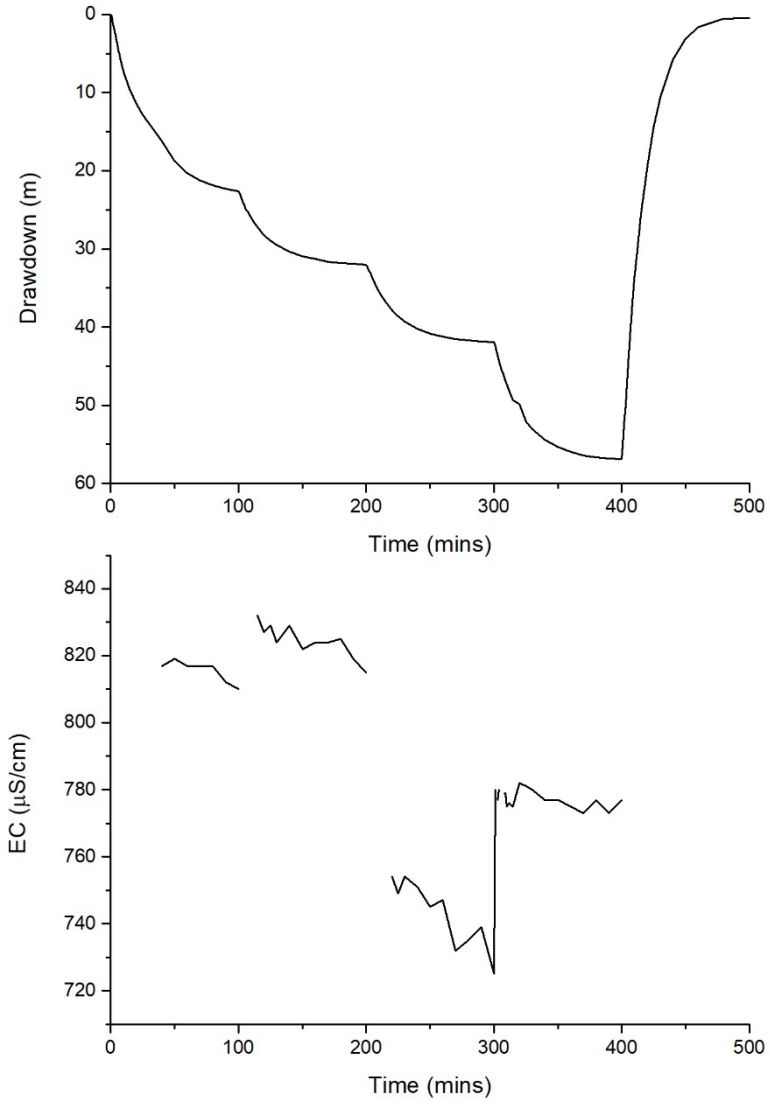

Figure 13. Drawdown in pumping bore and electrical conductivity of pump discharge during step test in RN 19385 (Site 1) conducted using pumping rates of 0.5, 0.7, 0.9 and 1.2 L/s, each for a period of 100 minutes.

835 μS/cm, after which is slowly decreased to 815 μS/cm after a further 100 minutes of pumping. Increasing the pumping rate to 0.9 L/s, resulted in an abrupt decrease in EC to 766 μS/cm, after which it continued to decrease, and was approximately 725 μS/cm after 100 minutes of pumping at 0.9 L/s. Increasing the pumping rate to 1.2 L/s, resulted in a rapid increase in EC to 780 μS/cm. EC was relatively stable at 773-782 μS/cm until the end of the test. During the 7-day pumping test, the EC rapidly decreased from approximately 760 μS/cm to 700 μS/cm, and subsequently fluctuated between approximately 670 and 710 μS/cm (Figure 14). The changes in electrical conductivity that are concident with changes in pumping rate indicate a change in water sourced by the pump. The rapid nature of these changes most likely indicates that hydraulic head is different in different

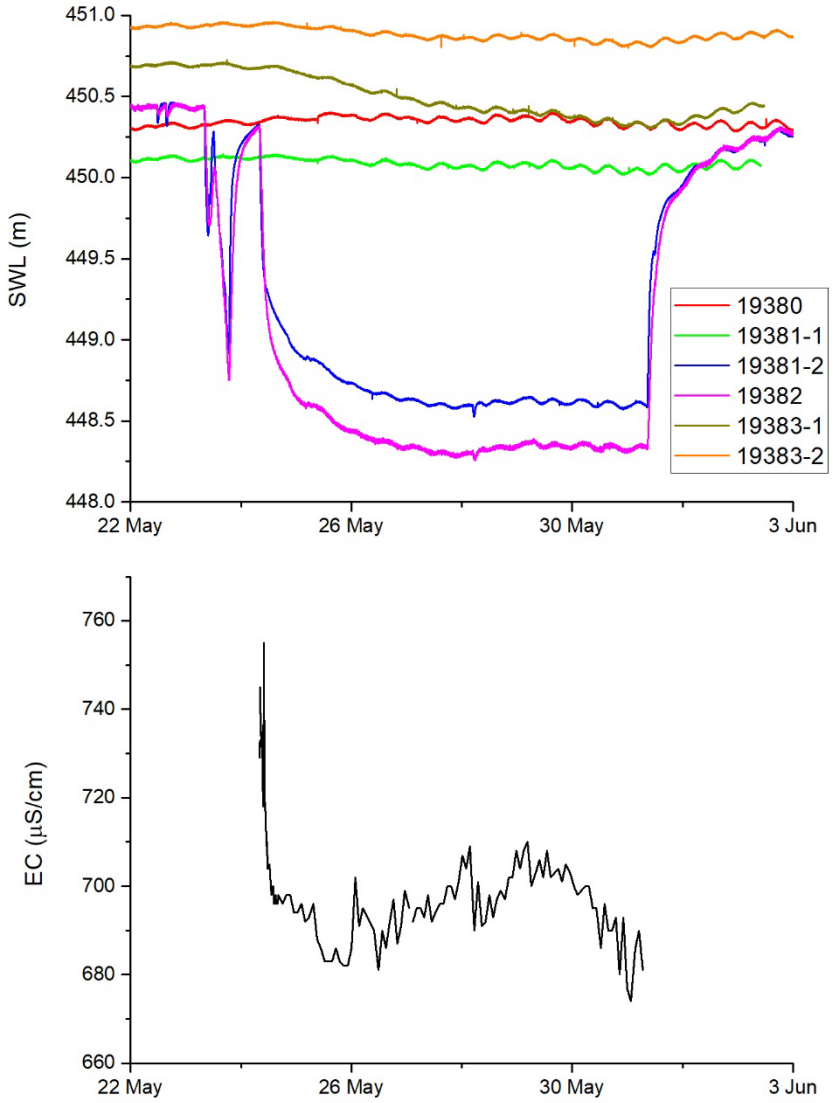

Figure 14. Drawdown in observation bores during pumping of RN 19385 (Site 1) at 0.9 L/s for 7 days, and EC of pump discharge.

producing zones intersected by the well, and hence flow from each zone changes when the pumping rate changes. As pumping rate increases, the proportion of water sourced from zones with higher head would be expected to increase.

The constant rate pumping tests at Sites 1 and 2 were analysed in FEFLOW using a homogeneous, layered model (see Appendix 1). At Site 2, estimated hydraulic conductivity values for the different layers ranged between 0.01 and 1.7 m/day, with highest conductivity between 280 and 286 m. Specific storage values ranged from 10^{-7} to 4.0 x 10^{-4}. At Site 1, hydraulic conductivity ranged between 2. 7 x 10^{-4} and 1.0 m/day, with highest hydraulic conductivity between 278 and 198 m depth. Specific storage values ranged from 3 x 10^{-7} to 10^{-4}. Although each layer within the model was assumed to be isotropic, the estimated vertical variation in hydraulic conductivity implies a

strong anisotropy, with horizontal hydraulic conductivity much greater than vertical hydraulic conductivity. At Site 2, the transmissivity over the 350 m interval of aquifer modelled (neglecting the upper 50 m, which is unsaturated) is calculated to be 110 m^2/day. The same value is calculated for the 450 m interval of aquifer modelled at Site 1. Mean hydraulic conductivities are therefore estimated to be 0.24 and 0.32 m/day, at Sites 2 and 1 respectively. Mean specific storage values are 2.3 x 10^{-4} and 1.5 x 10^{-3} for Sites 2 and 1, respectively. Mean vertical hydraulic conductivities are estimated as:

$$K_v = \frac{1}{\sum \frac{z_i}{K_i}} \quad (2)$$

where K_i are the layer vertical hydraulic conductivities (which are the same as their horizontal hydraulic conductivities, as they were modelled as isotropic) and z_i are the layer thicknesses. Mean vertical hydraulic conductivity of the formation is therefore estimated to be 0.12 m/day at Site 2 and 0.002 m/day at Site 1. These values indicate anisotropy ratios of between 2.6:1 and 110:1. The large range of values reflects the sensitivity of the anisotropy ratio to thin layers of low permeability.

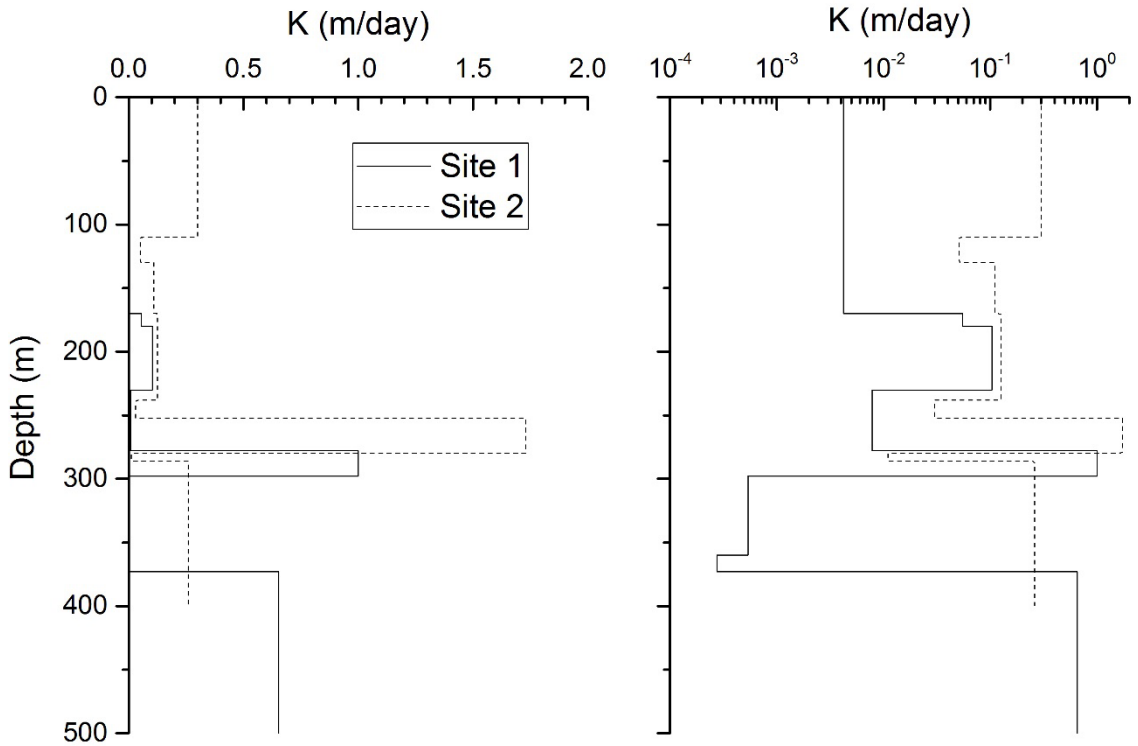

Figure 15. Hydraulic conductivity versus depth from numerical modelling of pumping tests. Results are shown both on linear and logarithmic scales.

4.4 Porosity and Specific Yield

Aquifer porosity and specific yield data is available from analysis of core samples. A large variation in porosity values is apparent, with values varying between 0.06 and 0.29 (Figure 16). However, most values (67%) are between 0.2 and 0.3. The mean of all values is 0.20, with a mean value for the Pacoota sandstone of 0.11 (five samples), and a mean for the Hermannsburg and Mereenie sandstones of 0.22 (23 samples, combined). Figure 17 shows the relationship between water content and matric potential for fourteen samples, including each of the main geological formations within the Rocky Hill area. Read and Paul (2000) calculate the specific yield based on the difference between the porosity and the specific retention at 33 kPa. Such a value is perhaps appropriate for short-term response of the water table to pumping or recharge pulses. However, to calculate long-term drawdown in response to pumping of the well field, the difference between porosity and water content at 240 kPa probably provides a better indication of specific yield. Values of specific yield calculated in this way vary between 0.01 and 0.23, with most of the samples from the Pacoota Sandstone being significantly lower than those from the other formations (Figure 18). The mean value for the Pacoota Sandstone is 0.07, and for the other formations in 0.15.

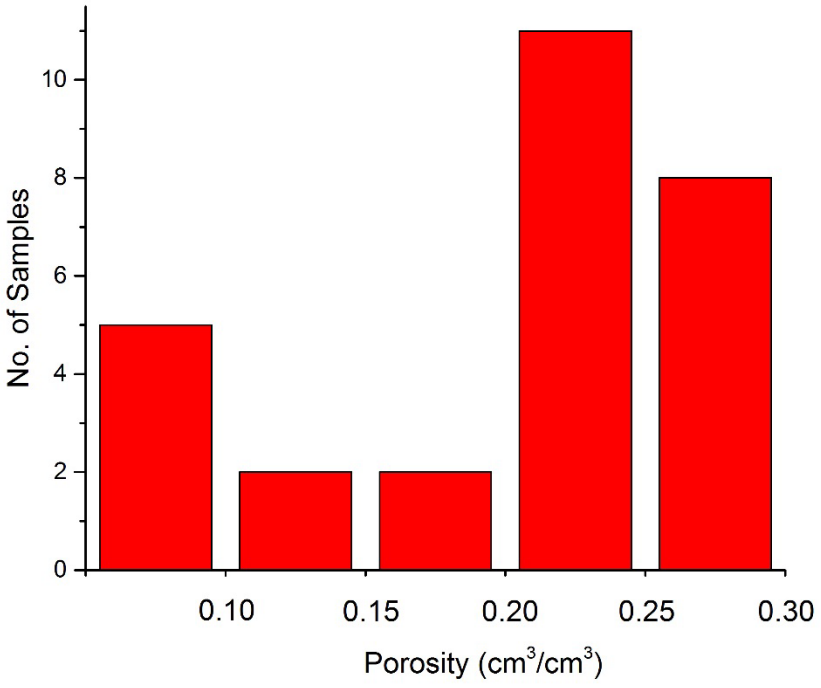

Figure 16. Histogram of porosity data from Rocky Hill core samples.

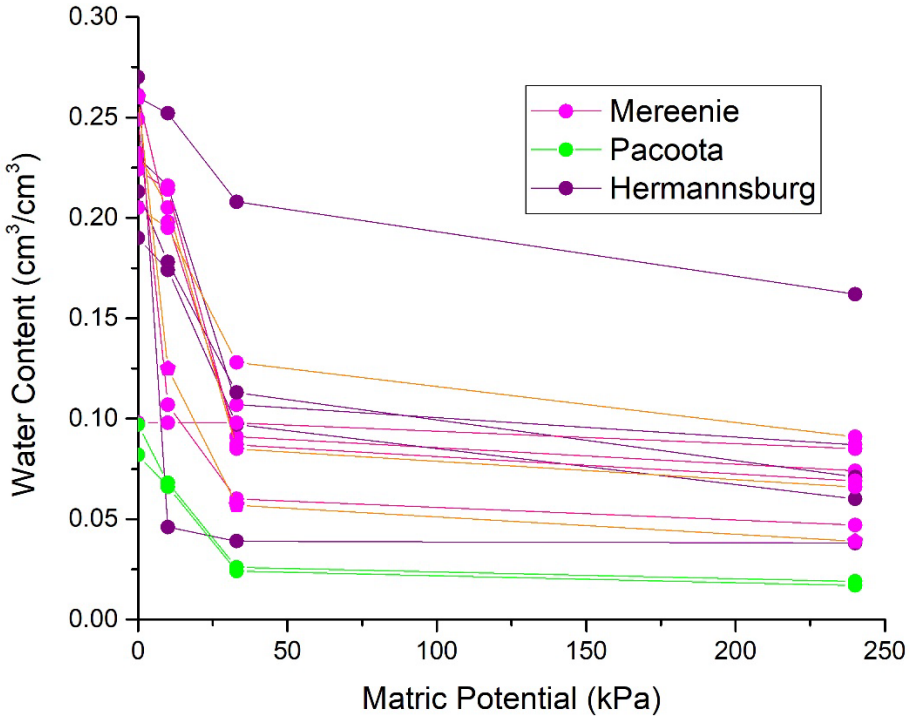

Figure 17. Relationship between water content (specific retention) and matric potential for core samples from geological formations within the Rocky Hill area. Data from Read and Paul (2000, 2002).

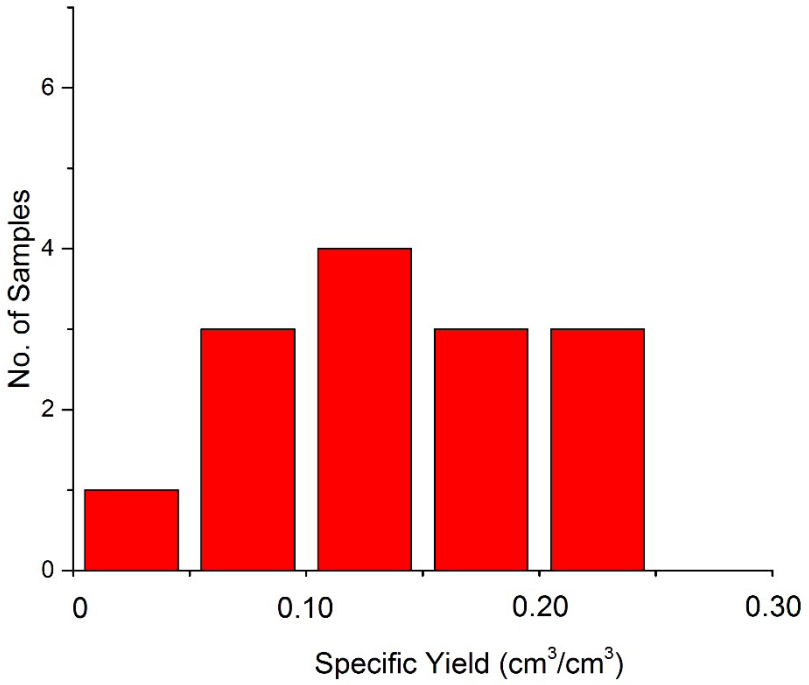

Figure 18. Histogram of specific yield data from Rocky Hill core samples. Specific yield is calculated as the difference between water content at saturation and 240 kPa.

Modelling of the pumping tests within the proposed borefield produced specific yield values of 0.24 at both Sites 1 and 2 (see Appendix 1). These values are significantly higher than results obtained on core samples (0.15 for the Hermannsburg and Mereenie sandstones) and appear too high when compared with estimated porosity values (mean of 0.22 for Hermannsburg and Mereenie sandstones). The difference could be related to the presence of highly fractured zones in the upper part of the aquifer at the drilling sites (loss of circulation was a problem during drilling) but may also represent uncertainty associated with modelling of the pumping tests. The specific yield value of 0.15 obtained from core sample analyses seems more likely.

5. POTENTIOMETRIC SURFACE AND WATER LEVEL TRENDS

5.1 Potentiometric Surface

The 2018 potentiometric surface map for the Rocky Hill area shows highest head across the northern boundary of the region, with heads decreasing towards the west, south and east (Figure 19). The general pattern is similar to that shown in the potentiometric surface map for July 2001 (Read and Paul, 2002), although heads are lower in 2018, particularly in the west of the study area. The main features of the potentiometric surface are:

(i) an area of low head in the northwest of the region, associated with pumping from Roe Creek borefield;
(ii) a groundwater mound in the north, thought to be due to recharge of the Cainozoic aquifers;
(iii) an area of low head in the northeast, likely related to groundwater discharge, although the discharge mechanism is currently unclear; and
(iv) a relatively flat potentiometric surface across the central part of the region.

It should be noted that this potentiometric map combines hydraulic head measurements from several geological units and from a number of different depths. In the northern part of the region, the Mereenie-Hermannsburg sandstones are absent, and bores are mostly screened in the overlying Cainozoic sediments or the underlying Pacoota Sandstone. The connection between the Pacoota and the overlying aquifers is uncertain, and so determining flow directions and flow rates from this map may not be straightforward. It is noteworthy that drawdown from pumping of the Roe Creek borehole extends to the southeast as a narrow tongue. This has created a very steep hydraulic gradient, of almost 50 m over a horizontal distance of less than 2 km (compare RN 4481 and RN 4688, for example). This steep head gradient approximately coincides with the boundary between the Pacoota and Goyder/Shannon formations (see Figure 6), and probably indicates that there is some restriction to flow between these units. Nevertheless, Figure 19 shows that drawdown associated with the Roe Creek borefield has reached the edge of NT Portion 4704.

5.2 Temporal Trends

Figure 20 shows the change in potentiometric surface between 2000 and 2018. Water level declines in excess of 0.4 m/y have occurred in the northwestern part of the region, with declines of more

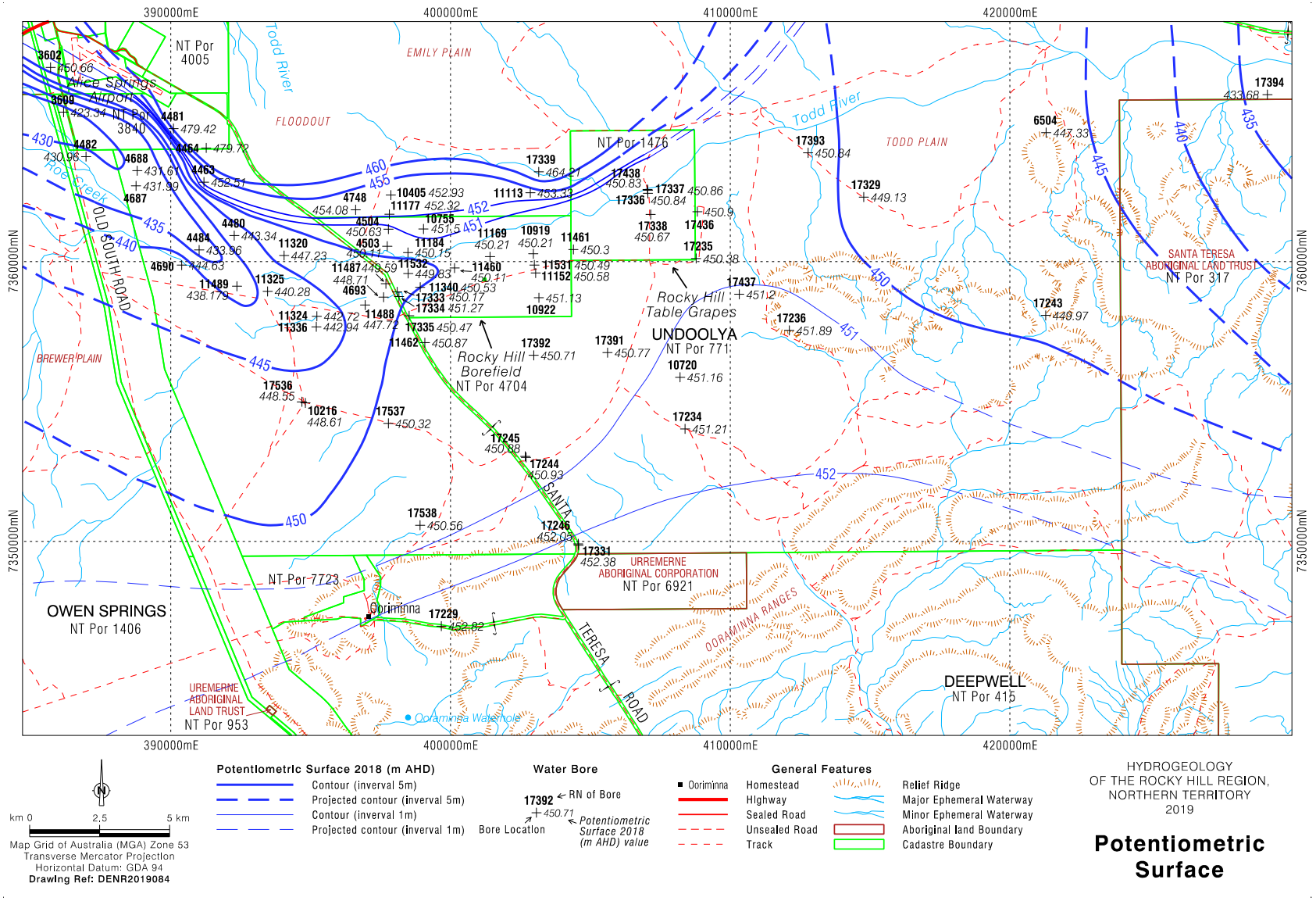

Figure 19. Potentiometric surface map for 2018. (Most measurements were made between in 7-10 August 2018; see Appendix 2.)

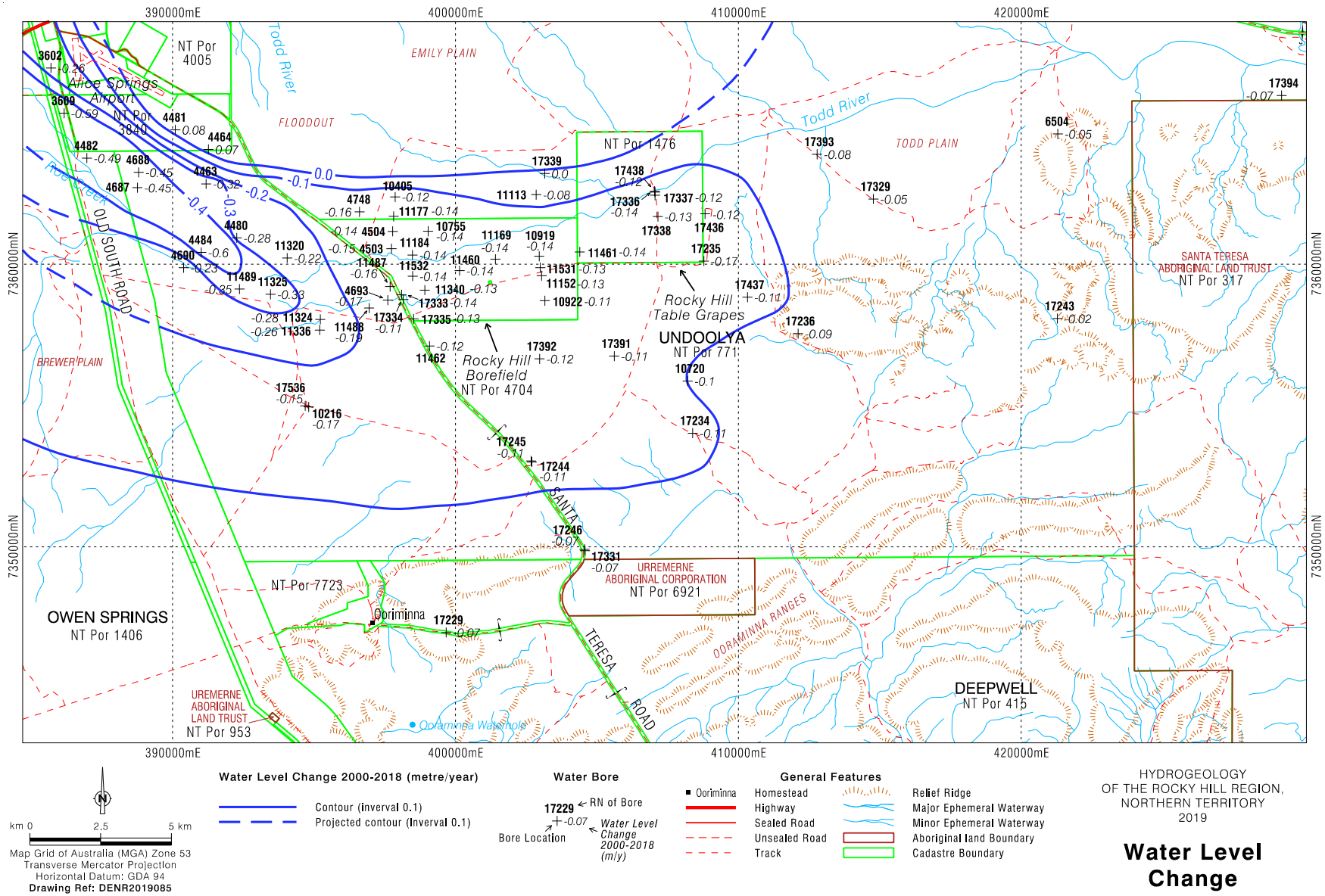

Figure 20. Change in water level between 2000 and 2018 (metres per year).

than 0.1 m/y extending as far east as 410000. However, significant declining trends are apparent much further east. The water table rise in the extreme northwest of the region has been attributed to cessation of pumping in the Amoonguna area (Read and Paul, 2000) and recent recharge of aquifers in this area (Verhoven, 1979).

Changes in hydraulic head between 1977 and 2016 along an approximate east-west transect are presented in Figure 21. Read and Paul (2000) constructed a similar figure, using data only up to 1997. The plot shows a gradient from west to east in the 1960s, reflecting flow from west to east, but with rapid declines in water levels in the west of the region since that time. A gradual, and relatively uniform decline occurs further east. Largely based on this figure, and data up until 1997, Read and Paul (2000) identified the eastern extent of drawdown from the Roe Creek borefield at approximately 402500 East. However, analysis of subsequent data shows that large drawdowns have not extended further east in the subsequent 19 years, and the declines observed in the eastern part of the region are not attributed to extraction from Roe Creek. The discontinuity in the water level trend occurs between RN 4690 and RN 4693. To the west, water levels show a rapid rate of decline, but with the rate of decline decreasing to the east. However, east of RN 4693 water levels of all wells have declined at a similar rate, which has been relatively constant with time. This point may reflect a change in geological structure, most likely an increase in the width of the aquifer system, and perhaps a decrease in hydraulic conductivity. The Mereenie aquifer dips at 30 - 35° to the south in the Roe Creek area and is overlain by the relatively impermeable Brewer Conglomerate. The dip is much less in the Rocky Hill area, and so a much greater area of Mereenie Sandstone occurs close to the surface, allowing flow towards Roe Creek from a much greater area of aquifer. The drawdown cone from Roe Creek is expected to extend further east in future years, but its rate of expansion will slow due to the change in the geological structure. However, the declining water levels which have been recorded to date in areas south and east of NT Portion 4704 are not attributed to pumping from the Roe Creek bore field. Rates of water level decline in the extreme south and east of Rocky Hill average 0.05 m/y and may due to groundwater use by deep-rooted vegetation. Higher rates of decline of 0.1 – 0.15 m/y immediately south and east of NT Portion 4704 may partly reflect a relaxation of water levels following historic periods of higher recharge. Nevertheless, the reason for declining water levels in the extreme south and east of the region remains somewhat uncertain as groundwater discharge mechanisms are not well understood. The mean rate of storage reduction in the area east of the Santa Teresa Road for the 2000 – 2018 period is approximately 3000 – 4000 ML/y. In comparison, groundwater extraction for agricultural activities in the region has been approximately 950 ML/y since 2012/2013 (Cook et al., 2017).

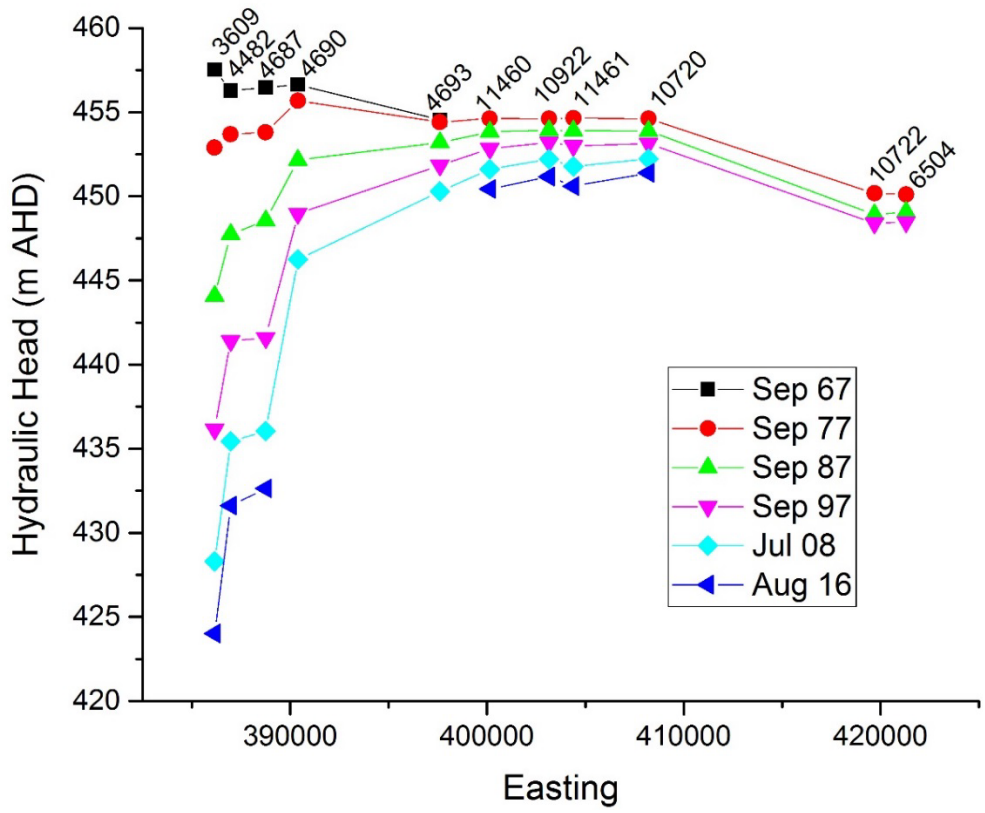

Figure 21. Potentiometric surface along an approximate east-west transect through the Rocky Hill area. Note: Water levels in each bore were measured within the month indicated in the legend, except that the water level in RN 10720 was measured in November 1977, and water levels in RN 10722 and RN 6504 were measured in June 1977, rather than September 1977. Bore locations are shown in Figure 1.

Figure 22 shows hydrographs for three bores from the Mereenie aquifer. The bores show a clear decline from the early 1980s. RN 4693, which is immediately west of NT Portion 4704, shows an average rate of water level decline of 0.14 m/y since 1980. RN 11152 and RN 11340 are located 1.3 and 5.4 km further east, respectively, both within NT Portion 4704. Both show very similar hydrographs, with average rates of water level decline of 0.1 m/y since 1980. The higher rate of water level decline in RN 4693 is attributed to pumping of the Roe Creek borefield. RN 11152 and RN 11340 show an increasing rate of decline since 2005, with rates of decline since that time of 0.13 and 0.14 m/y, respectively. Water level declines on these bores since the 1980s are attributed in part to relaxation following historic periods of high recharge. The increased rate of decline since 2005 may be related the expansion of the drawdown cone from pumping from the Roe Creek borefield.

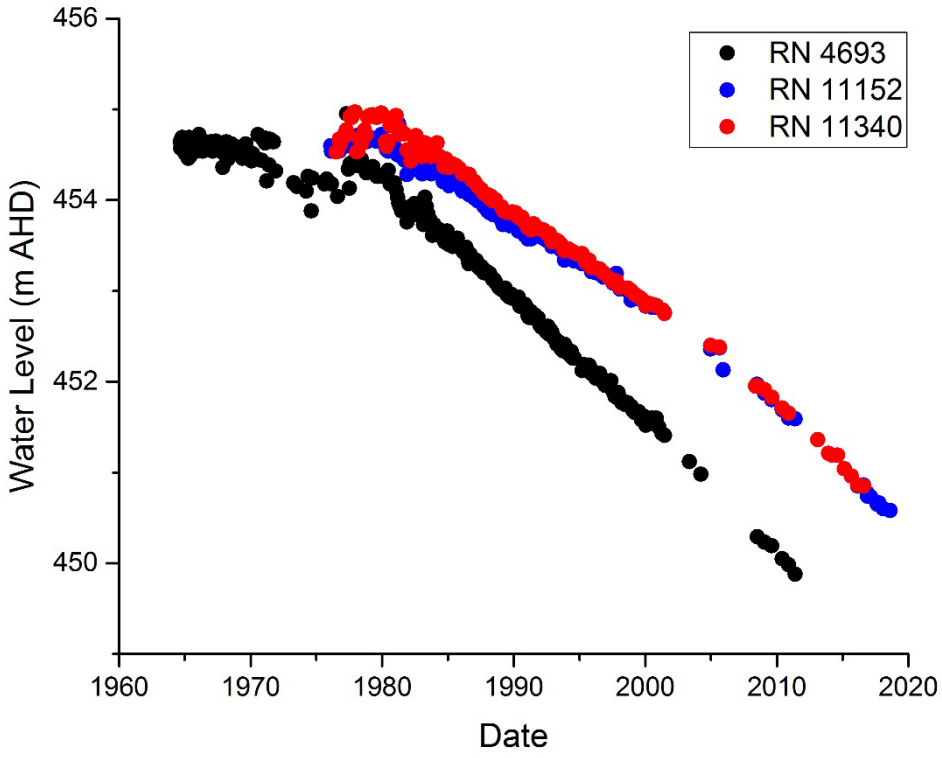

Figure 22. Hydrographs from three bores screened within the Mereenie aquifer located within or adjacent to NT Portion 4704. Bore locations are shown in Figure 1.

Figure 23 shows hydrographs for three bores that are predominantly open to the Pacoota aquifer; all three bores are in the north western part of the study area, where the Pacoota occurs relatively close to the land surface. Up to the early-1980s, hydrographs in these bores are relatively flat. Hydrographs show a declining trend after the early-1980s, in response to pumping from the Pacoota aquifer at Roe Creek borefield. The rate of decline between 1985 and 1995 was 0.7 m/y in RN 4463, located 8 km east of the Stuart Highway, but less further east (0.2 m/y in RN 4748 and 0.1 m/y in RN 10405, both located between 15 and 16 km east of the Stuart Highway). Monitoring of RN 4463 ceased in 1999, although RN 4463 and RN 10405 show continuing declines.

Three bores located in the NW of the area screened in Cainozoic aquifers show a sharp rise in water level after 1975 (Figure 24). (These bores are located further north than the Pacoota bores discussed above.) Read and Paul (2000) attributed this to cessation of pumping in the Amoonguna area around this time, although Verhoven (1979) attribute it to recharge to the Cainozoic aquifers due to flow in Todd River following high rainfall through the 1970s. (Alice Springs airport recorded 3786 mm of rainfall for the 1974-1977 period, with high rainfall also recorded in 1978 and 1979.) Although the rate of rise has slowed over time, these bores continue to show a gradual rise in water level. A sharp rise in water level was also observed after 2001, particularly in RN 4458 and RN 4461. This is likely due to recharge associated with high rainfall in 2000 and 2001, with Alice Springs

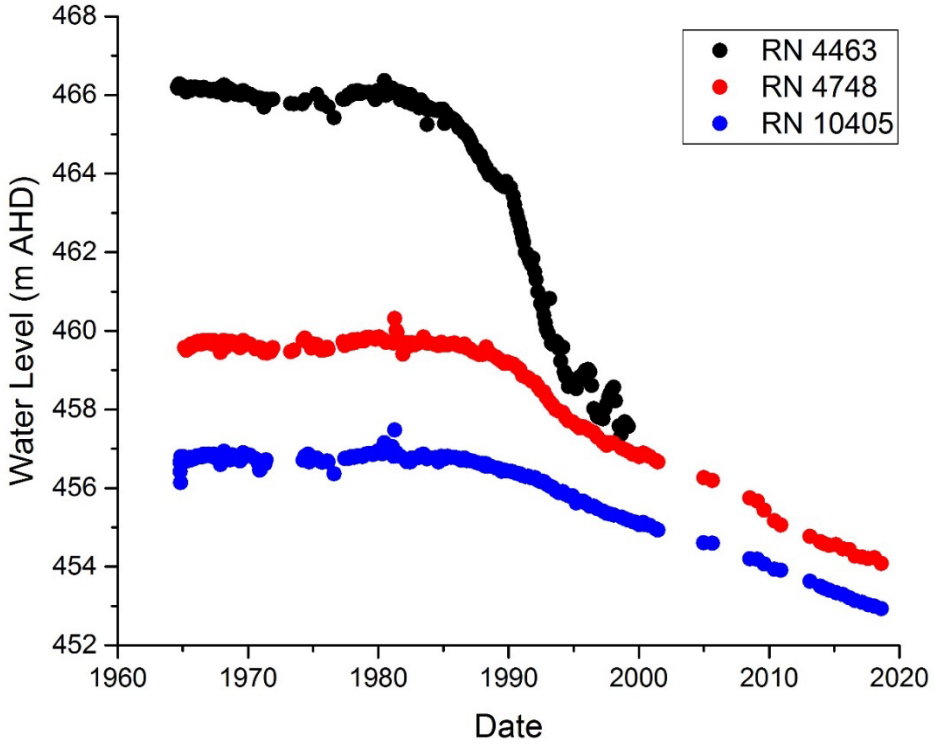

Figure 23. Hydrographs from three bores screened within the Pacoota aquifer, in the northwest of the study area. Updated from Read and Paul (2000). Bore locations are shown in Figure 1.

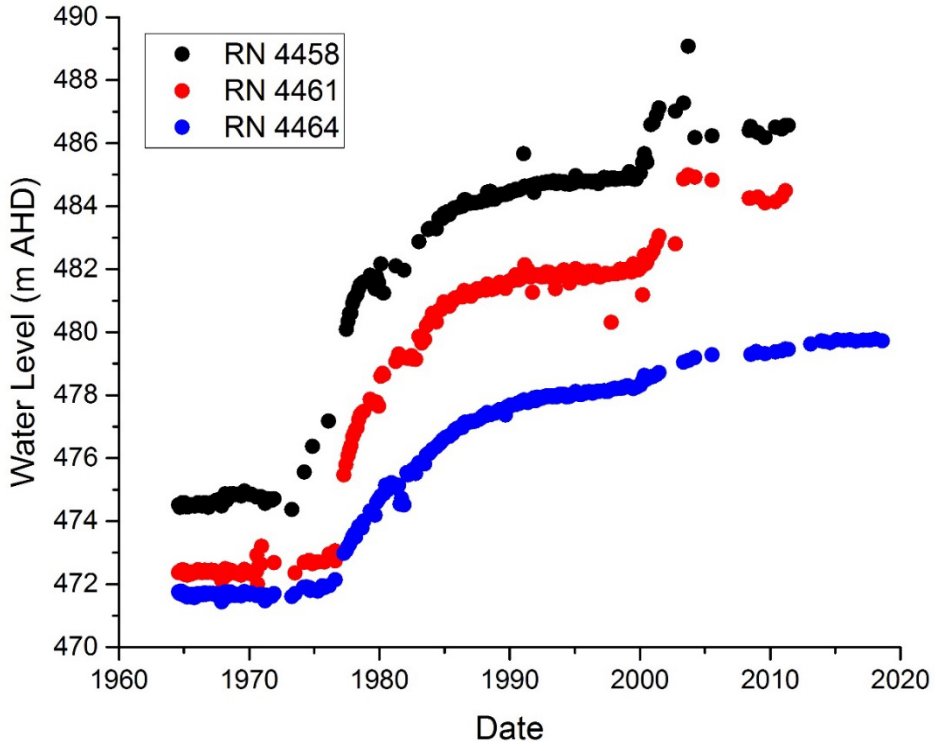

Figure 24. Hydrographs from three bores screened within the Cainozoic aquifer, in the northwest of the study area. Updated from Read and Paul (2000). Bore locations are shown in Figure 1.

airport recording 1405 mm for these two years. Both the Todd River and Roe Creek also recorded amongst their highest flows in 2000. At this time, water level increases of up to 1 m were also observed in bores in the northeast of the area between January 2000 and July 2001 (Figure 25). RN 17329 also shows a water level rise in 2011. There is also some evidence of a rise in water levels in RN 4458 and RN 4461 in 2011, before monitoring was discontinued (Figure 24). February – March 2011 was also very wet, with 228 mm of rainfall recorded at the airport in this two-month period.

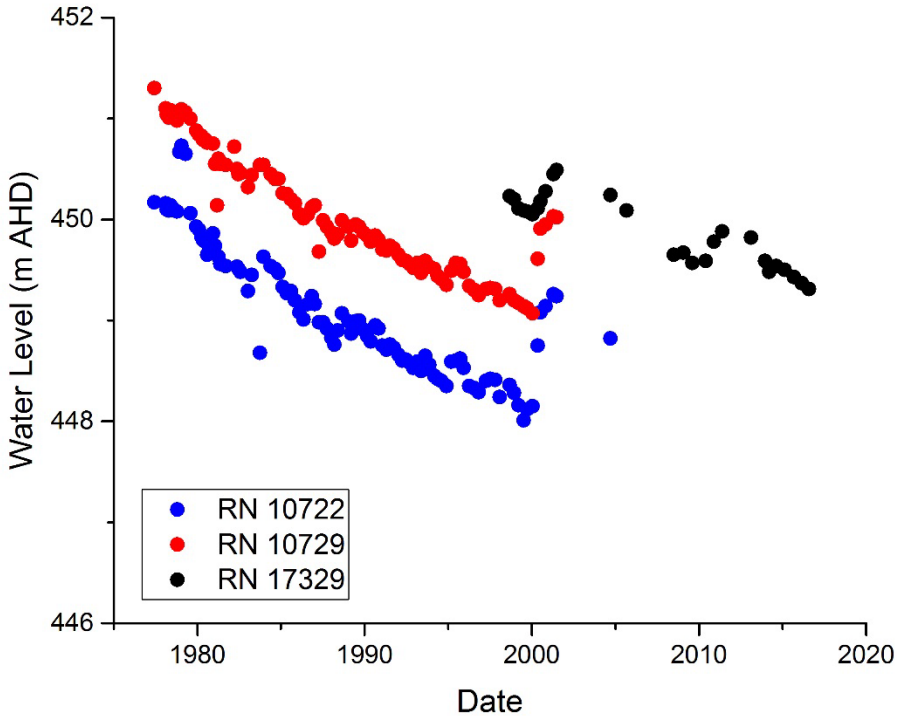

Figure 25. Hydrographs from three bores in the northeast of the study area, screened within the Mereenie aquifer. Bore locations are shown in Figure 1.

5.3 Aquifer Connectivity

Figure 26 shows representative bores from the Hermannsburg, Mereenie and Pacoota aquifers that are in close proximity, and located in the northwest of the study area. All three bores show declines in water levels, although the rate of decline is most rapid in the Mereenie aquifer and slowest in the Pacoota aquifer. Significant head differences are observed between the Pacoota aquifer and the other aquifers, which led Read and Paul (2000) to conclude that they are hydraulically separated. However, they also noted that the analysis was complicated because most bores are open over long intervals and may be in connection with more than one aquifer.

Figure 27 compares water levels in the Pacoota aquifer with those in other aquifers for bores further southeast than those shown in Figure 26. RN 4463 is mostly open to the Pacoota aquifer, while RN 4467 is mostly open to the Mereenie aquifer and RN 4464 (which is further north) is in Cainozoic sediments. Again, water levels in the Pacoota aquifer are higher than in the Mereenie aquifer, and lower than those in the Cainozoic aquifer. However, the comparison shown in both Figures 26 and 27 is complicated because available bores in the Pacoota aquifer are located further north than those in the Mereenie and Hermannsburg aquifers, and there is a pronounced decline in the potentiometric surface moving from north to south in this part of the study area. Nevertheless, the disparity between the rising water level trend in the Cainozoic aquifer, and the declining trends in the Mereenie and Pacoota aquifers, suggests that the Cainozoic aquifers are not strongly connected to the Mereenie – Pacoota aquifer system. This may be due to low permeability layers in the Goyder/Shannon Formation, or at the boundary between the Pacoota and Goyder/Shannon Formation, as discussed above.

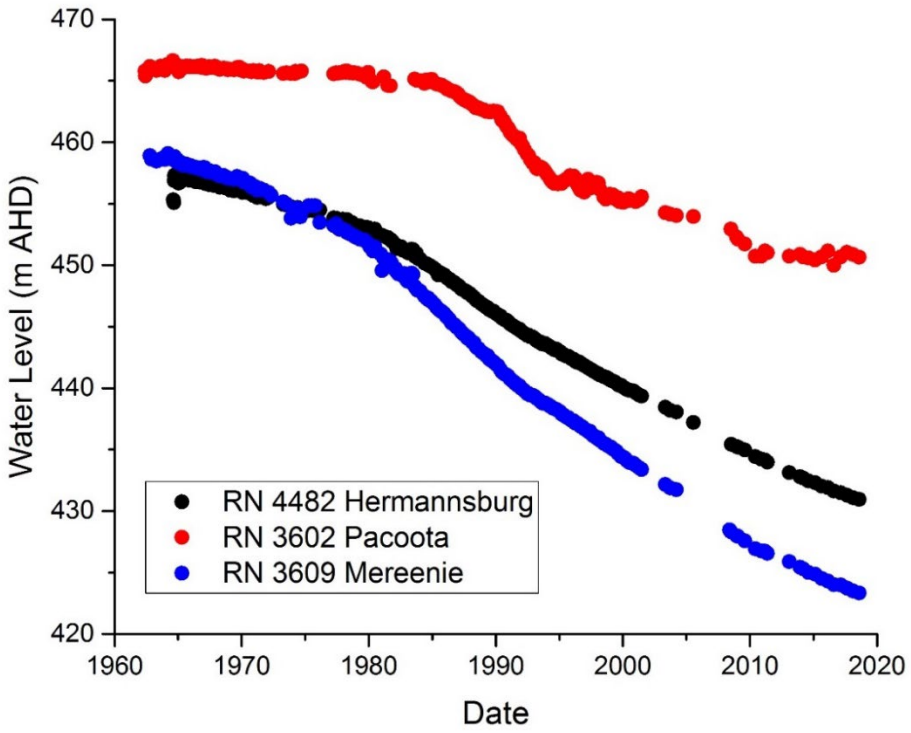

Figure 26. Comparison of hydrographs for bores from different aquifers, located in the northwest of the study area. Updated from Read and Paul (2000). Bore locations are shown in Figure 1.

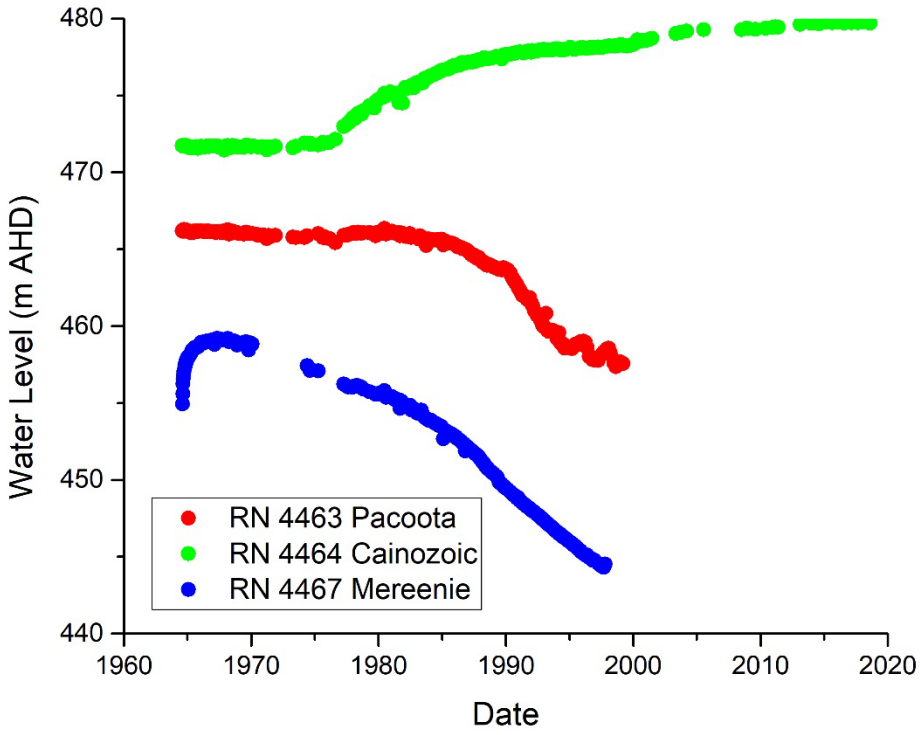

Figure 27. Comparison of hydrographs for bores from different aquifers, in the northwest of the study area. Bore locations are shown in Figure 1.

The vertical hydraulic gradient within the has been assessed on new piezometers installed at Site 1 and Site 2 within NT Portion 4704 (Figure 28). Hydraulic head data measured in March 2019 indicate a downward gradient of approximately 1.5 x 10^{-3} between the water table and almost 500 m depth. The deepest piezometer at Site 1 is screened in sediments identified by Read and Paul (2002) as the Pacoota Formation. The similarity of heads and continuity of the head gradient indicates a good hydraulic connection between the Pacoota and overlying aquifers, at least at this location. However, the Pacoota aquifer has a lower hydraulic conductivity than the overlying Hermannsburg and Mereenie aquifers, and this would explain the reduced drawdown in the Pacoota aquifer compared to the overlying aquifers that is observed elsewhere (Figure 26). Assuming a vertical hydraulic conductivity of 0.002 – 0.12 m/day measured at Sites 1 and 2, and the observed hydraulic gradient, would give a downward flux of 0.001 – 0.06 m/y, consistent with modern day recharge to the aquifer in the Rocky Hill region. The relaxation time for this gradient can be calculated from

$$t = \frac{x^2 S}{K_v} \tag{3}$$

where K_v is the vertical hydraulic conductivity, S is the specific storage, x is distance and t is time. Assuming K_v = 0.002 – 0.12 m/day, 10^{-4} m^{-1} < S < 10^{-5} m^{-1} and using x = 350 m, we get t = 0.03 – 17

years. This indicates that the vertical head gradient reflects hydrologic conditions over periods of months to years, and hence recharge over this period.

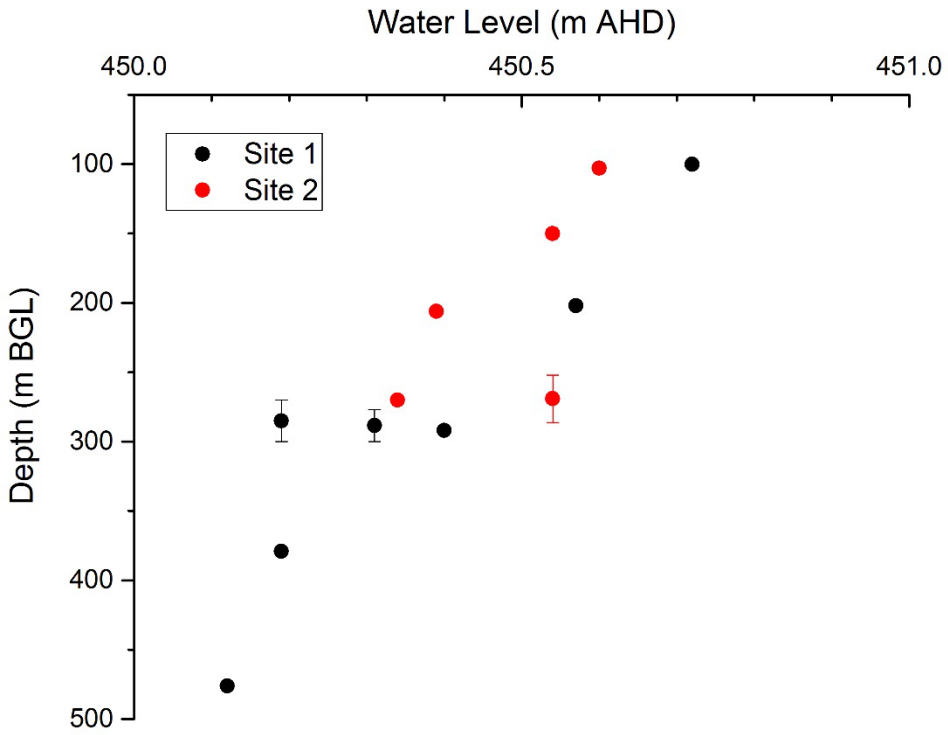

Figure 28. Vertical head profile from wells at Site 1 and Site 2.

6. GROUNDWATER SALINITY AND WATER QUALITY

6.1 Salinity Distribution

A contour map of total dissolved solids (TDS) in groundwater in the Rocky Hill region was prepared by Read and Paul (2000) based on data available at that time. The map shows low TDS groundwater (< 500 mg/L) in an area along Roe Creek, where it was hypothesised that infiltration of ephemeral surface flows could recharge the Mereenie and Hermannsburg aquifers. The area of low TDS groundwater generally coincided with the location of the proposed Rocky Hill borefield. This map was updated by Read and Paul (2002) based on additional information obtained following a drilling program in 2000.

The map produced by Read and Paul (2000, 2002) was based on water quality data obtained during drilling of wells, or from subsequent sampling. The authors noted that, in most cases, data from the deepest water sample analysed for each bore was used and this usually had the highest TDS value. Where drilling and test pumping samples were available from the same bore then the test pumping TDS result was used. Cozens (2017) undertook a review of the salinity data used by Read and Paul (2000, 2002). This review analysed the database for early data not included in the Read and Paul assessments, more recent data, and examined sampling methodology and well depth. Cozens (2017) noted that recent TDS data (post 2002) is mostly lower than the data used by Read and Paul in 2002. Figure 29 compares TDS results for groundwater samples obtained in 2016 – 2017 with samples obtained from the same wells prior to 2010 (and mostly prior to 2000). Only data with samples obtained after well purging are shown in Figure 29, as these are considered more reliable. The comparison shows that recent TDS results are between 7 and 15% lower than earlier values, although the reasons for this difference are unclear. Recent recharge associated with flooding of the Todd River and Roe Creek in 2000-2001 and 2011 may have contributed to a reduction in TDS of groundwater, and all bores shown in the comparison are located close to these creeks and their flood-outs. However, it is not possible to rule out analytical uncertainty and laboratory calibration issues. The strong linear relationship between pre- and post-2010 samples provides some support for the latter explanation.

Figure 30 shows an updated salinity map, based on the original map of Read and Paul, the review of salinity data by Cozens (2017), and more recent data obtained during the 2017 – 2018 drilling program. The map also covers a greater region than that of Read and Paul (2002), which focussed on the area underlain by the Mereenie Sandstone. The TDS map shows the extent of the low salinity (TDS < 500 mg/L) groundwater to be significantly greater than previously thought and extending throughout much of NT Portion 4704. The increased mapped extent of low salinity groundwater is, in part, due to lower TDS values recently measured in several bores, and also partly due to new drilling results. The increased northerly extent of low TDS groundwater is inferred from

re-sampling of RN 10755, RN 11532, RN 11460 and RN 11487, and an increase in the area of low salinity water along Roe Creek is inferred from re-sampling of RN 11491. To the northeast, an increase in the area of low TDS groundwater is indicated from results on new wells RN 17817 and RN 19678.

Groundwater having salinity less than 600 mg/L extends east of the Undoolya Rocky Hill Agricultural Block (NT Portion 1476), and as far south as NT Portion 415. Groundwater becomes increasingly saline further east, with a maximum salinity of 7650 mg/L measured in RN 17394, in the extreme east of the region. Cozens (2017) noted that close to the proposed borefield the samples have mostly been collected with methods that result in high quality samples – following purging of at least three well volumes, or after pump tests, where it can also be assumed that the well was sufficiently purged. However, in other parts of the region, data quality is poorer.

High TDS groundwater to the southeast of NT Portion 4704 was measured in bores RN 12045 and RN 10720. Read and Paul (2000) note that drilling records for RN 12045 show that there was saline water encountered between 58 and 62 m depth in the Tertiary sediments overlying the Hermannsburg Sandstone. Chemical analysis of a water sample collected during drilling yielded an electrical conductivity of 31,200 µS/cm (approximately 20,000 mg/L TDS). High TDS groundwater at

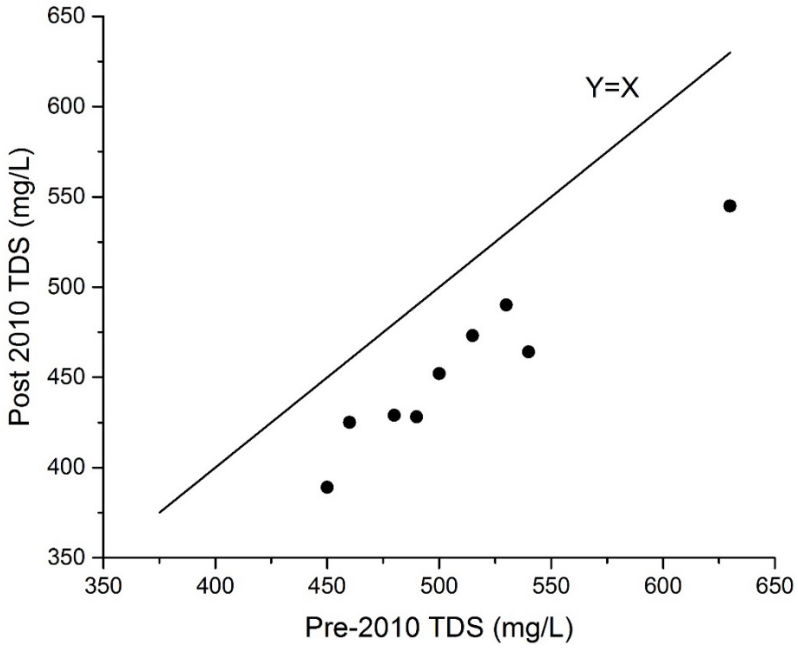

Figure 29. Comparison of pre-2010 and post-2010 TDS data. Pre-2010 data was most obtained from bores sampled in 1974-1977 but includes one bore that was sampled in 1999 and one that was sampled in 2007. Post-2010 data was obtained from samples collected in 2016-2017. Only TDS results on samples obtained following purging of wells are included (i.e., bailed and air-lifted samples have not been included).

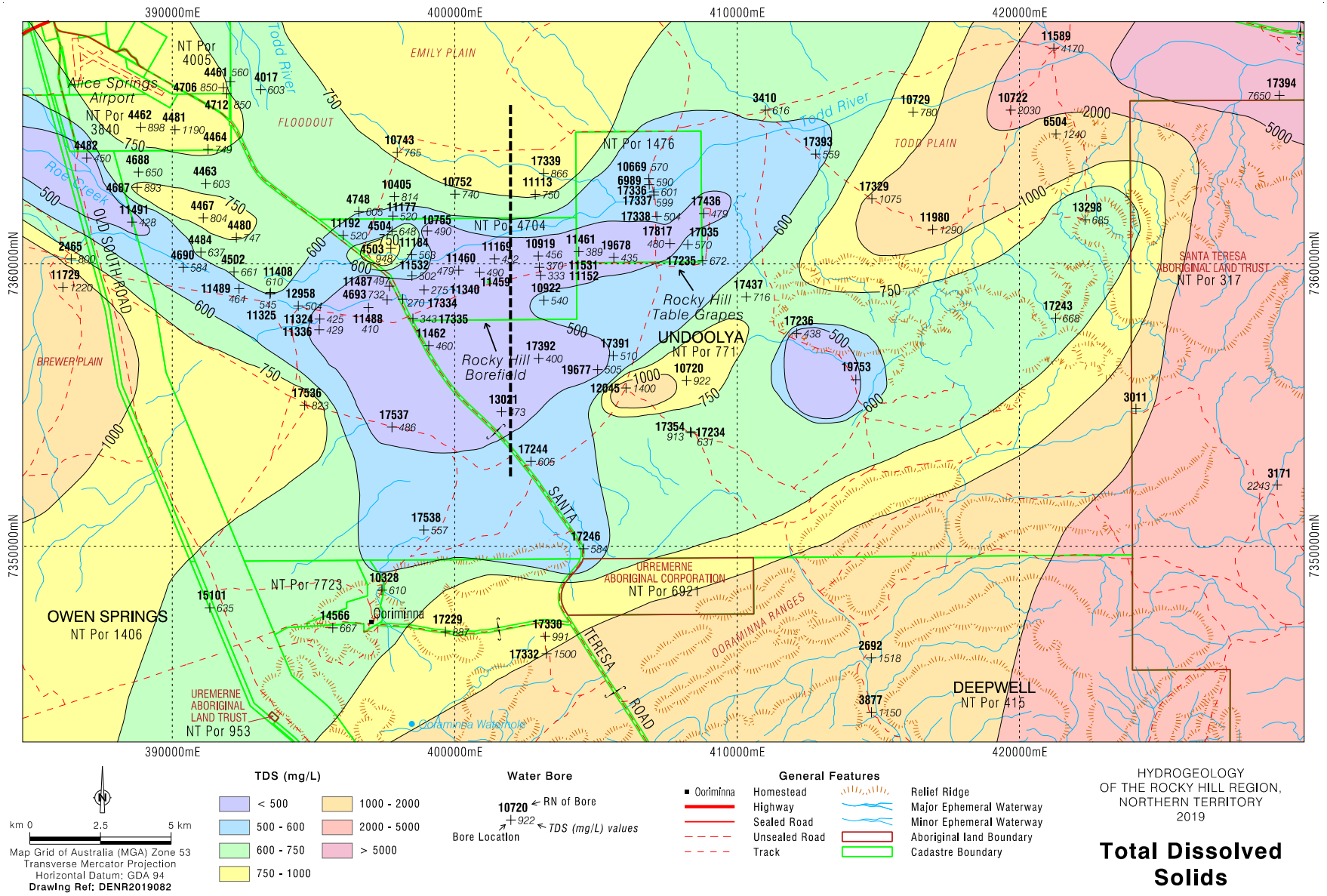

Figure 30. Groundwater salinity (total dissolved solids). The broken black line shows the location of the AEM transect in Figure 38.

this location is also supported by results from the aerial electromagnetic survey, that show high electrical conductivity in this region (Figure 31). An area of low TDS groundwater further east is indicated by RN 17236, and by EC results on RN 19753. The extent of this low TDS groundwater is unclear, as there is an absence of wells to the south and east. It is possible that it extends further to the southwest as far as RN 17246. The electromagnetic survey also shows a small area of high conductivity immediately east of NT Portion 4704 and south of NT Portion 1476, although this has not been confirmed by drilling.

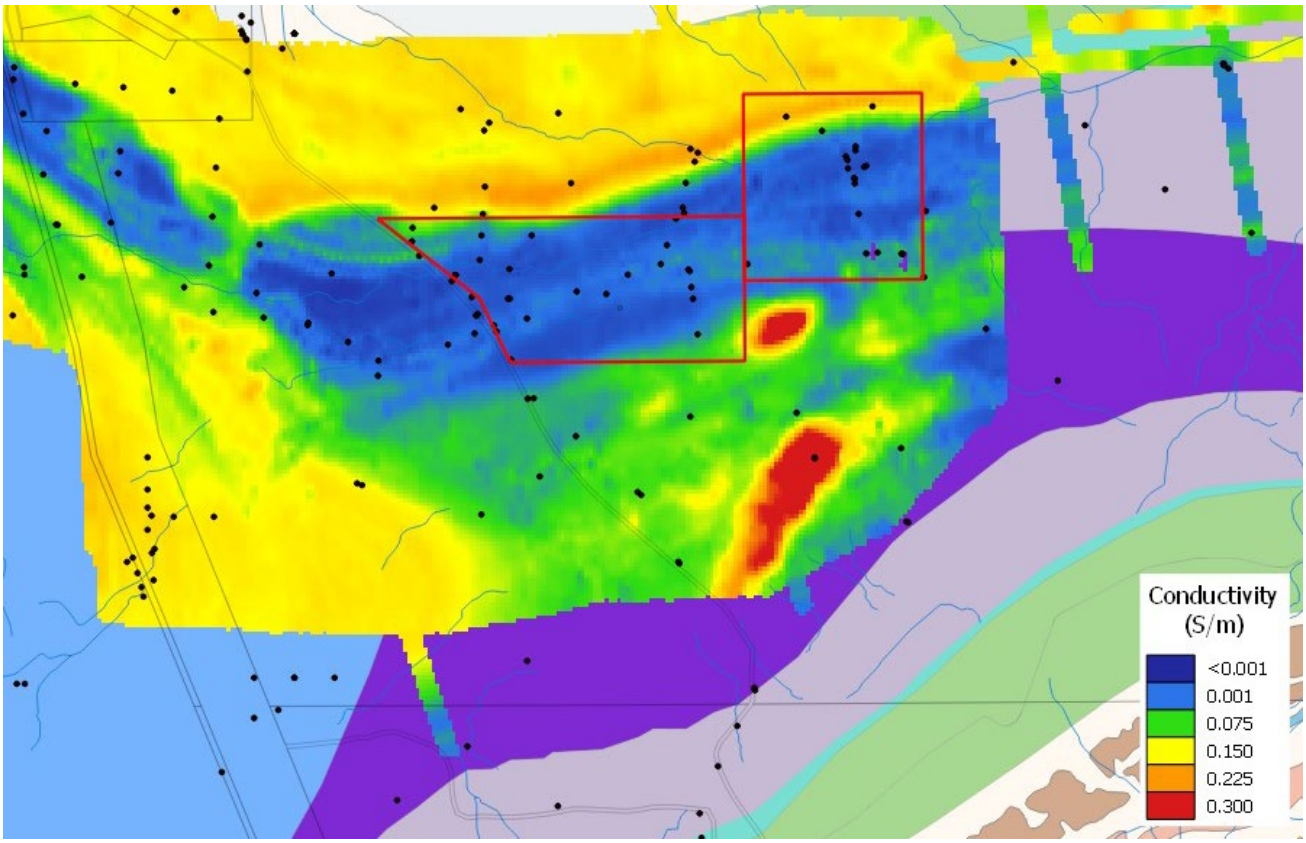

Figure 31. Aerial electromagnetic magnetic conductivity in the Rocky Hill area. The approximate boundaries of NT Portions 1476 and 4704 are marked in red, and the background map (where there is no electromagnetic data) from Figure 5. Electromagnetic data is from Ray (2019).

There remains some uncertainty regarding the southwestern extent of the fresh groundwater, due to a lack of bores in this area. The southwestern boundary is largely defined by RN 17536, RN 11462 and RN 17537. Groundwater in RN 17536 is significantly more saline than that in wells RN 11462 and RN 17537, located respectively 5 and 3.5 km to the northeast and east, respectively. There are several exploration bores further to the southwest (near Old South Road) that are not depicted on Figure 30 (RN 11888 – RN 11904 and RN 12955 – RN 12957). It is unclear from available records whether these bores were screened or backfilled immediately after drilling. The bores depths range from 30-216 m and some had groundwater samples collected by airlifting. EC results ranged from

790 μS/cm to 35,300 μS/cm. While the data quality is uncertain, it may suggest that the high TDS groundwater in the west of the region (as defined only by RN 11729) is more widespread than shown on Figure 30. The electromagnetic results are consistent with a decline in water quality south and east of RN 17536, but they do not indicate that the water is highly saline.

6.2 Salinity Variation with Depth

Following Cozens (2017), we examine trends in salinity with depth from bores that had airlift samples collected from at least three depths during drilling (a total of 31 bores). Although the bores would have been open, allowing mixing of water from different depths, several wells show increases in salinity with depth (Figures 32, 33). In RN 10722, RN 11340, RN 11491, RN 17394 and RN 17437, salinity increases by more than 20% between the shallowest and the deepest samples. Increases in salinity with depth are most apparent in areas with more saline groundwater (RN 10722 and RN 17394), where rates of increase with depth are between 21 and 29 μS/cm per metre. However, significant increases in salinity with depth are also apparent in areas with lower salinity groundwater. For RN 11340, the rate of salinity increase with depth is 28% per 100 m, and for

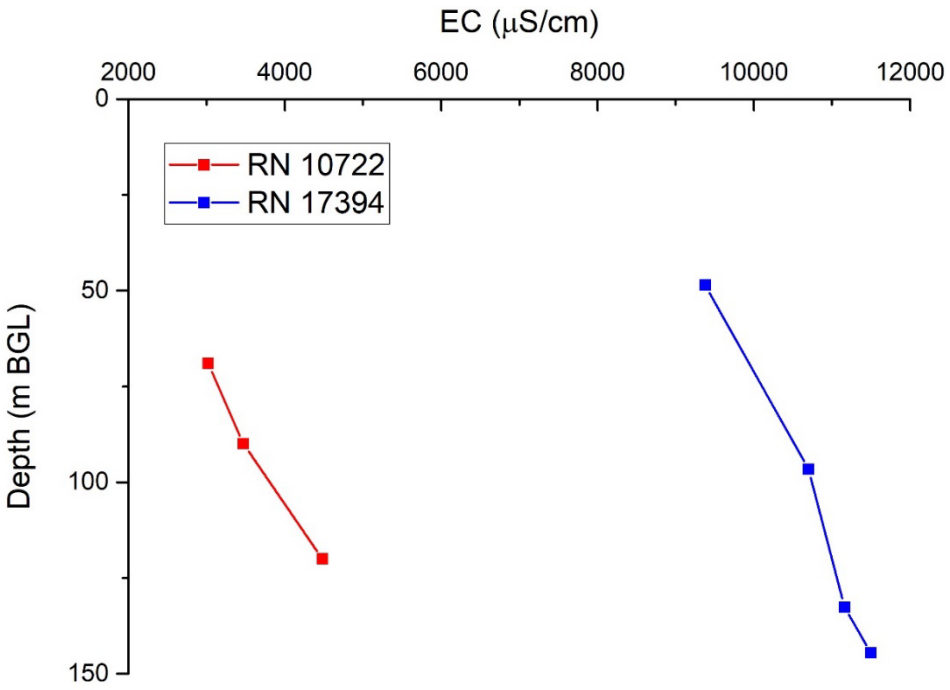

Figure 32. Electrical conductivity of groundwater samples collected by airlifting during drilling for two bores in areas of high salinity.

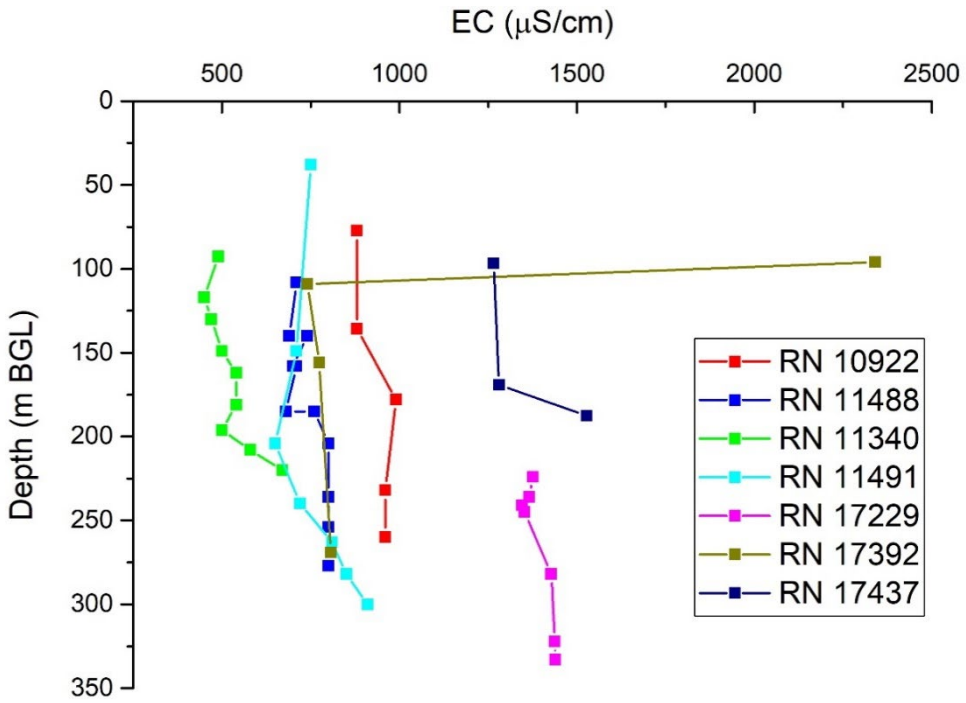

Figure 33. Electrical conductivity of groundwater samples collected by airlifting during drilling for seven bores that show significant increases in salinity with depth.

RN 17437 it is 23% per 100 m. However, for the other bores shown in Figure 33, it ranges between 4 and 9 % per 100 m.

In RN 17392, a high salinity was measured in the shallowest airlift sample (2340 µS/cm at 92 m), with much lower salinity between 109 and 269 m. (Salinity increases from 741 to 807 µS/cm between 109 and 269 m.) However, the yield from the upper portion of the aquifer was much lower (~0.2 L/s) than deeper in the bore (6+ L/s), so that this highly salinity zone is likely to have a small contribution to the salinity of a pumped sample from this bore. While samples from only two depths were collected from 12045, it is worth noting the significantly higher EC at 57 m (31,000 µS/cm) compared to just 2,880 µS/cm at 100 m. Very high EC near surface may also be the reason later samples from this bore are high. This was also noted by Read and Paul (2002) who recommended drilling of a new bore that would case off this upper saline water, so that representative samples from the underlying portion of the aquifer could be collected.

Considering all 31 bores, 17 show significant increases in salinity with depth, 7 show significant decreases, and 6 do not show a trend. Averaging all bores showing significant trends, salinity increases by approximately 2.1 µS/cm per metre of depth, or approximately 210 µS/cm for every 100 m. However, if the two most saline bores are excluded, the average trend is an increase in

salinity with depth of approximately 0.042 µS/cm per metre of depth, or 4.2 µS/cm for every 100 m.

Cozens (2017) obtained bore fluid electrical conductivity profiles to up to 300 m depth from 10 sites within the Rocky Hill area. A number of these profiles (notably RN 17437 and RN 17536; Figure 34) display step-like increases in electrical conductivity with depth. Although this data does not indicate salinity of the formation water at the respective depths, as it is influenced by flow within the borehole itself, the EC values measured within the bore must occur within the sampled interval of the formation. The depths at which step-like changes in electrical conductivity occur, have been previously interpreted to represent fracture zones or zones of high permeability, where water from the formation flows into the borehole (Morin et al., 1997). Thus, EC profiles in RN 17437 and RN 17536 would appear to indicate the existence of high permeability zones, with a spacing of 20 – 50 m. The increasing EC with depth in the borehole, also suggests that EC increases with depth within the aquifer. It is noteworthy, though, that such step-increases are not observed in all profiles (e.g., RN 17391; Figure 34).

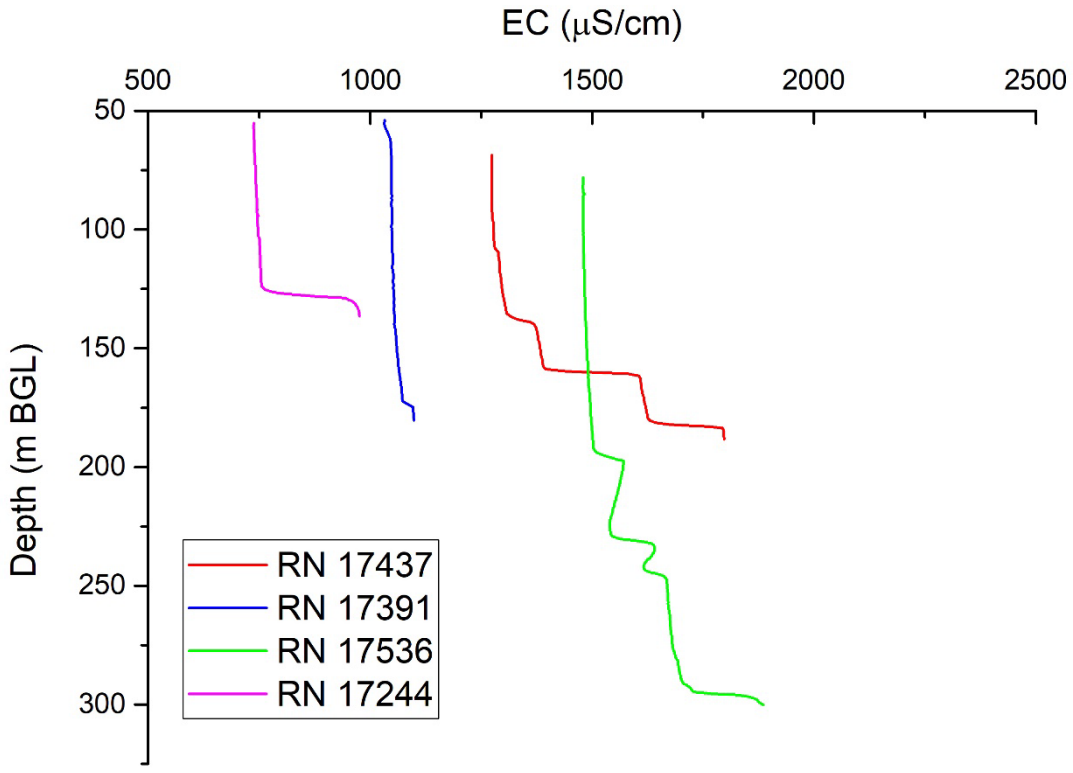

Figure 34. Electrical conductivity (specific conductance) logger data versus depth for four bores within the Rocky Hill area. Step-like increases in electrical conductivity with depth may indicate the location of preferential flow zones.

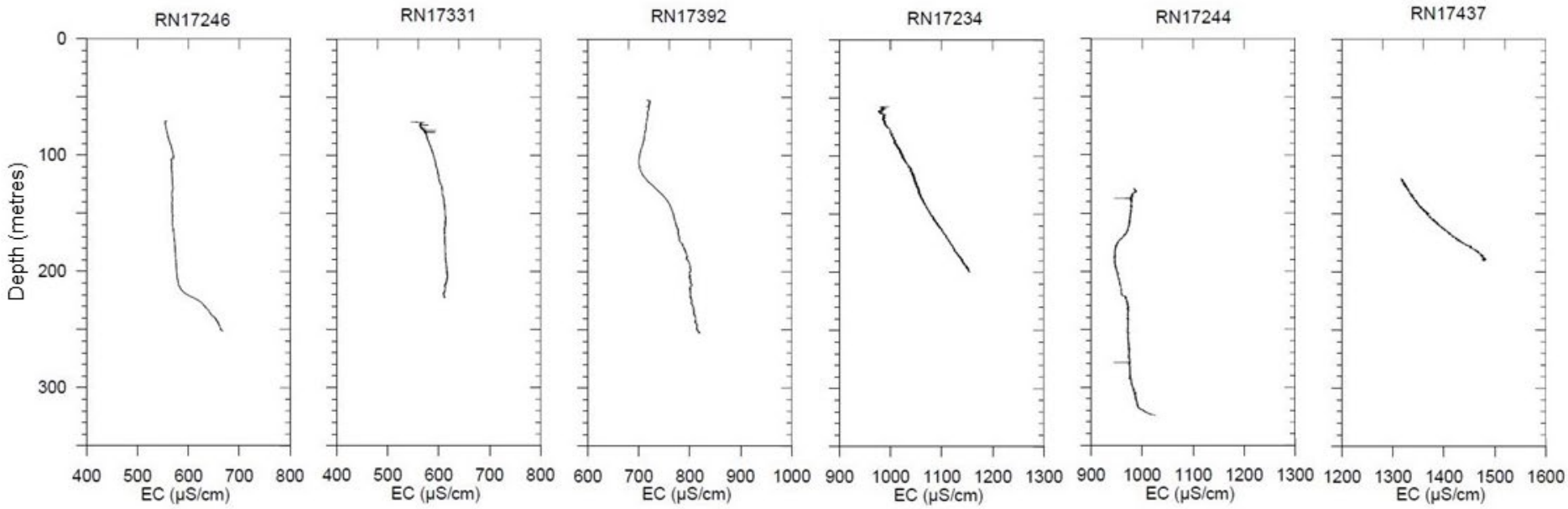

Figure 35. Fluid resistivity logs from six bores south and southeast of the proposed Rocky Hill Borefield. From Read and Paul (2000).

Read and Paul (2000) also present fluid resistivity logs for six bores and salinity data obtained on samples airlifted during drilling of these same bores (Figure 35). Four of the six bores presented show significant increases in salinity with depth. All these bores are south or southeast of the proposed Rocky Hill borefield. Also, since the fluid resistivity logs measure electrical properties of water within the bore, they can be affected by flow within the open hole. The dates on which the resistivity logs were obtained are not specified in the reports, but it is likely that they were obtained soon after drilling the wells. Mixing of water within the well during the drilling process might contribute to the relatively smooth resistivity profiles observed, and the lack of distinct and discrete step-increases, such as those shown in Figure 34.

Comparison of TDS and total depth data for bores used to construct the regional salinity map (Figure 30) does not show a clear increase or decrease in salinity with depth (Figure 36), although salinity of shallow groundwater (< 150 m bgl) appears to be more variable than samples from deeper within the aquifer. Similarly, airlifted samples collected during drilling of RN 19381, and samples collected from completed piezometers at Site 1 and Site 2 show little variation in electrical conductivity with depth (Figure 37). Aerial electrical conductivity data also shows no evidence of a significant increase in electrical conductivity with depth in the area of the proposed borefield (Figure 38).

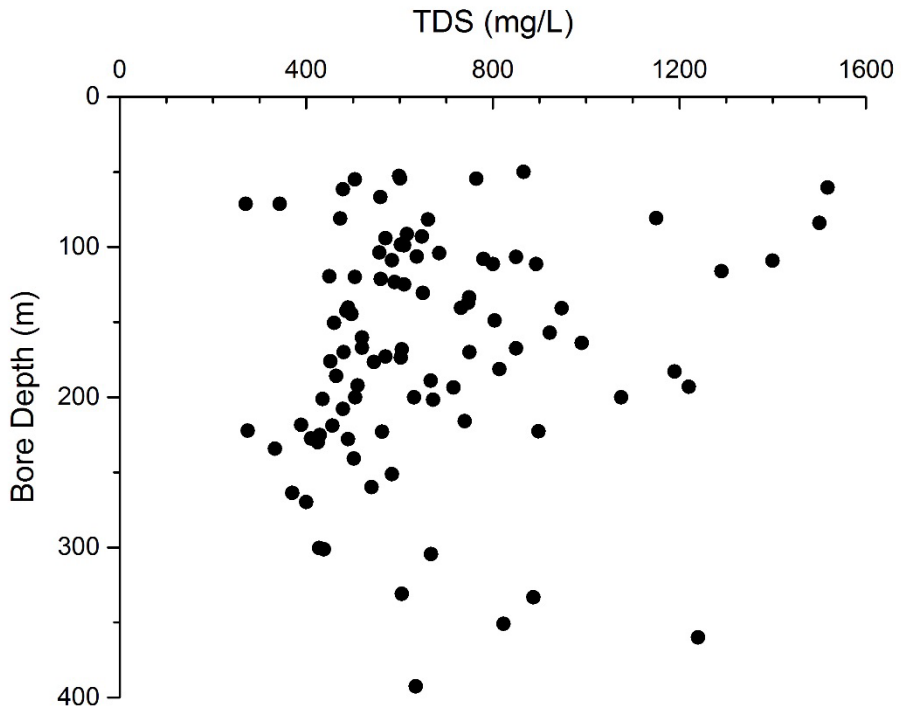

Figure 36. Total dissolved salts measured on bores within the Rocky Hill region plotted against total bore depth. Data for RN 10722 (2030 mg/L; 119 m depth), RN 11589 (4170 mg/L; 36.6 m depth) and RN 17394 (7650 mg/L; 144.6 m depth) are not shown.

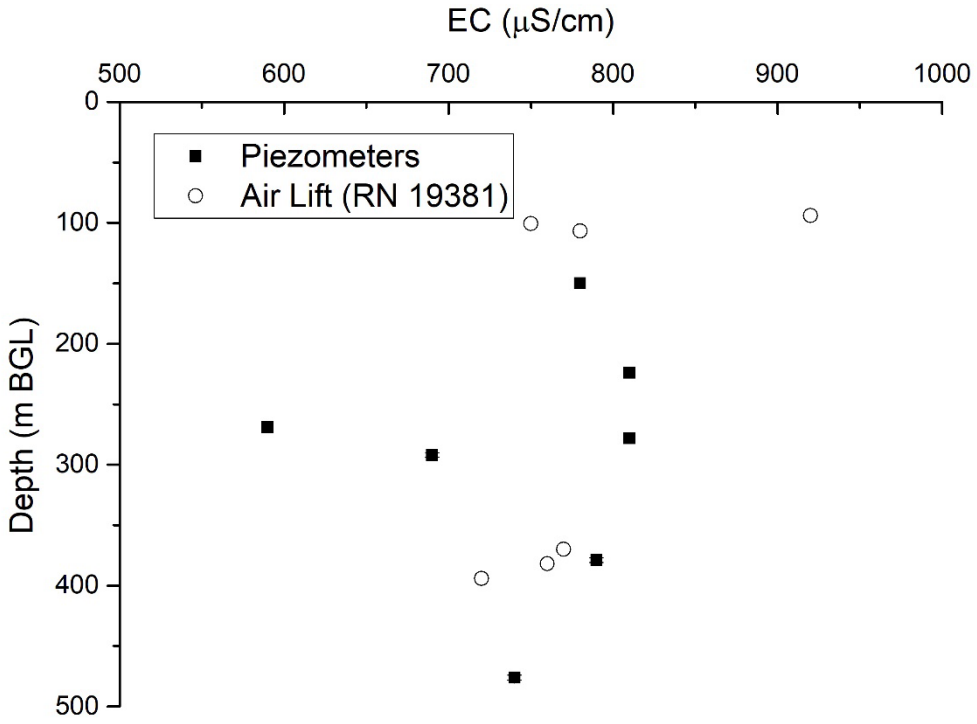

Figure 37. Vertical profile of electrical conductivity on pumped samples from piezometers at Site 1 and Site 2 and airlifted samples from RN 19381. Data from piezometers RN 19382, RN 19383-2 and RN 19383-1 is not shown, due to suspected contamination with drilling fluids (see Table 2).

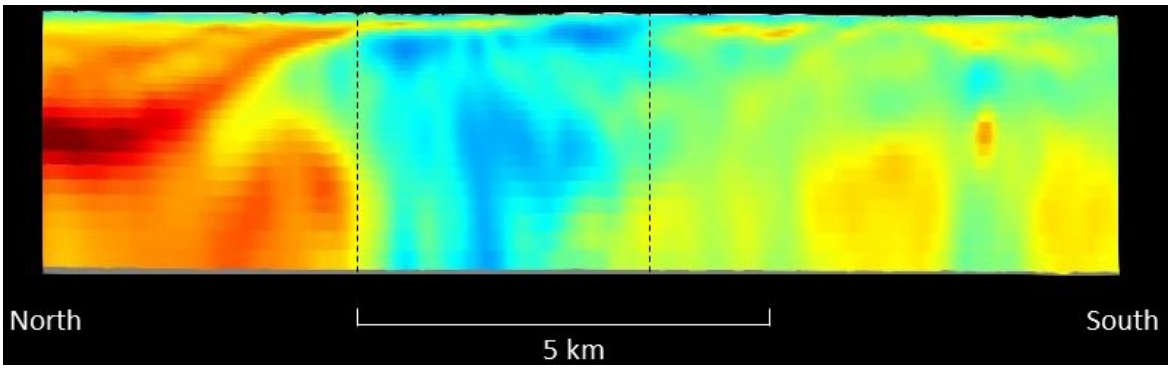

Figure 38. Electrical conductivity pseudo-section from inversion of aerial electromagnetic survey results for an approximate north-south flight line (line 113401) through NT Portion 4704. The vertical extent of the pseudo-section is approximately 500 m, and its approximate location is depicted in Figure 30. Broken black lines delineate the approximate boundaries of NT Portion 4704. Blue colours in the image indicate low electrical conductivity and orange and red colours indicate high electrical conductivity values. https://portal.ga.gov.au/

Thus, although several bores show evidence of increasing salinity with depth, data is somewhat contradictory. There is certainly no evidence of increasing salinity within the upper 400 – 500 m of aquifer within NT Portion 4704.

6.3 Volume of Fresh Water

The volume of usable groundwater stored within the Rocky Hill aquifers can be calculated from interpolation of the geological extent of the main aquifers, estimates of specific yield, the current water table surface and interpolated salinity distribution. For the purposes of this calculation, the western edge of the area has been taken as longitude line 133° 57', which is the boundary between the Rocky Hill – Ooraminna and Roe Creek management zones in the Alice Springs Water Allocation Plan (DLRM, 2016). It is also assumed that salinity does not vary with depth, and so the salinity distribution depicted in Figure 30 is assumed to be representative of the entire aquifer thickness.

The results show an extractable volume of 2 300 GL of low salinity groundwater (< 500 mg/L) to 300 m depth in the Mereenie and Hermannsburg aquifers (Table 5). Considerable additional volume is contained in the Pacoota and Goyder/Shannon aquifers; almost most of this is located below 400 m depth. The extractable volume more than doubles to 5 200 GL if groundwater of TDS between 500 – 600 mg/L is also included. Australian Drinking Water Guidelines (NHMRC, NRMMC,2011) recommend a maximum TDS value of 600 mg/L, whereas Alice Springs Water Allocation Plan refers to a value of 1000 mg/L. The extractable volume of groundwater with TDS less than 1000 mg/L in the Mereenie and Hermannsburg aquifers to 300 m depth is estimated to be 10 700 GL.

Table 5. Volume of groundwater stored in the Rocky Hill aquifers below various salinity cut-off values. A specific yield of 0.15 has been used for the Mereenie and Hermannsburg aquifers, whereas 0.07 has been used for the Pacoota and Goyder/Shannon aquifers.

	Depth Range	Volume (GL)		
		< 500 mg/L	< 600 mg/L	< 1000 mg/L
Mereenie and Hermannsburg	Entire Thickness	3 500	8 100	16 900
	< 400 m bgl	2 900	6 700	14 000
	< 300 m bgl	2 300	5 200	10 700
Pacoota and Goyder/Shannon	Entire Thickness	2 000	7 200	18 300
	< 400 m bgl	300	1 200	4 200
	< 300 m bgl	100	600	2 700
TOTAL	Entire Thickness	6 500	15 300	35 200
	< 400 m bgl	3 200	7 900	18 200
	< 300 m bgl	2 400	5 800	13 400

Read and Paul (2002) estimated the volume of extractable groundwater having TDS less than 1000 mg/L to 300 m as 2677 GL. This is approximately 25% of the value estimated in the current report. The major difference seems to be the omission of groundwater stored in the Hermannsburg aquifers from the Read and Paul (2002) figure. The higher value of specific yield used in the current report (0.15 for the Mereenie and Hermannsburg aquifers, compared to 0.1 used by Read and Paul, 2002) also explains some of the difference. However, specific yield remains somewhat uncertain, and based on core samples from a small number of bores. Jolly et al. (2005) present a total volume of 3750 GL, which is the figure given by Read and Paul for the Mereenie and Pacoota aquifers to 300 m depth, but still excludes the Hermannsburg aquifer.

7. GROUNDWATER GEOCHEMISTRY

Major ion chemistry data is available for several bores within the Rocky Hill region. There have also been a number of studies (Calf, 1978; Jacobson et al., 1989; Cresswell et al., 1999; Hostetler, 2000; Kulongoski et al., 2007) that have measured the isotope composition of groundwater samples from the Amadeus Basin, including a number of samples from the Roe Creek and Rocky Hill regions. Interpretation of this data is described in the following sections.

7.1 Major Ion Chemistry

The major ion geochemistry of groundwater from the Rocky Hill region is dominated by Ca, Na, HCO_3 and Cl ions. Anion composition in low TDS groundwater is dominated by bicarbonate, whereas higher TDS groundwater is dominated by chloride. Molar fractions of HCO_3 (compared to other anions) typically exceed 70% for TDS values less than 400 mg/L, with molar fractions of chloride typically exceeding 40% for TDS values greater than 600 mg/L and reaching almost 80% for the most saline samples. SO_4, Mg, Na and K all show positive correlations with chloride, whereas Ca and HCO_3 do not (Figure 39). This is evidence that groundwaters are close to saturation with respect to calcite. Ion exchange processes within the groundwater also result in loss of calcium and addition of other cations. The molar fraction of Na (compared to other cations) thus increases with increasing TDS, while that of Ca decreases. While SO_4 generally increases with increasing chloride concentration, some samples with low chloride concentrations also have high sulphate concentrations. In general, the highest molar SO_4/Cl ratios are restricted to the northern part of the region, and probably related to the geological source rock.

Read and Paul (2000, 2002) observed an area of high HCO_3/Cl ratios centred in the southwest of the proposed Rocky Hill borefield, approximately coinciding with the area of fresh groundwater. Molar ratios in excess of two were measured across a large area extending from Undoolya Rocky Hill Agricultural Block through most of NT Portion 4704, and along Roe Creek as far as Alice Springs airport, and as high as five in some parts of this region. They argued that this was evidence of young water and preferential recharge of water high in HCO_3. As the water moves away from this recharge area increases in major ions (including chloride) occur, resulting in higher TDS and lower HCO_3/Cl ratios. For comparison, Williams and Siebert (1963) measured a HCO_3/Cl ratio of 5.4 for a sample of Todd River surface water flow collected in October 1961, supporting the conclusion of Read and Paul (2000, 2002).

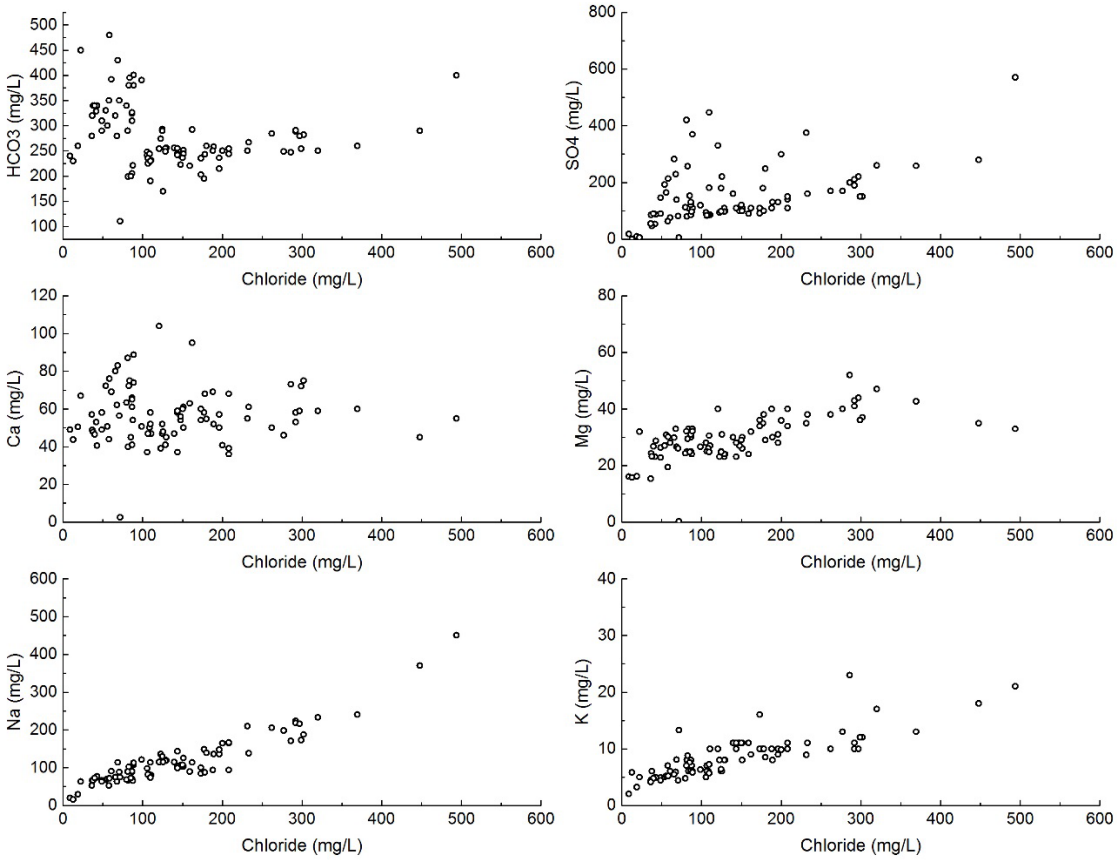

Figure 39. Plots of major ion concentrations versus chloride concentrations in groundwater. Major ions chemistry. Data is derived from Read and Paul (2000, 2002) and from sampling conducted in 2016 and 2017. Data is not shown for chloride concentrations above 600 mg/L.

Chloride concentration ranges between 9 and 3080 mg/L, with a mean of 250 mg/L and median of 100 mg/L (Figure 40). If values in excess of 1000 mg/L are excluded, then the mean concentration of the remaining samples is 150 mg/L. The mean chloride concentration for samples with less than 500 mg/L TDS is 65 mg/L. For comparison, the chloride concentration of Todd River flow has been measured at 5 mg/L (Williams and Siebert, 1963).

Chloride concentrations in groundwater have been commonly used for estimating rates of groundwater recharge, particularly in arid and semi-arid areas, using a chloride mass balance approach. The chloride mass balance is usually expressed:

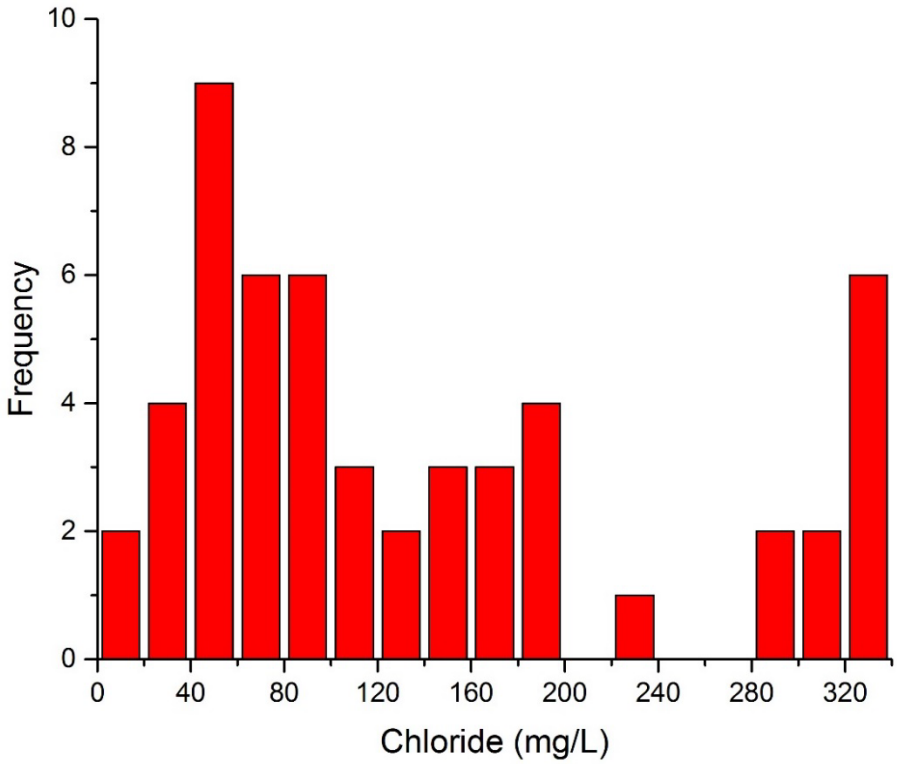

Figure 40. Histogram of chloride concentration measured on groundwater from 53 bores in the Rocky Hill area. (The last column indicates values above 320 mg/L.) Based on data in Calf (1978), Jacobson et al. (1989), Cresswell et al. (1999), Kulongoski et al. (2007), Read and Paul (2000, 2002) and more recent sampling in 2016 and 2017.

$$C_P P = C_R R \tag{4}$$

where C_p is the chloride concentration in precipitation, P is the mean annual precipitation rate, C_R is the chloride concentration in groundwater recharge, and R is the mean annual recharge rate. The equation assumes steady state conditions, and that chloride is sourced only from precipitation and dryfall and is not derived from weathering processes within the catchment (Scanlon et al., 2002). It also assumes that chloride concentrations in groundwater have not been elevated by direct evaporation from groundwater (i.e., in salt lakes).

The chloride mass balance method is usually applied to estimate diffuse rates of recharge but can also be applied to estimate recharge by other processes, if groundwater recharge is the only process by which salt can leave the catchment. We can re-write the chloride mass balance as:

$$R_t = \frac{C_P P A_t f}{C_R} \tag{5}$$

where R_t is the total recharge through Todd River floodouts at Rocky Hill, A_t is the total catchment area upstream of this point, and f is the fraction of chloride fallout that leaves the catchment as groundwater recharge in the Rocky Hill area. If significant recharge occurs upstream of Rocky Hill, then f will be less than one. However, assuming f=1 gives a maximum value for recharge.

The chloride concentration in rainfall in the Alice Springs area was estimated from samples collected between 1957 and 1962 (Hutton, 1983) and between 1991 and 1993 (Keywood et al., 1997). The earlier study measured a mean chloride concentration in rainfall of 0.9 mg/L, while the later study measured a mean chloride concentration of 0.25 mg/L. Based on these studies, we assume a mean chloride in rainfall in the Rocky Hill region of approximately 0.5 mg/L. The catchment area upstream of the gauging station on the Todd River at Rocky Hill is 2500 km^2. Assuming a mean chloride concentration in groundwater of 150 mg/L thus gives a maximum recharge of 2083 ML/y. Assuming a floodout area of 50 km^2, then gives an equivalent recharge rate of 40 mm/y. Distributed across the entire region (approximately 500 km^2) is this equivalent to a mean recharge rate of approximately 4 mm/y.

7.2 ^{18}O and ^{2}H

Variations in δ^2H and δ^{18}O values in natural waters arise mostly from isotopic fractionation during evaporation and condensation processes, whereby the heavy isotopes of water preferentially remain in the liquid phase during evaporation or pass into the liquid phase during condensation. They are therefore useful indicators of groundwater recharge processes and rainfall patterns. The mean amount-weighted δ^{18}O and δ^2H ratios for Alice Springs rainfall are -4.5 and -24.3 ‰, respectively (IAEA/WMO, 2018). Wetter months are usually associated with more depleted (more negative) ^{2}H and ^{18}O compositions, and comparison with groundwater data suggests that recharge usually occurs during months with more than 60 mm of rainfall (Figure 41). Months with more than 60 mm rainfall also corresponds with periods of highest flows in the Todd River and in Roe Creek.

Figure 42 compares the stable isotopic composition (^{2}H and ^{18}O) of groundwater from the Roe Creek and Rocky Hill areas with those from other areas within the eastern Amadeus Basin. For the purpose of this analysis, the Roe Creek area is defined by the rectangle bounded by eastings of 375000 and 385000, and northings of 7365000 and 7369000. The Rocky Hill area is defined by the rectangle bounded by eastings of 388000 and 425000, and northings of 7347000 and 7366000. Other samples are from areas further west and south. Samples from the Roe Creek and Rocky Hill areas are more depleted than other samples, with Rocky Hill samples (including those from Sites 1 and 2) amongst the most depleted. A single ^{18}O value of -10.9 ‰ for the Todd River is reported by Calf (1978), but the date and

location of sampling is not specified. This value is more depleted than all the groundwater ^{18}O values.

All the ^{2}H and ^{18}O data shown in Figure 42 are derived from groundwater with TDS values less than 2500 mg/L. The only data available from the area of high salinity groundwater in the northeast of the region is a single ^{18}O value of -7.6 ‰ that was obtained from water extracted from a core sample collected less than 1 m below the water table during drilling of RN 18334. This sample had a chloride concentration of 4700 mg/L. The lack of apparent enrichment in ^{18}O on this sample suggests that the saline groundwater in the extreme east of the region is not due to evaporation directly from the groundwater.

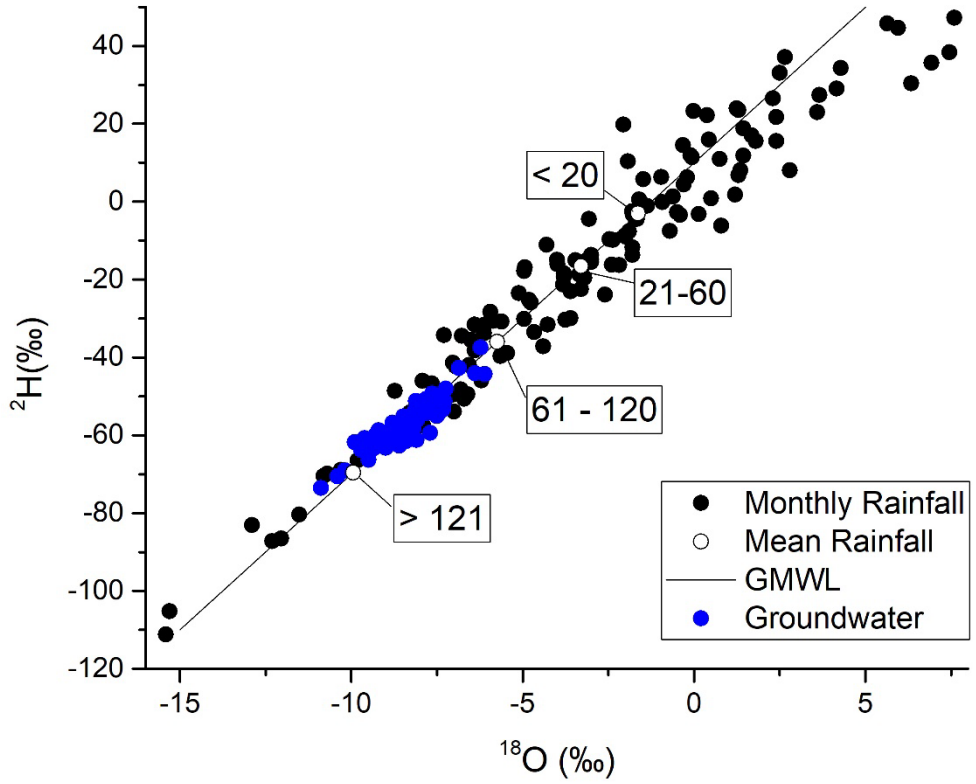

Figure 41. Comparison between ^{18}O and ^{2}H composition of groundwater from eastern Amadeus Basin with Alice Springs rainfall. Alice Springs rainfall data represents mean amount-weighted monthly values between 1962 and 1987 (IAEA data). The Global Meteoric Water Line (GMWL), which reflects the mean composition of global rainfall is also shown. Open circles on this line reflect the mean amount-weighted ^{2}H composition of Alice Springs rainfall, for months with total rainfall volumes of < 20, 21 –60, 61 – 120, and > 121 mm. Groundwater data is derived from Calf (1978), Jacobson et al. (1989), Cresswell et al. (1999), and Kulongoski et al. (2007), and presented in Appendix 4.

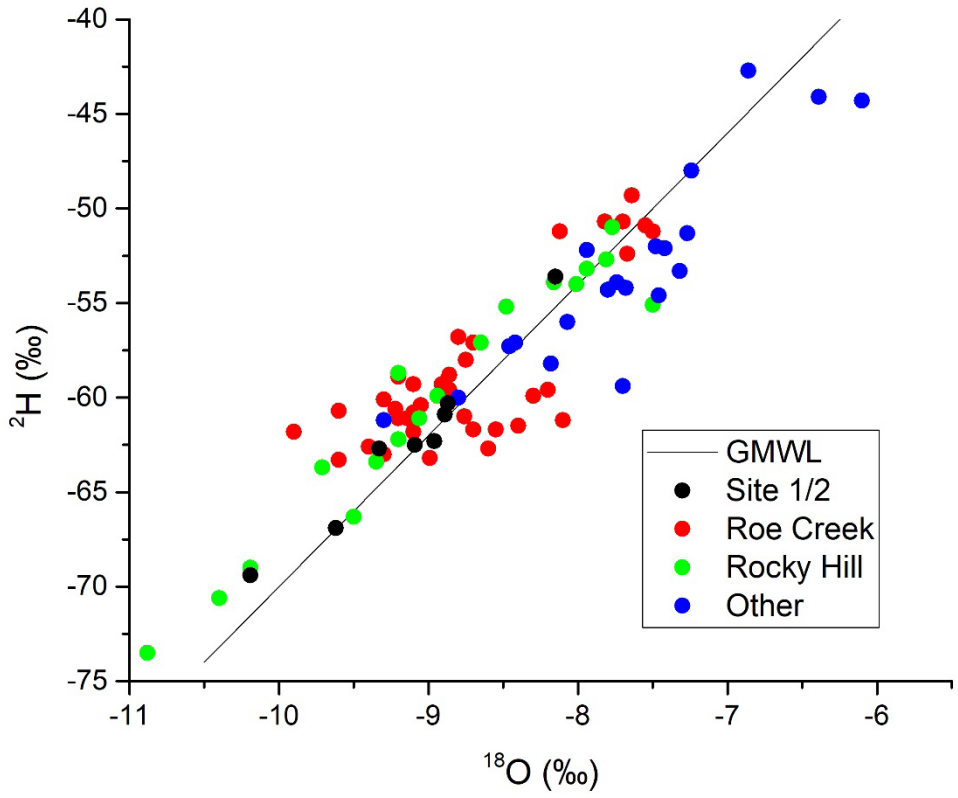

Figure 42. ^{18}O versus ^{2}H plot for groundwater samples from the eastern Amadeus Basin. GMWL refers to the Global Meteoric Water Line. The two most depleted values are repeat samplings from RN 10922. Data is from Calf (1978), Jacobson et al. (1989), Cresswell et al. (1999) and Kulongoski et al. (2007).

7.3 ^{14}C and ^{13}C

$\delta^{13}C$ values in groundwater from arid landscapes can provide information on recharge processes. Although atmospheric CO_2 has a $\delta^{13}C$ composition of approximately -7 ‰, this is altered by photosynthetic uptake of CO_2 within the soil zone. The $\delta^{13}C$ value of soil CO_2 in ecosystems dominated by C3 plants is typically between -24 and -30 ‰. However, C4 plants are more common in arid systems, and usually associated with $\delta^{13}C$ values of -10 to -16 ‰ (i.e., spinifex with $\delta^{13}C$ of -14.5 ‰; Cook and Dawes-Gromadzki, 2005). Due to an isotopic fractionation factor of approximately +8 ‰ between $^{13}CO_2$ in unsaturated zone gas and ^{13}C in DIC in groundwater (Clark and Fritz, 1997), water in equilibrium with soil CO_2 would be expected to have $\delta^{13}C$ values in TDIC of -16 to -22 ‰ in landscapes dominated by C3 plants and -2 to -8 ‰ in C4-dominated systems. Vertical profiles of $^{13}CO_2$ in unsaturated zone beneath open woodlands of the Ti Tree Basin showed values ranging from -13.5 to -16.8 ‰ (Wood et al., 2014), consistent with respiration from C4 grasses. The ^{13}C composition of DIC in underlying groundwater mostly ranged from -5.5 to -8.5 ‰, consistent with inputs from

an unsaturated zone dominated by C4 grasses. However, $\delta^{13}C$ values in the Ti Tree Basin were more depleted in groundwater close to the Woodforde River (-9 to -12 ‰) and in the perched aquifer beneath the river (-16 to -17 ‰) (Wood et al., 2016). These values likely represent inputs from unsaturated zone gas from a riparian zone where a mixture of grasses and C3 trees are present (Wood et al., 2016).

$\delta^{13}C$ values in groundwater from the Rocky Hill and Roe Creek areas are mostly -9 to -12 ‰, with values from other parts of the eastern Amadeus Basin mostly -6 to – 10 ‰ (Figure 43). The latter are similar to values from most of the Ti Tree Basin and consistent with diffuse recharge through thick unsaturated zones and vegetation dominated by C4 grasses. $\delta^{13}C$ values from Rocky Hill and Roe Creek areas are similar to values in groundwater near the Woodforde River in the Ti Tree Basin, and probably indicate recharge from the Todd River and from Roe Creek, where there will be a mixture of C3 and C4 plants.

Following recharge, $\delta^{13}C$ and ^{14}C activities can be affected by chemical reactions involving DIC that might occur in the saturated zone, usually leading to more enriched ^{13}C values and lower ^{14}C activities. Values of $\delta^{13}C$ of carbonates obtained from drill cuttings of bores from the Rocky Hill region range between -2.4 and -7.8 ‰, with a mean value of -6.3 ‰ (Calf, 1978). A correlation between ^{14}C activity and ^{13}C is apparent for groundwater samples from the eastern Amadeus Basin (Figure 43), which might indicate addition of old carbonate from aquifer materials to groundwater. However, there is no relationship between ^{13}C value and DIC concentration for groundwater samples, suggesting that weathering processes do not dominate the DIC composition. Similar conclusions were reached for the Ti Tree Basin, where samples obtained from nested piezometers showed little variation in $\delta^{13}C$ with depth.

Calculating groundwater ages based on ^{14}C activities requires assumptions concerning initial ^{14}C activities in groundwater recharge, and reactions that might occur in the saturated zone that would affect carbonate concentrations. Work in the Ti Tree Basin observed low ^{14}C activities above the water table where the unsaturated zone is thick, probably due to dissolution-precipitation of calcite releasing CO_2 with a low ^{14}C activity (Walvoord et al., 2005; Gillon et al., 2009; Wood et al., 2014). For the purpose of calculating groundwater ages, we assume an initial ^{14}C activity of 60 pmC, which is consistent with the Ti Tree Basin studies that measured ^{14}C activities in soil gas close to the water table of 55-85 pmC (Wood et al., 2014), and is the approximate upper limit of ^{14}C measured in the Roe Creek and Rocky Hill areas (Figure 43). The groundwater age is then calculated using

$$t = -\lambda^{-1} ln\left(\frac{c}{c_0}\right) \quad (6)$$

where c and c_0 are the measured and initial ^{14}C concentrations, and $\lambda = 1.21 \times 10^{-4}$ y^{-1} is the decay constant. Groundwater ages calculated in this way range from modern to 25,000 years, with a mean age of approximately 6700 years for both Rocky Hill and Roe Creek regions.

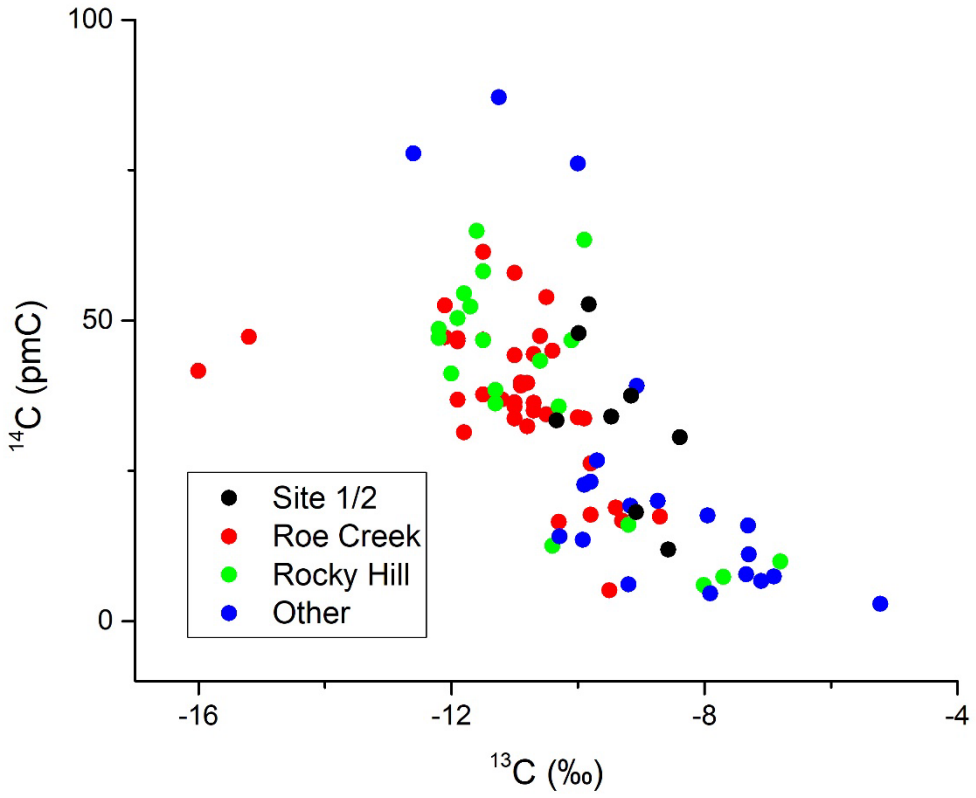

Figure 43. Comparison of ^{13}C and ^{14}C data on groundwater samples from the eastern Amadeus Basin.

There is an apparent relationship between ^{14}C activity and ^{18}O value (Figure 44), with lower ^{14}C values (older groundwater) corresponding with more enriched ^{18}O values (i.e., closer to zero), and higher ^{14}C values corresponding with more depleted (i.e., more negative) ^{18}O values. A similar relationship has been identified for groundwater from the Finke River region and explained in terms of a change in recharge processes over time (Love et al., 2013). Other factors being equal, the rainfall will be more depleted in heavy isotopes (lower $\delta^{18}O$ and $\delta^{2}H$ values) during heavy rainstorms than during lighter storm events (Ingraham, 1998). It is therefore possible that rainfall under the current climate is restricted to very high intensity events, whereas in the past recharge was not restricted to such high intensity rainfall events. A shift in seasonality of recharge (from summer-dominated to winter-dominated recharge) could also be a factor.

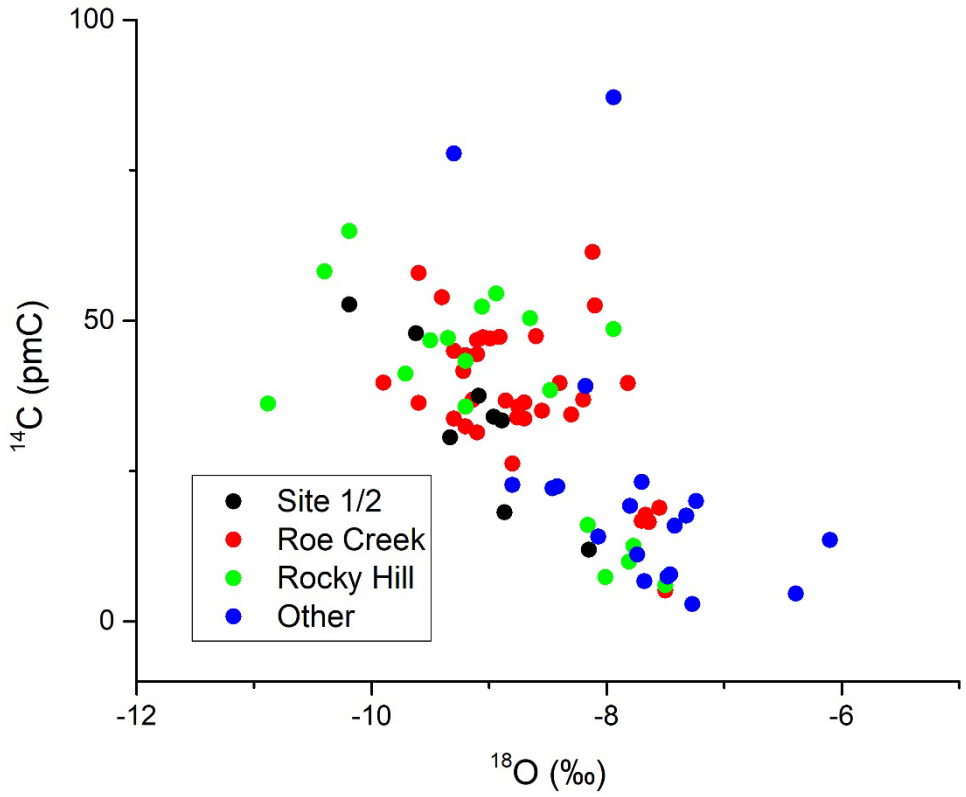

Figure 44. Comparison of ^{14}C and ^{18}O data on groundwater samples from the eastern Amadeus Basin.

In simple unconfined aquifers, aquifer recharge rates can sometimes be determined from vertical profiles of groundwater age (Cook et al., 1995). At Rocky Hill, past well construction practices did not effectively isolate different aquifer depths, and so it is difficult to determine the depths represented by samples obtained from these wells. However, the piezometer nests at Site 1 and Site 2 were installed with short screens that were isolated with bentonite. For these piezometers, ^{14}C activities decrease (and hence groundwater age increases) with depth (Figure 45). Curves representing expected ^{14}C activities assuming vertical flow at velocities of 0.02 and 0.1 m/y bound the measured values. Assuming a porosity of 0.2, these vertical water velocities are equivalent to recharge rates of 0.004 and 0.02 m/y, respectively. We therefore infer a mean recharge rate of between 4 and 20 mm/y over the Holocene period. This is generally consistent with recharge estimates based on the chloride mass balance (Section 7.1, above).

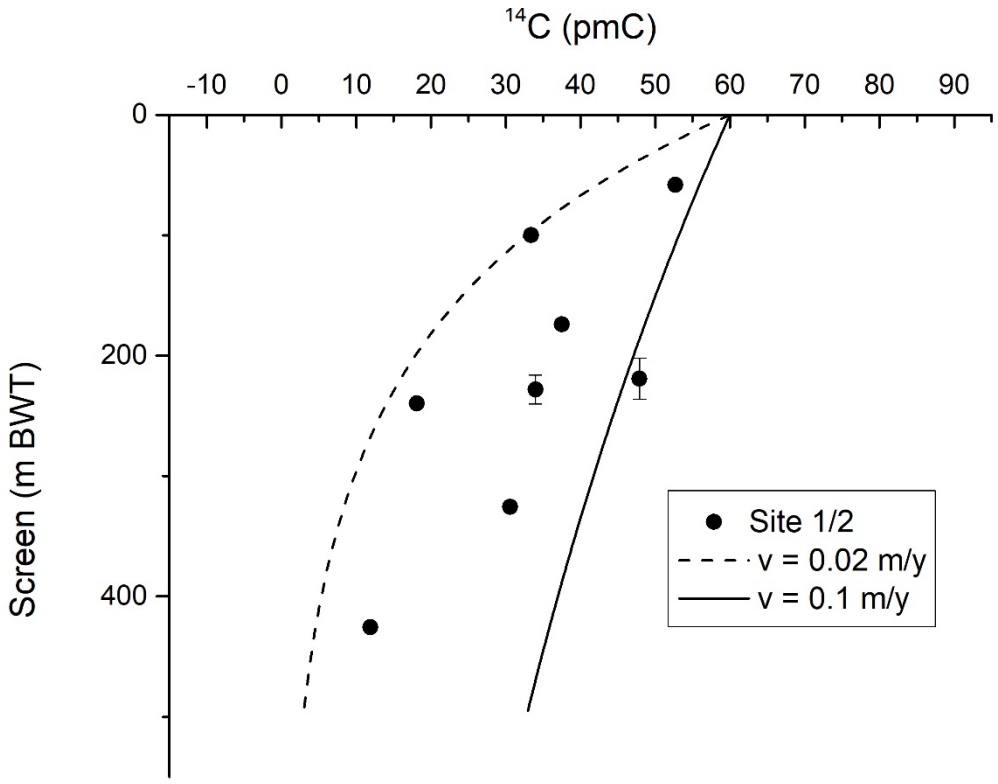

Figure 45. Measured ^{14}C activities at Sites 1 and 2 plotted versus depth below the water table. Vertical error bars denote the length of the well screens, although for most points the well screen is too small to be shown on the figure. Curved lines depict expected ^{14}C activities with depth based on an initial activity of 60 pmC and vertical water velocities between 0.02 and 0.1 m/y.

7.4 ^{36}Cl and ^{3}H

Dating of groundwater using the ^{36}Cl technique is somewhat analogous to ^{14}C, and as all sources and sinks of ^{36}Cl should be accounted for before determining age. Use of ^{36}Cl is further complicated by the fact that the ratio of radioactive ^{36}Cl to stable Cl in rainfall varies spatially due to latitude and continental effects (Phillips, 2000). Thus, some local knowledge of the likely $^{36}Cl/Cl$ ratio in precipitation is required so groundwater age can be estimated from the amount of observed radioactive decay (Davis et al., 1998). $^{36}Cl/Cl$ ratios less than the rainfall value indicate radioactive decay and hence old groundwater.

$^{36}Cl/Cl$ ratios in the eastern Amadeus Basin range between 43 x 10^{-15} and 200 x 10^{-15} (Appendix 4), and the relationship between $^{36}Cl/Cl$ ratio and ^{14}C activity in the eastern Amadeus Basin displays a very large amount of scatter (Figure 46). The current $^{36}Cl/Cl$ ratio in rainfall in central Australia is estimated to be approximately 350 x 10^{-15} (i.e., one ^{36}Cl atom for every 3 x 10^{17} ^{35}Cl atoms). This is based on an estimated ^{36}Cl fallout of 11 atoms m^{-2} s^{-1}

(Keywood et al., 1998) and chloride fallout of 0.6 kg ha^{-1} y^{-1} (Keywood et al., 1997). However, uncertainty in the concentration of chloride in rainfall (see Section 7.1), and hence in the chloride fallout, means that the $^{36}Cl/Cl$ ratio in modern rainfall could be as low as 200 x 10^{-15}. ^{36}Cl has a half-life of approximately 301,000 years (λ = 2.3 x 10^{-6} in Equation 6), and so low values of $^{36}Cl/Cl$ are indicative of very old water or mixing with old chloride. The solid line in Figure 46 indicates the expected relationship between $^{36}Cl/Cl$ ratio and ^{14}C activity for groundwater, based on initial values of 350 x 10^{-15} for $^{36}Cl/Cl$ and 100 pmC for ^{14}C, and the respective decay rates of these isotopes. The broken line shows the same relationship for an initial $^{36}Cl/Cl$ ratio of 200 x 10^{-15}. Because the half-life of ^{14}C is much shorter than that of ^{36}Cl, groundwater that is between 50,000 and 300,000 years old would be expected to have high $^{36}Cl/Cl$ ratios (between 100 and 175, depending on the assumed initial value), but negligible ^{14}C. The shaded area in Figure 46 denotes possible ^{14}C and $^{36}Cl/Cl$ values that could be derived from mixing of groundwater of different ages, assuming an initial $^{36}Cl/Cl$ value of 200, and assuming no additional sources of ^{36}Cl. Most of the data fall within the mixing zone, indicating that groundwater samples represent mixing between young and old groundwater. Interestingly, the samples from the piezometer nests at Site 1 and Site 2 fall close to the broken line, indicating that they have undergone less mixing with very old water than most of the other samples. This likely reflects the well construction of these piezometers, that isolated individual zones to minimise mixing associated with long or poorly isolated well screens.

Tritium data are available for 24 wells from the eastern Amadeus Basin, although only four samples were above the detection limit of 0.3 TU. Two of these were measured to be 0.4 TU, which is very close to the detection limit, and so may not be significant. The highest value, 3.3 TU, was measured on a well south of Rocky Hill (RN 17246) which had relatively low ^{14}C and $^{36}Cl/Cl$ values (48.6 pmC and 124, respectively). This suggests that the ^{3}H value may be in error. One well located in the Alice Springs Town Basin was measured at 3.5 TU, and had the highest ^{14}C activity of any sample, suggesting very young water.

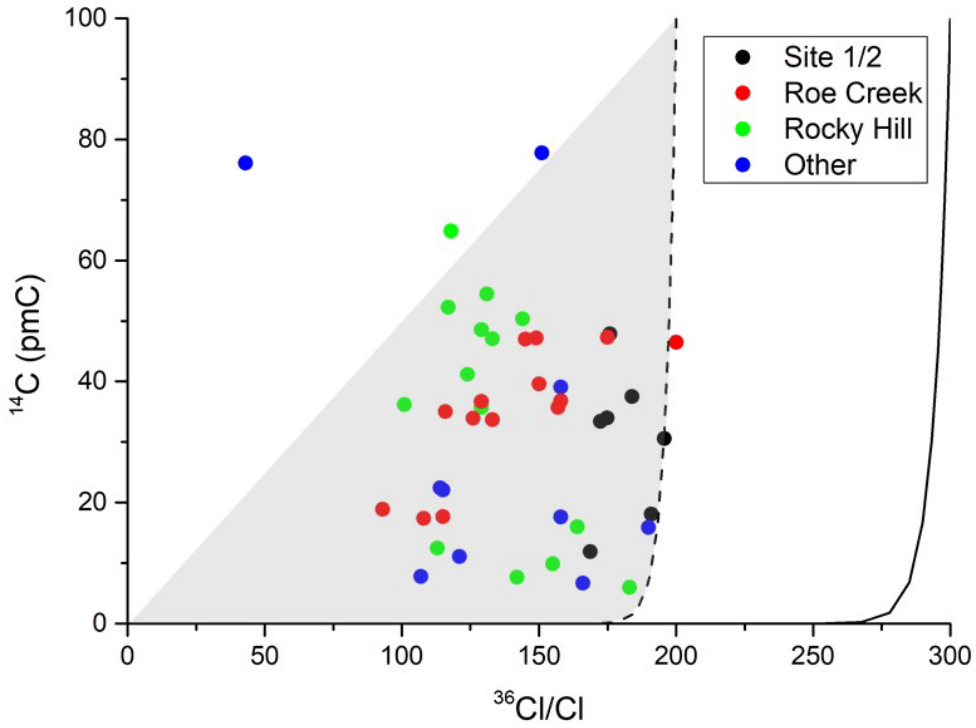

Figure 46. Relationship between ^{36}Cl/Cl ratio and ^{14}C activity on groundwater samples from the eastern Amadeus Basin. The solid line depicts the ratio that would be expected to occur in groundwater assuming initial values of 350 x 10^{-15} for ^{36}Cl/Cl and 100 pmC for ^{14}C. The broken line shows the same relationship for an initial ^{36}Cl/Cl ratio of 200 x 10^{-15}. Assuming an initial ^{36}Cl/Cl ratio of 200 x 10^{-15}, the shaded area indicates concentrations that might arise due to mixing of groundwater of different ages. Note that data from piezometers RN19833-1 and RN19833-2 is believed to be contaminated by KCl added to drilling mud, and so is not included.

8. CONCEPTUAL MODEL

Prior to development of the Roe Creek borefield, groundwater in the Rocky Hill area flowed from west to east. Groundwater recharge occurred in the vicinity of NT Portion 4704, and east of this area, associated with the flood-out areas of Todd River and Roe Creek, and from local runoff from the eastern McDonnell Ranges. Groundwater discharge occurred in the east, although the location and mechanism of groundwater discharge has not been clearly identified. The increase in salinity currently observed in this area may suggest groundwater discharge by vegetation, which may have occurred at a higher rate in the past, when the water table in this area may have been shallower. The land surface falls from west to east, and so water tables are shallower to the east. Groundwater use by vegetation in this area has been suggested from soil profile data (Cook et al., 2008), although it is likely to occur at a relatively low rate under current conditions due to the large depth to the water table. There is no evidence of local enrichment of ^{2}H and ^{18}O in the groundwater, and so the salinity is unlikely to be due to direct evaporation from a shallow water table.

Since commencement of pumping at Roe Creek, the groundwater flow direction has reversed at least as far as 400 000E. Further east, groundwater levels are currently declining at about 0.1 m/y, and this is believed to be a natural phenomenon. It indicates that groundwater discharge is currently greater than groundwater recharge, and that groundwater recharge was probably higher in the past than it is today. Currently, the reduction in aquifer storage in areas not affected by Roe Creek pumping is approximately 3000 – 4000 ML/y. However, in the central part of the region, east of the Roe Creek drawdown, there is very little hydraulic gradient, indicating little groundwater flow. The water table decline probably represents a combination of relaxation in groundwater levels following historically higher recharge rates, and groundwater use by vegetation across the region.

Short-term water table rises have been observed in years with high rainfall, notably in 2000-2001 and 2010-2011. This is despite a deep water table, which would dampen any rise, and thus suggests very high rates of recharge. Water level increases of up to 1 m were observed in Mereenie aquifer bores in the northeast of the area between January 2000 and June 2001 (Figure 25). Using a specific yield of 0.1, Read and Paul (2002) calculated an increase in storage in the aquifer of 9×10^{7} m^{3} (90,000 ML). This was one of only four occasions in which more than 1000 mm were recorded in an 18-month period at Alice Springs airport since records commenced in 1942. Thus, assuming a 1 in 15-year event, this gives recharge volume of 6000 ML/y in this part of the aquifer. However, groundwater samples from these bores have TDS values between 780 and 2030 mg/L, somewhat in contradiction with the high inferred rate of recharge. It is possible that lower TDS water from recent recharge overlies more saline groundwater in this area, and there is some evidence for this in airlift

samples from RN 10722 (Figure 32). Large flows of Todd River also occurred in February and April 2000 and rises in water levels of up to 4 m are observed near the Todd River floodout. However, there are insufficient bores in this area to calculate the size of the groundwater mound, and hence estimate recharge from the magnitude of the water level rise. Water level rises were also observed in 2010/2011 in the northeast of the study area and in bores near the Todd River floodout. Rainfall in the 18-month period from January 2010 – June 2011 was similar to that from January 2000 – June 2001. There is little evidence of rise in water table in the Roe Creek area (south of the airport) at these times. This might be due to the increased water table depth in this area due to the influence of pumping from Roe Creek. Increases in infiltration following large rainfall events are buffered during passage through thick unsaturated zones, so that for the same amount of recharge, the water table rises will be much greater where the water table is shallow. ^{2}H and ^{18}O data are consistent with recharge from episodic creek flows following high intensity rainfall events.

The area of lowest TDS groundwater in the Rocky Hill region coincides with the area immediately downstream of the Todd River and Roe Creek flood-outs and is believed to be predominantly recharged from these two sources. The groundwater HCO_3/Cl ratios in these areas correspond to that measured on the Todd River. $\delta^{13}C$ ratios in groundwater are also consistent with river recharge following large flow events. A chloride mass balance calculation suggests a maximum recharge rate of approximately 2000 ML/y through river recharge over the Holocene period – equivalent to a recharge rate of approximately 40 mm/y in this part of the basin, but a much lower rate (approximately 4 mm/y) when averaged across the entire Rocky Hill region. The ^{14}C data from the newly established piezometer nests within the proposed borefield suggest a recharge rate of 4 – 20 mm/y in this area, which is consistent the chloride mass balance calculation.

The area having < 600 mg/L TDS groundwater is more than 140 km^2. Assuming a depth of 400 m, unsaturated zone thickness of 50 m, and porosity of 0.2, this gives a volume of approximately 10^7 ML. At a recharge rate of 2000 ML/y, this gives a mean residence time of 5,000 years. While this is consistent with ^{14}C data obtained from the piezometer nests, ^{36}Cl data indicates that some of the groundwater is much older – at least several hundred thousand years old. These old groundwaters reflect much lower recharge rates in some parts of the basin. Thus, the relatively young, low salinity groundwater that is recharged beneath the ephemeral creeks sits within a regional aquifer containing much older, more saline groundwater.

9. CONCLUSIONS AND RECOMMENDATIONS

The subsurface geology in the Rocky Hill area (particularly depths and thicknesses of the main aquifers) is not well defined due to absence of deep wells, but recent drilling has confirmed that the main aquifer units extend to at least 475 m within the proposed borefield (NT Portion 4704). Although it is difficult to differentiate between the Mereenie and Hermannsburg units based on drilling records and gamma logs, available evidence suggests that the hydraulic properties of these units are similar. Available data does not show any significant differences in water levels between the different formations, except in the extreme west of the area where water levels are greatly affected by drawdown from Roe Creek pumping.

The aquifer transmissivity in the Rocky Hill area is approximately 10 times lower than in the Roe Creek region. However, there is still some uncertainty regarding hydraulic properties of the main aquifer units, and hence how they will respond to pumping from a future borefield. This uncertainty is due to poor well construction for most of the bores within the region, which contributes to large uncertainties associated with hydraulic conductivity data obtained from pump testing, and the difficulties in constructing and developing new bores within the proposed borefield. Hydraulic conductivity data from core samples significantly underestimates behaviour of the formation at large scales. This may indicate the role of fractures in groundwater flow. Hydraulic conductivities from pumping tests mostly range between 10^{-1} and 10^{2} m/day, with a mean of 4 m/day and median of 1 m/day. However, lower values of 0.24 and 0.32 were estimated for two test production bores installed within the proposed borefield. The large variability may also reflect the importance of preferential flow zones. Porosity and specific yield have been determined on core samples, with porosity of most samples between 0.2 and 0.3. The specific yield of the Hermannsburg and Mereenie sandstones is estimated to be 0.15.

Water level data shows that drawdown associated with pumping from the Roe Creek bore field has reached the edge of the proposed Rocky Hill borefield. Over the last 18 years, water levels near the western boundary of the proposed borefield have been declining at almost 0.2 m/year. Further east, water levels have been declining at approximately 0.1 m/year for the past 30-40 years, and this is attributed to a relaxation of water levels following historic periods of higher recharge.

Increases in salinity during pumping represents one of the largest risks to a new Rocky Hill borefield. The area of lowest TDS groundwater coincides with the area immediately downstream of the Todd River and Roe Creek flood-outs and is believed to be predominantly recharged from these two sources. Groundwater salinity within NT Portion 4704 and the surrounding area is low. Total dissolved solids (TDS) is less than 600 mg/L over

an area of more than 140 km^2, including the whole of NT Portion 4704 as well as areas to the south and east. Recent drilling has confirmed that this good quality water extends to at least 475 m depth. An area of high salinity occurs approximately 2.5 km to the southeast of NT Portion 4704, as indicated by analysis of groundwater samples and aerial electromagnetic survey data.

The extractable volume of good quality groundwater (TDS < 600 mg/L) to 300 m depth in the Mereenie and Hermannsburg aquifers within the Rocky Hill – Ooraminna Management Zone of the Water Allocation Plan is estimated to be 5 200 GL. This increases to 10 700 GL if groundwater with TDS up to 1000 mg/L is considered. Considerable additional volume is contained in the Pacoota and Goyder/Shannon aquifers, although almost most of this is located below 400 m depth.

9.1 Recommendations

Several uncertainties remain, particularly related to the nature of groundwater flow and possible role of preferential pathways, recharge rates and water quality trends. To overcome some of these uncertainties, and improve the hydrogeological understanding, a number of recommendations are proposed:

1) Continue monitoring of water levels across the Rocky Hill region, at six-monthly or more frequent intervals, as this data is critical for assessing water level trends and for groundwater model calibration. It is particularly important that monitoring be continued in bores with long water level records. Some thought should therefore be given to re-establishing monitoring at RN 4458, RN 4461, RN 4463, RN 4464, RN 4693, RN 6504, RN 10722 and RN 10729, as these bores provide valuable long-term data. All bores constructed as part of the 2016 – 2018 drilling program should be added to the monitoring network.

2) Pressure transducers and water level loggers should be installed in bores near the Todd River and Roe Creek floodouts, including bores RN 4458, RN 4461, RN 10722, RN 10729 and RN 17329. These bores show water level responses to high rainfall events, and high-resolution water level data may assist quantification of flood recharge. Further work is needed to better understand recharge processes across the region.

3) Groundwater chemistry should be measured regularly on selected bores. Currently there is a lack of data on temporal trends in water quality, and much of the water

chemistry data is of poor quality. Wells need to be purged prior to collection of groundwater chemistry data. Highest priority would be the bores constructed as part of the 2016 – 2018 drilling program, as these bores effectively isolate different depths within the aquifer. Sampling should occur at least annually.

4) Groundwater levels should be monitored in areas where groundwater is extracted for irrigation, as this is equivalent to a large-scale pumping test. If pumping volumes are known and drawdown can be observed, then this is likely to provide a more reliable estimate of large-scale aquifer properties than is currently available. Drilling additional wells may be necessary so that the drawdown from this pumping can be accurately determined.

5) Investigations should take place to better quantify the role of preferential flow within the aquifer systems. Understanding preferential flow is critical for prediction of contaminant transport, including changes in salinity that may occur during operation of the proposed borefield.

6) Additional studies to examine the connection between the Pacoota Formation and Cainozoic aquifers to the north should be considered. The degree of this connectivity this will affect the northward propagation of pumping from the proposed Rocky Hill borefield and may also impact the risk of contamination of the pumped groundwater from industrial activities in areas overlying the Cainozoic aquifers.

7) The groundwater model should include uncertainty analysis that fully represents the uncertainty of aquifer parameters at Rocky Hill. It should also include scenarios that represent the possible role of preferential flow on water quality and travel times.

10. ACKNOWLEDGMENTS

This work was funded by Power and Water and the Northern Territory Department of Environment and Natural Resources. The authors are indebted to the Northern Territory Department of Environment and Natural Resources drilling and pumping test crews and cartography unit for their contribution to the work. We also wish to thank Geoscience Australia for access to aerial electromagnetic data.

11. REFERENCES

Calf GE (1978) The isotope hydrology of the Mereenie Sandstone aquifer, Alice Springs, Northern Territory, Australia. *J.Hydrol.*, 38, 343-355.

Cook GD and Dawes-Gromadzki TZ (2005) Stable isotope signatures and landscape functioning in banded vegetation in arid-central Australia. *Landscape Ecol.,* 20, 649-660.

Cook PG, O'Grady AP, Wischusen JDH, Duguid A, Fass T and Eamus D (2008) Ecohydrology of sand plain woodlands in central Australia. Report to Natural Heritage Trust (Project number 2005/147).

Cook PG, Knapton A and White N (2017) The potential impact of irrigated agriculture on groundwater quality in the Rocky Hill region, Northern Territory. National Centre for Groundwater Research and Training, Australia.

Cook PG, Solomon DK, Plummer LN, Busenberg E and Schiff SL (1995) Chlorofluorocarbons as tracers of groundwater transport processes in a shallow, silty sand aquifer. *Water Resour. Res.,* 31, 425-434.

Cozens G (2017) Groundwater Salinity Assessment – Proposed Rocky Hill Borefield. Masters Thesis, Flinders University.

Cresswell RG, Jacobson G, Wischusen J and Fifield LK (1999) Ancient groundwater in the Amadeus Basin, Central Australia: evidence from the radio-isotope ^{36}Cl. *J.Hydrol.*, 223, 212-220.

DLRM (2016) Alice Springs Water Allocation Plan 2016-2026. Northern Territory Department of Land Resource Management, Report No. 01/2016A.

Davis SN, Cecil D, Zreda M and Sharma P (1998) Chloride-36 and the initial value problem. *Hydrogeology Journal*, 6, 104-114.

Hutton JT (1983) Soluble ions in rainwater collected near Alice Springs, N.T., and their relation to locally derived atmospheric dust. *Royal Society of South Australia, Transactions*, 107, 138.

Gillon M, Barbecot F, Gibert E, Corcho Alvarado JA, Marlin C, and Massault M. (2009) Open to closed system transition traced through the TDIC isotopic signature at the aquifer recharge stage, implications for groundwater ^{14}C dating. *Geochim. Cosmochim. Acta,* 73, 6488-6501.

Hostetler S (2000) Age of Groundwater, Alice Springs, NT. Bureau of Rural Sciences, November 2000. NT Water resources Branch external report number A1186.

IAEA/WMO (2018). Global Network of Isotopes in Precipitation. The GNIP Database. Accessible at: https://nucleus.iaea.org/wiser

Ingraham NL (1998) Isotopic variations in precipitation. Chapter 3 in C Kendall and JJ McDonnell (ed) *Isotope Tracers in Catchment Hydrology*. Elsevier, Amsterdam, p87-118.

Jacobson G, Calf GE, Jankowski J and McDonald PS (1989) Groundwater chemistry and palaeorecharge in the Amadeus Basin, central Australia. *J.Hydrol.*, 109, 237-266.

Jolly P, Chin D, Prowse G and Jamieson M (1994) Hydrogeology of the Roe Creek borefield. Power and Water Authority, Report No. 10/1994A.

Jolly P, Knapton A, Read R, Paul R and Wischusen J (2005) Volume of groundwater stored in the Mereenie aquifer system in the Pine Gap / Roe Creek / Ooraminna Region. Department of Natural Resources, Environment and the Arts. Natural Resources Division, Report No. 36/2005A.

Northern Territory Government, Keywood MD, Chivas AR, Fifield LK, Cresswell RG and Ayers GP (1997) The accession of chloride to the western half of the Australian continent. *Aust J. Soil Res.,* 35, 1177-1189.

Keywood MD, Fifield LK, Chivas AR and Cresswell RG (1998) Fallout of chlorine 36 to the Earth's surface in the southern hemisphere. *J. Geophys. Res.,* 103(D7), 8281-8286.

Kulongoski JT, Hilton DR, Cresswell RG, Hostetler S and Jacobson G (2007) Helium-4 characteristics of groundwaters from Central Australia: Comparative chronology with chlorine-36 and carbon-14 dating techniques. *J.Hydrol.,* 348, 176-194.

Love AJ, Wohling D, Fulton S, Rpousseau-Gueutin P and de Ritter S (2013) Allocating Water and Maintaining Springs in the Great Artesian Basin, Volume II: Groundwater Recharge, Hydrodynamics and Hydrochemistry of the Western Great Artesian Basin, National Water Commission, Canberra, 238p.

Morin RH, Carleton GB and Poirier S (1997) Fractured-aquifer hydrogeology from geophysical logs: The Passiac Formation, New Jersey. *Ground Water,* 35(2), 328-338.

NHMRC, NRMMC (2011*) Australian Drinking Water Guidelines Paper 6 National Water Quality Management Strategy. National* Health and Medical Research Council, National Resource Management Ministerial Council, Commonwealth of Australia, Canberra. Version 3.5. Updated August 2018.

Phillips FM (2000) Chlorine-36. In Cook P and Herczeg AL (eds) *Environmental Tracers in Subsurface Hydrology*. Kluwer, Boston, p299-348.

Ray A (2019) Southern Stuart Corridor AEM SkyTEM® airborne electromagnetic data. Geoscience Australia, Canberra. http://pid.geoscience.gov.au/dataset/ga/131098.

Read RE and Paul RJ (2000) Rocky Hill – Ooraminna groundwater investigation 1998 & 1999. Northern Territory Department of Lands, Planning and Environment. Report No. 16/1998A (2 volumes).

Read RE and Paul RJ (2002) Rocky Hill – Ooraminna groundwater investigation 2000. Northern Territory Department of Infrastructure, Planning and Environment. Report No. 05/2000A.

Roberts KP (1974) Analysis and prediction of the effects of pumping from the Mereenie Sandstone aquifer – Alice Springs. Water Resources Branch, Dept of N.T. Technical Report WRA74003.

Scanlon BR, Healy RW and Cook PG (2002) Choosing appropriate techniques for quantifying groundwater recharge. *Hydrogeology J.,* 10(1), 18-39

Seiler C, Gow L, Christensen N, Wischusen J, Lawrie K, Cathro D, Buchanan S, Smith M and Tan KP (2018) An integrated hydrogeophysical approach to exploring for groundwater resources in southern Northern Territory. Presentation at Australian Exploration Geoscience Conference, Sydney, February 2018.

SKM (2006) Risk assessment to the recharge area of the Roe Creek borefield.

Verhoeven T and Knott G (1982) Hydrogeology of the Pacoota Sandstone & Goyder Formation near Alice Springs. NT Department of Transport and Works, Water Division. Unpublished Technical Report No. WRA82022.

Verhoven TJ, Read RE and Macqueen AD (1979) Alice Springs Water Supply Future Development. September 1977. Northern Territory Department of Transport and Works, Water Division. Project 12. Report 3/1979.

Walvoord MA, Striegl RG, Prudic DE and Stonestrom DA (2005) CO_2 dynamics in the Amargosa Desert: fluxes and isotopic speciation in a deep unsaturated zone. *Water Resour. Res.,* 41. http://dx.doi.org/10.1029/2004WR003599

Williams WD and Siebert BD (1963) The chemical composition of some surface waters in central Australia. *Aust. J. Mar. Freshw. Res.,* 14, 166-175.

Wischusen JDH (2020) Drilling and Stratigraphy, Rocky Hill Investigation 2017-2019. NT DENR Water Resources Branch Report.

Wood C, Cook PG, Harrington GA, Meredith K and Kipfer R (2014) Factors affecting carbon-14 activity of unsaturated zone CO_2 and implications for groundwater dating. *J.Hydrol.,* 519, 465-475.

Wood C, Cook PG, Harrington GA, and Knapton A (2017) Constraining spatial variability in recharge in an arid environment through modelling carbon-14 transport in groundwater. *Water Resour. Res.*, 53, 142–157, doi:10.1002/2015WR018424.

Woolley D (1966) Geohydrology of the Emily and Brewer Plains area, Alice Springs, N.T. Department of Northern Territory, Mines Branch. Technical Report WRA66007.

APPENDIX 1. PUMPING TESTS AT SITE 1 AND SITE 2

Introduction

Pumping tests were carried out on RN 19385 (Site 1) and RN 19386 (Site 2) to examine aquifer transmissivity within NT Portion 4704 and vertical connectivity between aquifer layers. An initial step test was used at each production bore to determine the pumping rate for a subsequent constant rate pump test. Data from the constant rate test was analysed in FEFLOW using a homogeneous, layered model.

Model setup

A three-dimensional model was set up, with a domain extent of 5000 m x 5000 m (Figure A1.1). Layering at each site was based on lithology and gamma logs. Eight layers were used

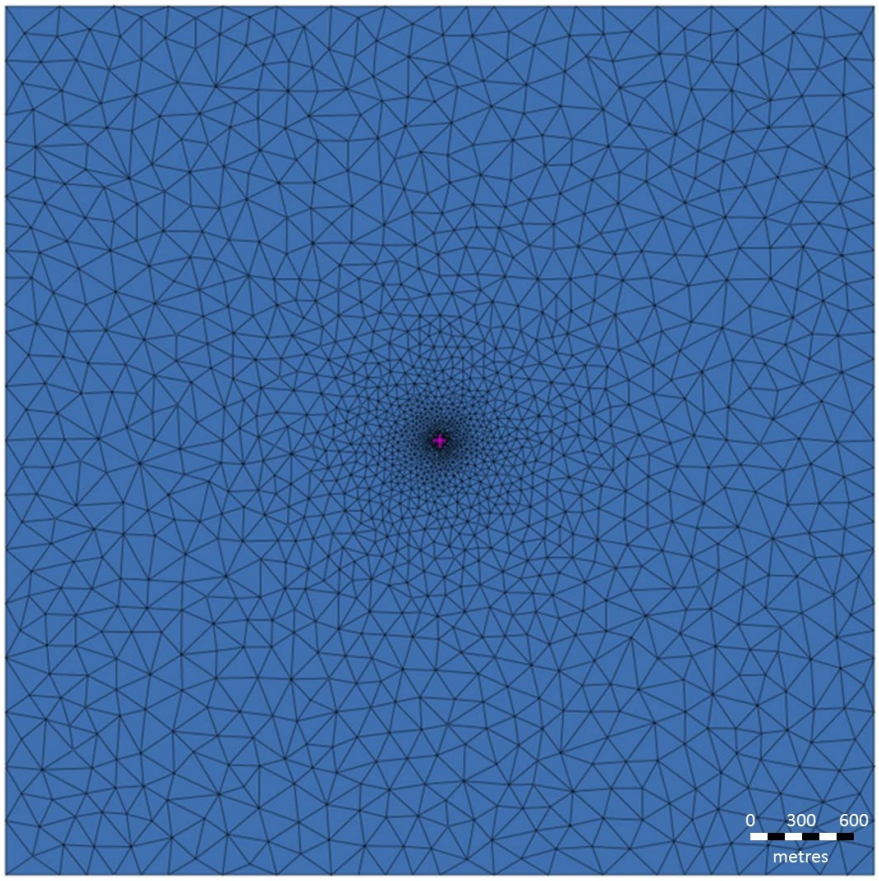

Figure A1.1. Model domain and mesh discretisation.

for the pumping test at RN 19385 and nine layers were used for the pumping test at RN 19386. The model lateral boundaries were no-flow and were located at sufficient distance so that they did not influence results of the simulation. The lower boundary was also no-flow. The pumping wells were located across the screened layer using a multi-layer well.

RN 19385 (Site 1)

Model layers at Site 1 were based on gamma logs for RN 19381 and RN 19385. The pumping well (RN 19385) is located across layer 5 using a multi-layer well.

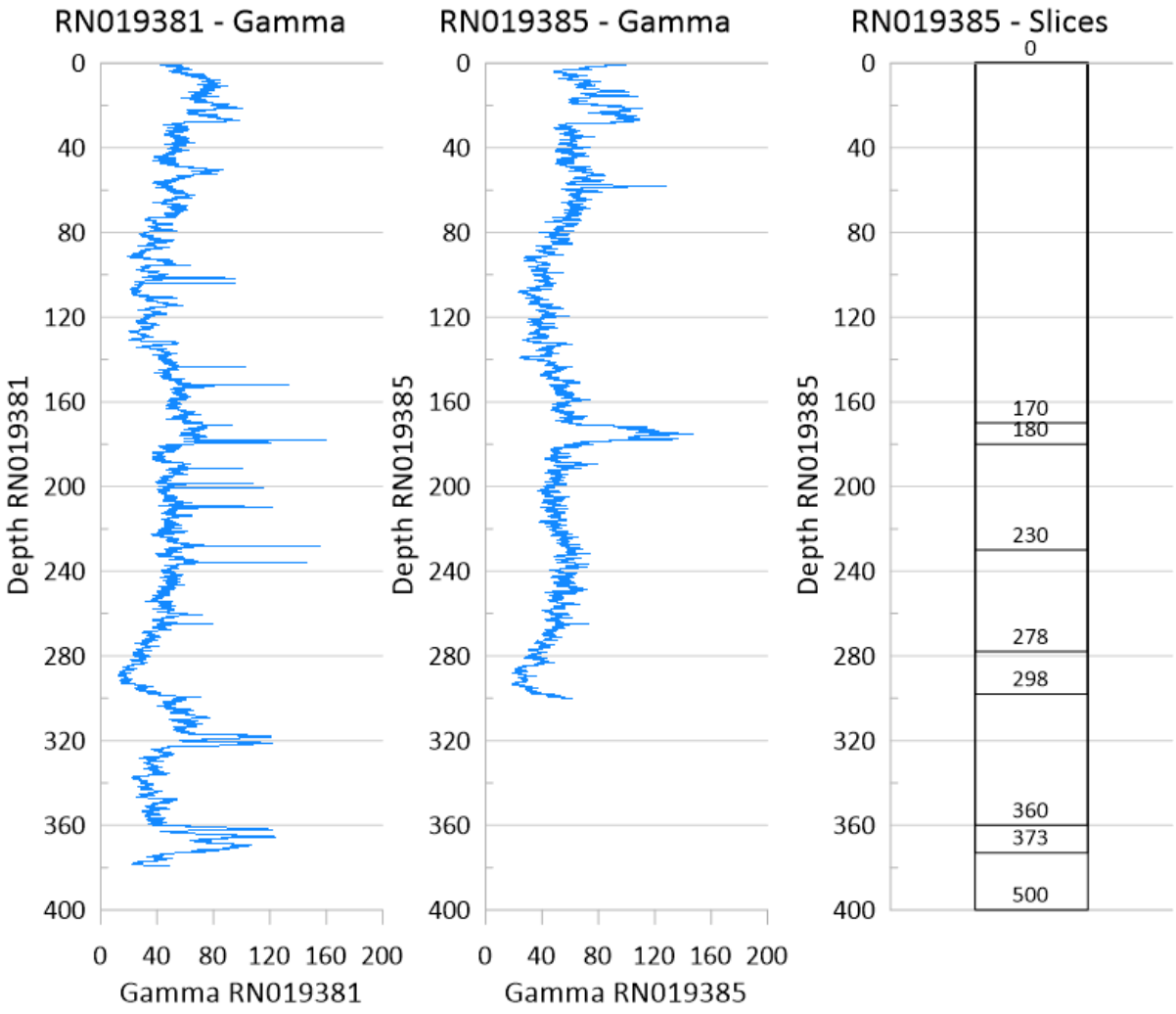

Figure A1.2. Gamma plots for RN 19381 and RN 19385 (pumped bore) versus slices in FEFLOW model. Note that the final slice extends to 500 m and is located below the bottom of the logs presented.

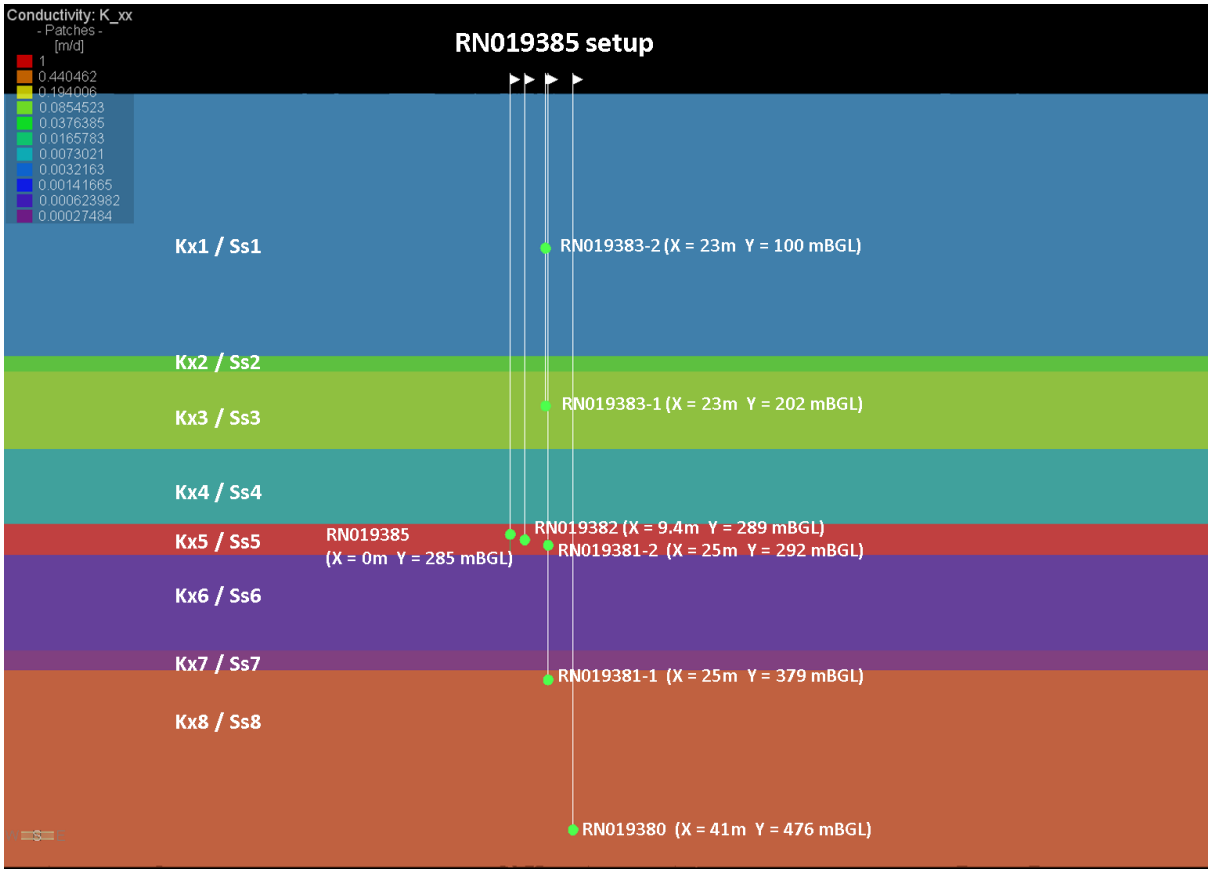

Figure A1.3. West to east section through the centre of the model domain showing layer configuration and observation bores.

The model was optimised using PEST and the final parameters are presented in Table A1.1. RN 19385, which has a low bore efficiency, was simulated with a low hydraulic conductivity zone (kx9) around the bore.

Table A1.1. Final parameters for pump test conducted at RN019385.

Layer Depth (m)	Hyd. Cond. Parameter	Value (m/day)	Storage Parameter	SS	Sy
0 – 170	kx1	4.217E-03	ss1, sy1	1.031E-06	2.402E-01
170 – 180	kx2	5.451E-02	ss2	8.841E-07	-
180 – 230	kx3	1.044E-01	ss3	1.383E-05	-
230 – 278	kx4	7.791E-03	ss4	3.124E-05	-
278 – 298	kx5	1.00E+00	ss5	5.644E-07	-
298 – 360	kx6	5.373E-04	ss6	3.667E-07	-
360 – 373	kx7	2.748E-04	ss7	7.744E-06	-
373 - 500	kx8	6.544E-01	ss8	1.040E-04	-
	Anisotropy	1			-

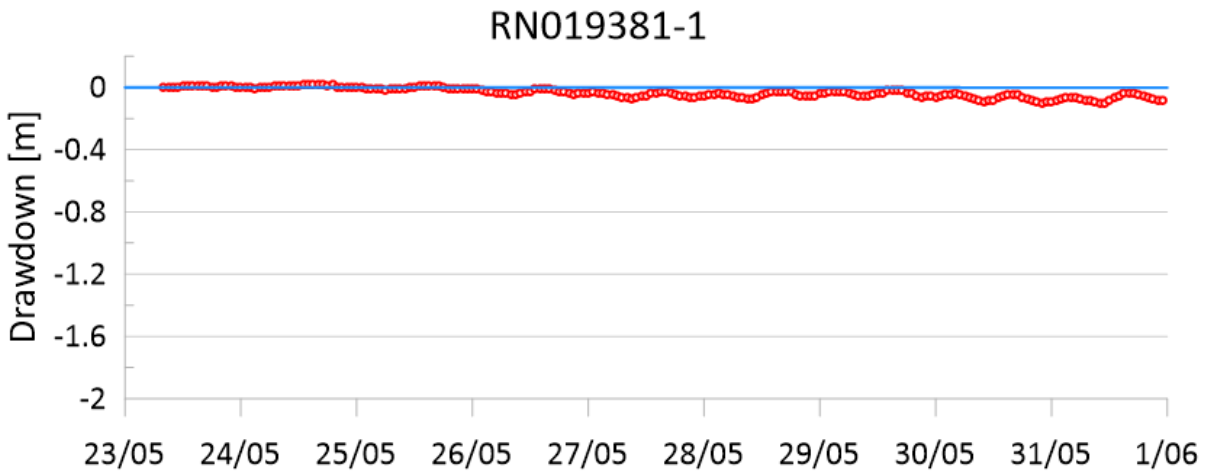
RN019381-1
Drawdown [m]
0
-0.4
-0.8
-1.2
-1.6
-2
23/05
24/05
25/05
26/05
27/05
28/05
29/05
30/05
31/05
1/06

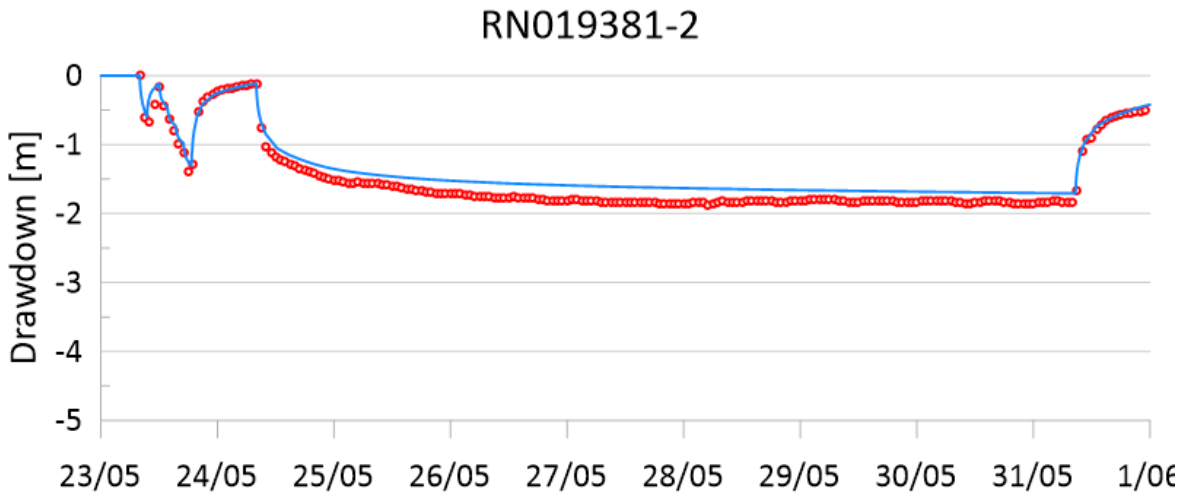
RN019381-2
Drawdown [m]
0
-1
-2
-3
-4
-5
23/05
24/05
25/05
26/05
27/05
28/05
29/05
30/05
31/05
1/06

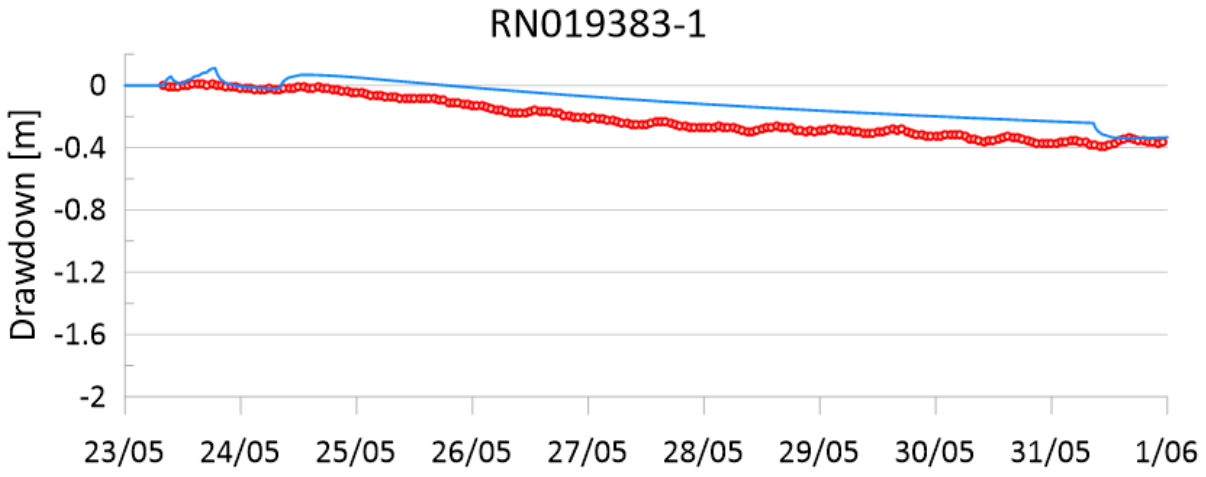
RN019383-1
Drawdown [m]
0
-0.4
-0.8
-1.2
-1.6
-2
23/05
24/05
25/05
26/05
27/05
28/05
29/05
30/05
31/05
1/06

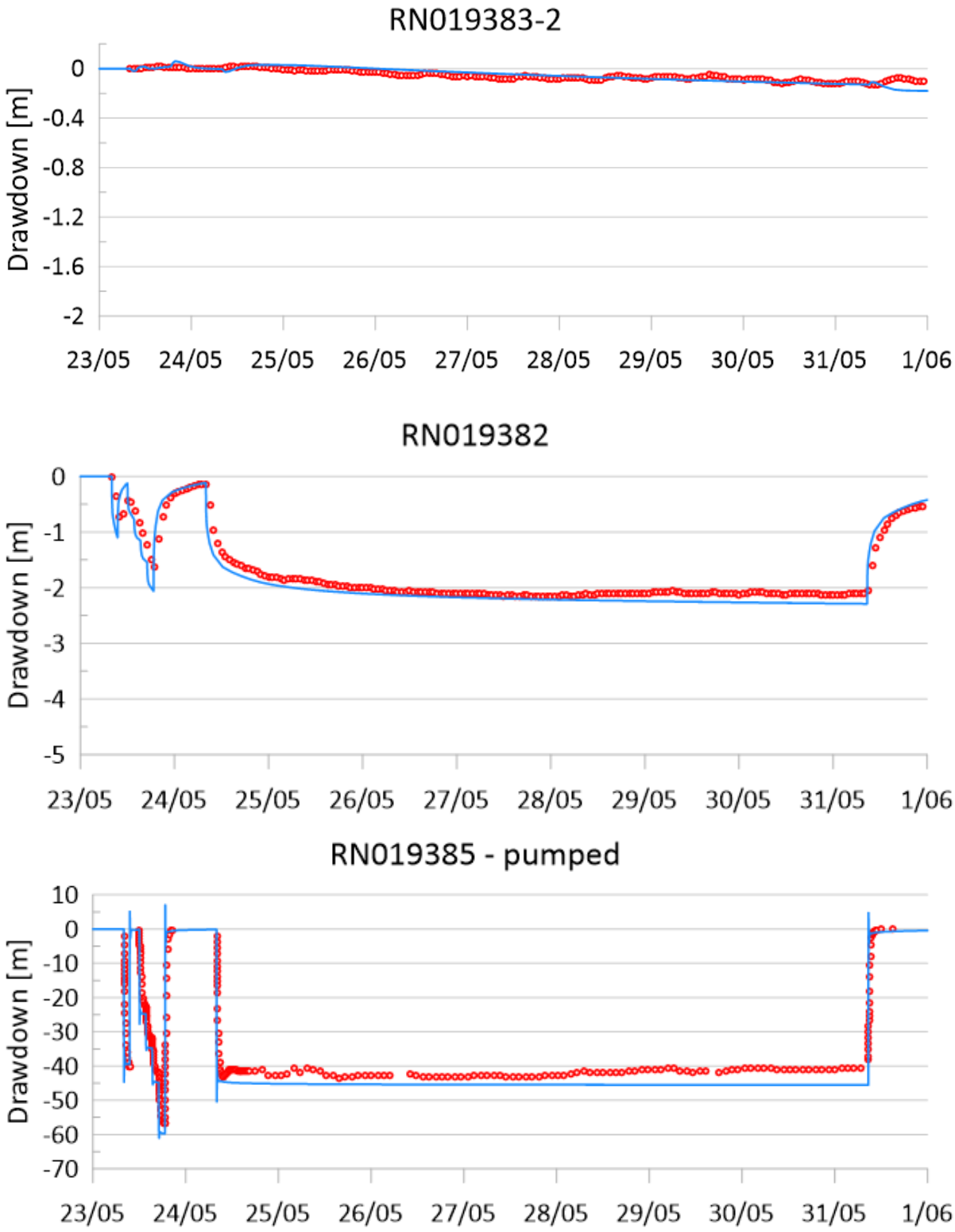

Figure A1.4. Observed (red circles) and simulated (blue line) drawdown for pumping bore and observation bores.

RN 19386 (Site 2) pumping test

The model comprises nine layers. It includes an additional layer to the previous model to provide separation between RN 19387 and observation bore RN 19384-1.

The production bore and monitoring bore construction compared to the gamma log for RN 19384 is presented in Figure A1.5 reference. The model layering (Figure A1.6) was based on the gamma log for RN 19384. The gamma log for RN019381 (from Site 1) is also presented in Figure A1.6 as it shows some similarities with a 50 m vertical offset. The pumping well located across layer 6 using a multi-layer well.

The model was optimised using PEST and the final parameters are presented in Table A1.2 and Figure A1.7.

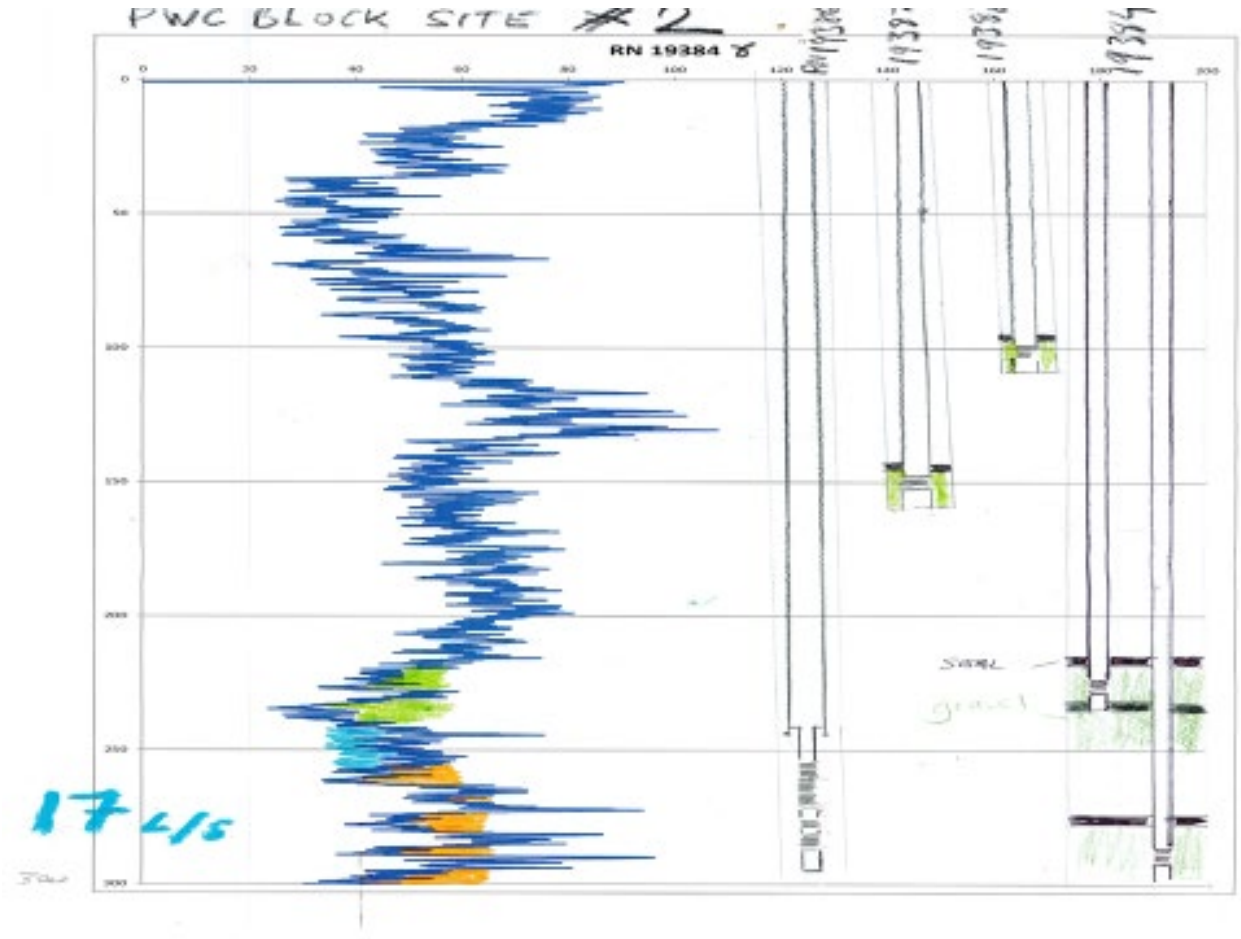

Figure A1.5. Gamma log RN 19384 and bore construction details of pumped bore and observation bores.

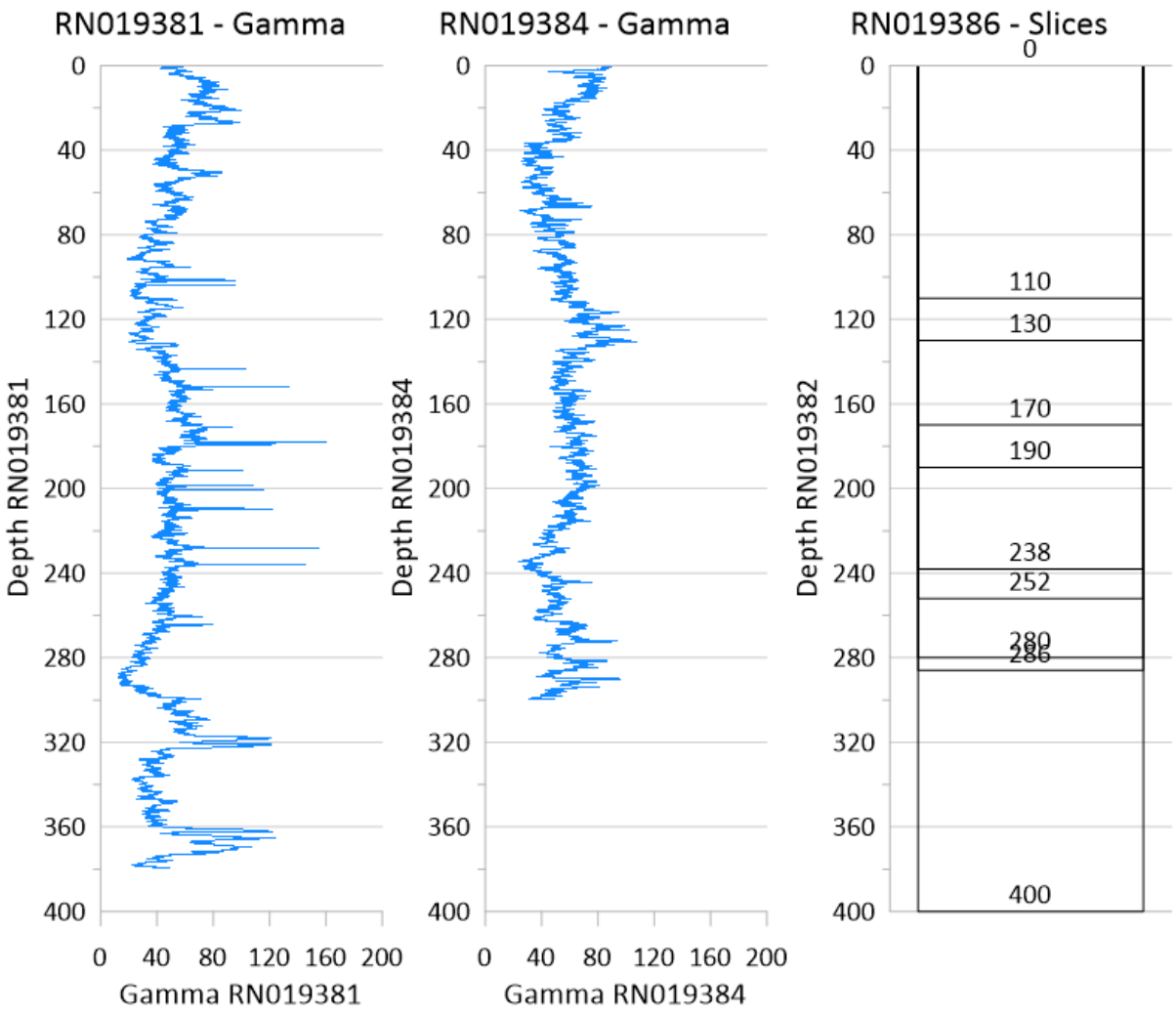

Figure A1.6. Gamma plots for RN 19381 and RN 19384 (observation bore) versus slices in FEFLOW model.

Table A1.2. Final parameters for RN019386.

Layer Depth (m)	Hyd. Cond. Parameter	Value (m/day)	Storage Parameter	SS	Sy
0 – 110	kx1	3.005E-01	ss1, Sy1	3.972E-04	2.400E-01
110 – 130	kx2	5.131E-02	ss2	9.846E-07	-
130 – 170	kx3	1.108E-01	ss3	7.449E-07	-
170 – 190	kx4	1.264E-01	ss4	1.000E-07	-
190 – 238	kx5	1.264E-01	ss5	1.000E-07	-
238 – 252	kx6	3.010E-02	ss6	9.588E-07	-
252 – 280	kx7	1.73E+00	ss7	4.897E-06	-
280 – 286	kx8	1.101E-02	ss8	1.154E-06	-
286 - 400	kx9	2.613E-01	ss9	1.394E-06	-
	Anisotropy	1			-

Figure A1.7. West to east section through the centre of the model domain showing layer configuration and observation bores. RN 19386 is at the centre.

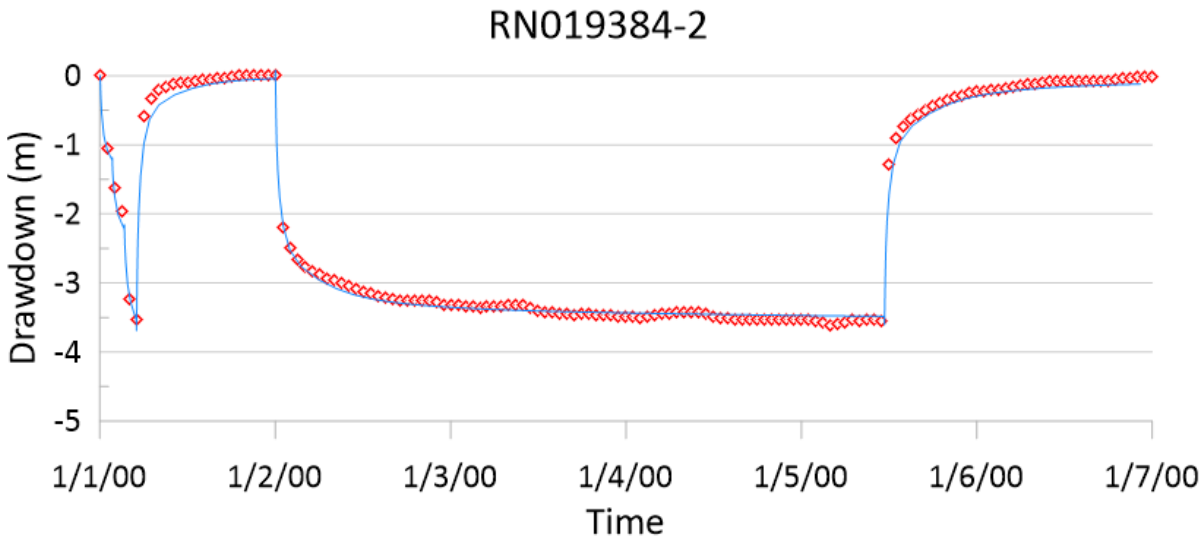
RN019384-2
0
-1
-2
-3
-4
-5
Drawdown (m)
1/1/00
1/2/00
1/3/00
1/4/00
1/5/00
1/6/00
1/7/00
Time

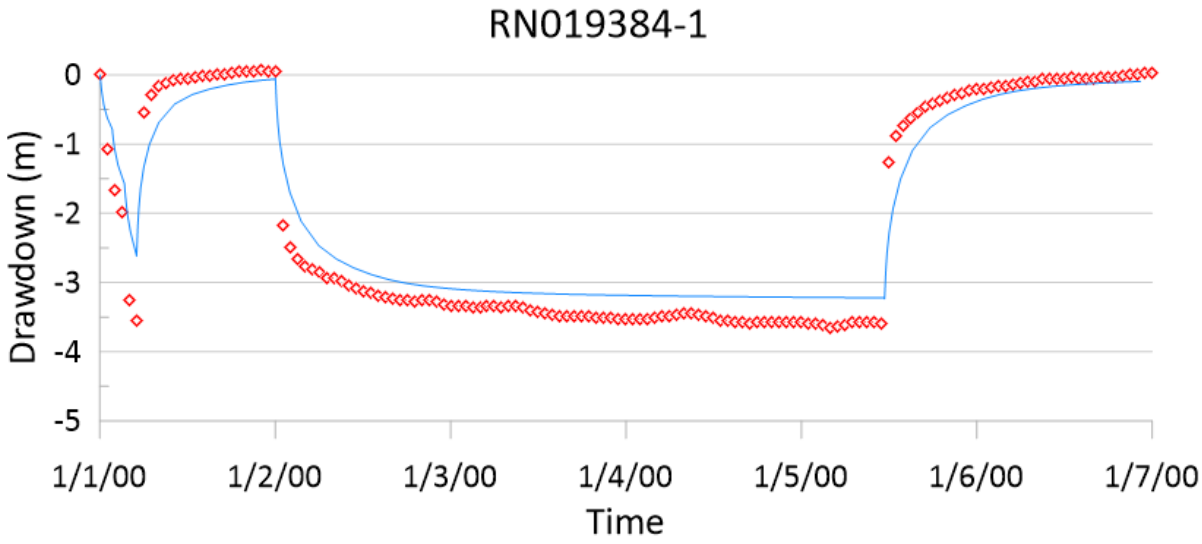
RN019384-1
0
-1
-2
-3
-4
-5
Drawdown (m)
1/1/00
1/2/00
1/3/00
1/4/00
1/5/00
1/6/00
1/7/00
Time

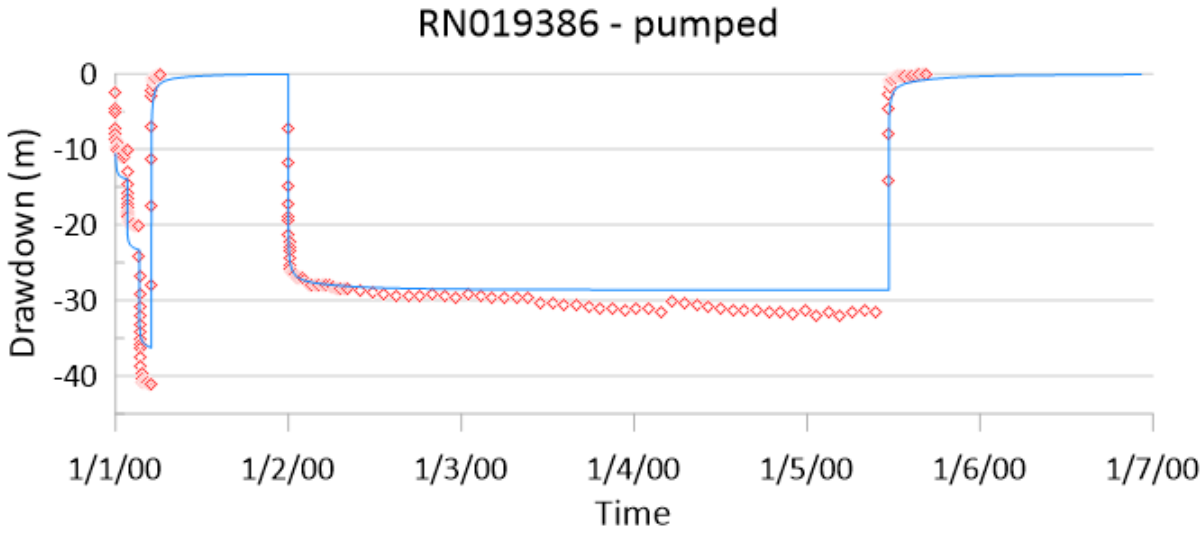
RN019386 - pumped
0
-10
-20
-30
-40
Drawdown (m)
1/1/00
1/2/00
1/3/00
1/4/00
1/5/00
1/6/00
1/7/00
Time

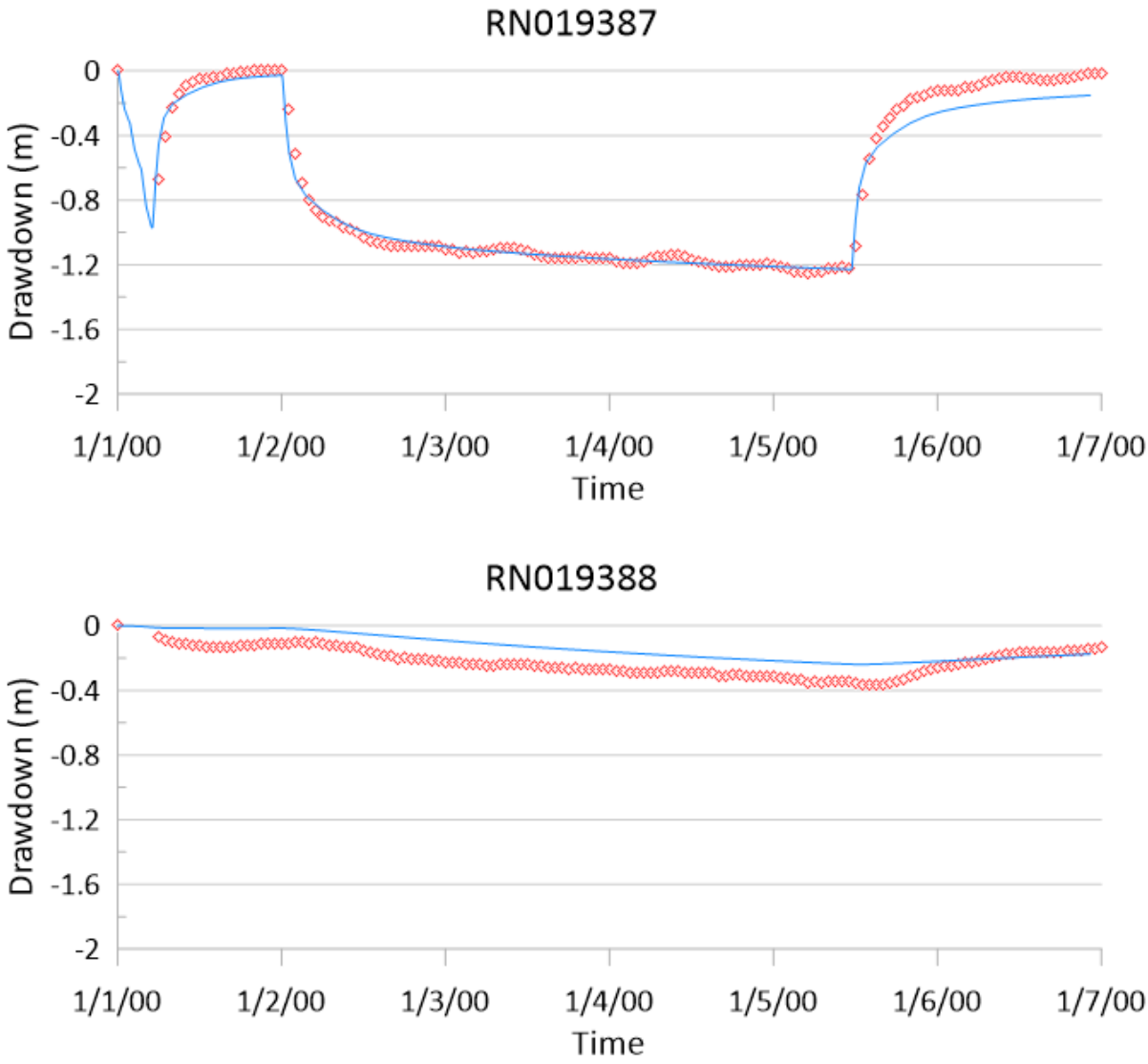

Figure A1.8. Observed (red circles) and simulated (blue line) drawdown for pumping bore and observation bores.

The pumping test results for RN 19386 were also simulated using a six-layer model and a summary of the results of this analysis are presented below. This simulation was designed to test whether a simpler conceptualisation would lead to similar estimated hydraulic parameters. The slices defining the layers compared to the gamma logs are presented below in Figure A1.9. For this configuration (shown in Figure A1.10), the pumping bore was represented using a well boundary condition at a node between layer 5 and 6 (this is different to the implementation used in the previous analysis where multi-layer wells were used).

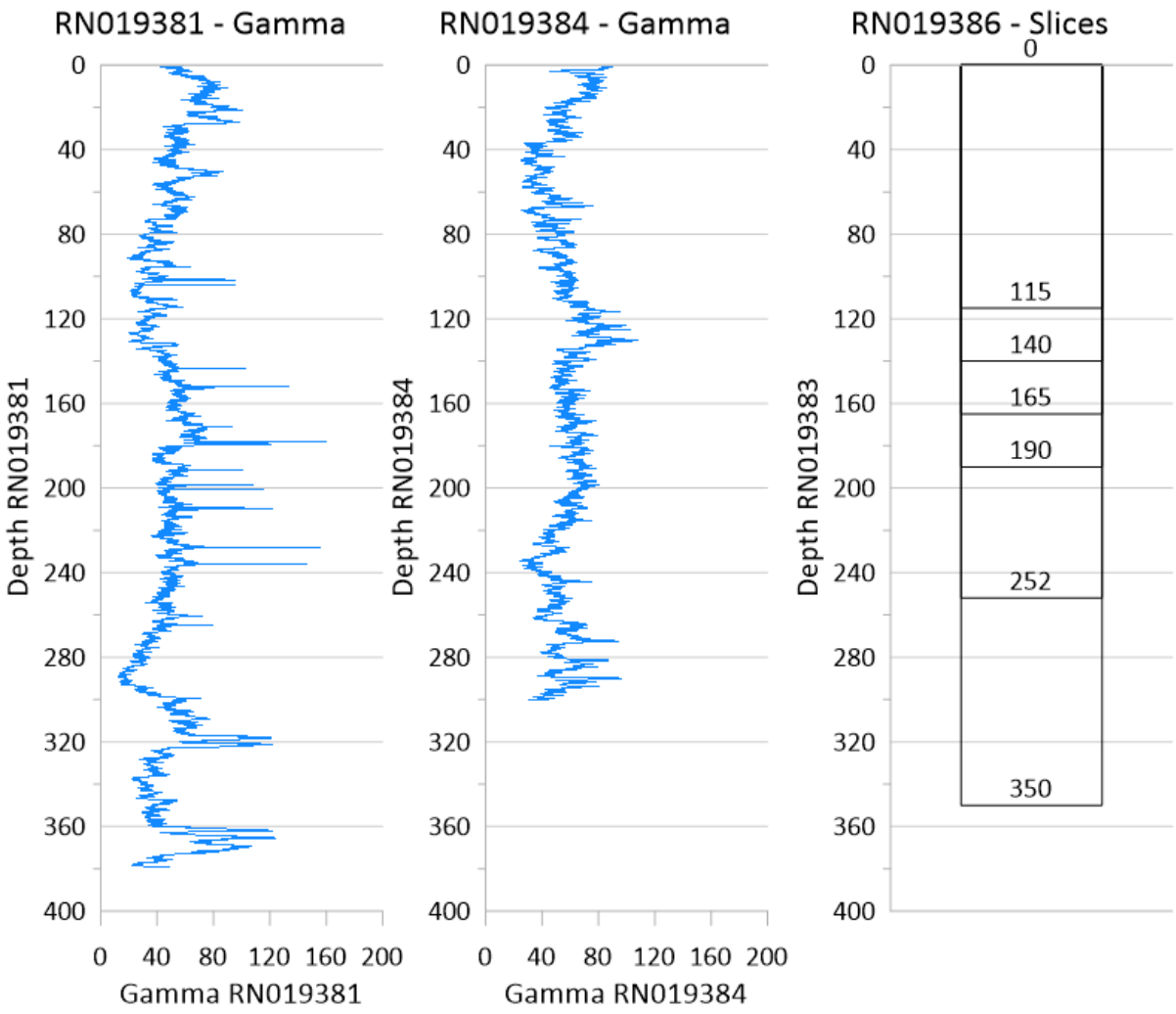

Figure A1.9. Gamma plots for RN 19381 and RN 19385 (pumped bore) versus slices in FEFLOW model. Note: the final slice is located below the bottom of the logs presented.

Final estimated parameter values are shown in Table A1.3. The results differ from the nine-layer model in that an anisotropy of 2.00 is used for each layer in the six-layer model conceptualisation, whereas individual layers in the nine-layer model were isotropic. Observed and modelled drawdown for six-layer model are depicted in Figures A1.11 and A1.12, and the derived hydraulic parameters for the two models are directly compared in Figure A1.13. The hydraulic conductivity profile for the six-layer model does not contain the low permeability layers of the nine-layer model, as the resistance to vertical flow is partly represented by anisotropy of the individual layers. The mean weighted horizontal hydraulic conductivity for the six-layer model is 0.13 m/day, compared with a mean value for the nine-layer model of 0.32 m/day. The mean vertical hydraulic conductivity is 0.12 m/day for both models.

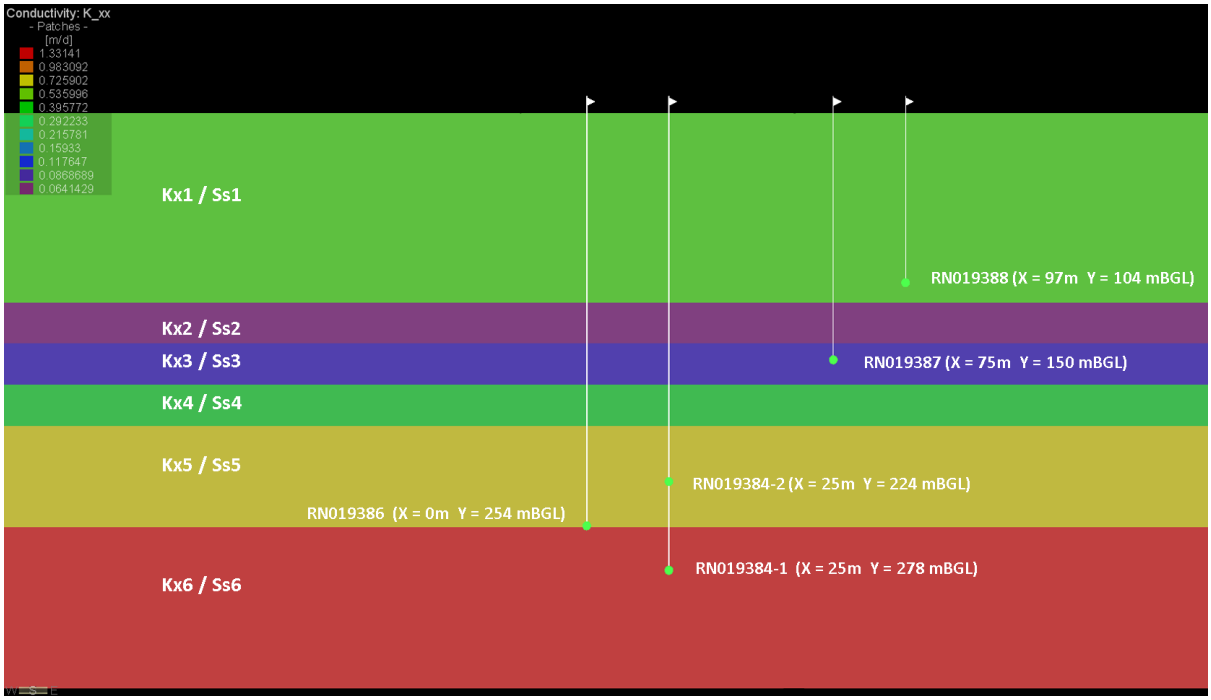

Figure A1.10. West to east section through the centre of the model domain showing layer configuration for six-layer model. Parameter names are indicated for reference.

Table A1.3. Six-Layer model final parameters.

Layer Depth (m)	Hyd. Cond. Parameter	Value (m/day)	Storage Parameter	SS	Sy
0 – 115	kx1	0.46	ss1, Sy	3.02E-06	2.00E-01
115 – 140	kx2	0.06	ss2	9.49E-07	-
140 – 165	kx3	0.10	ss3	4.46E-07	-
165 – 190	kx4	0.35	ss4	4.64E-07	-
190 – 252	kx5	0.75	ss5	3.99E-06	-
252 – 350	kx6	1.33	ss6	3.60E-06	-
	Anisotropy	2.0			

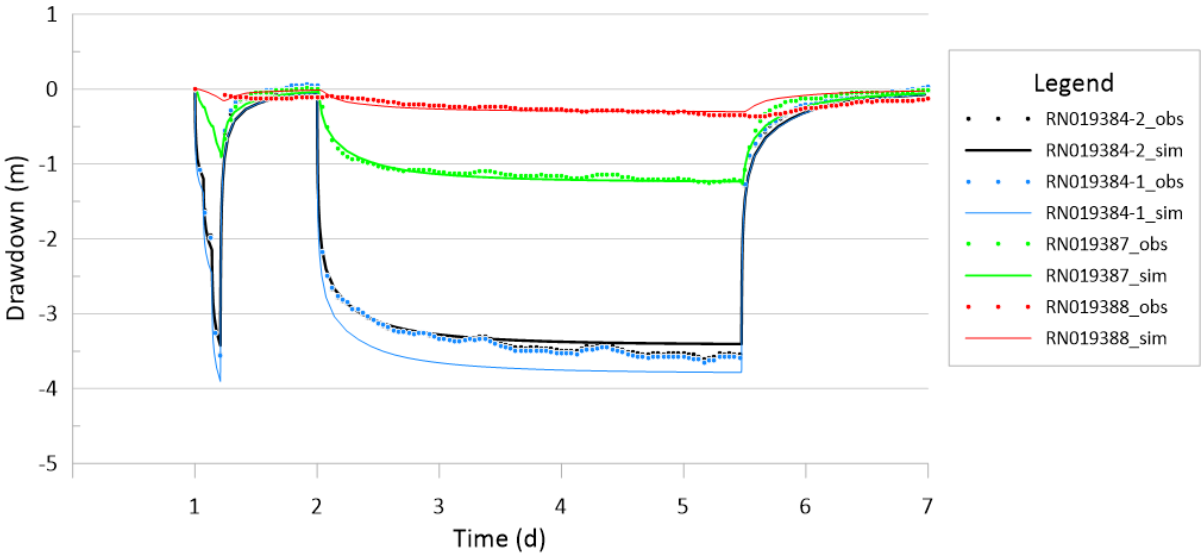

Figure A1.11. Observed drawdown for observation bores at Site 2, together with drawdown simulated by six-layer model. Note that time is offset by 1 day.

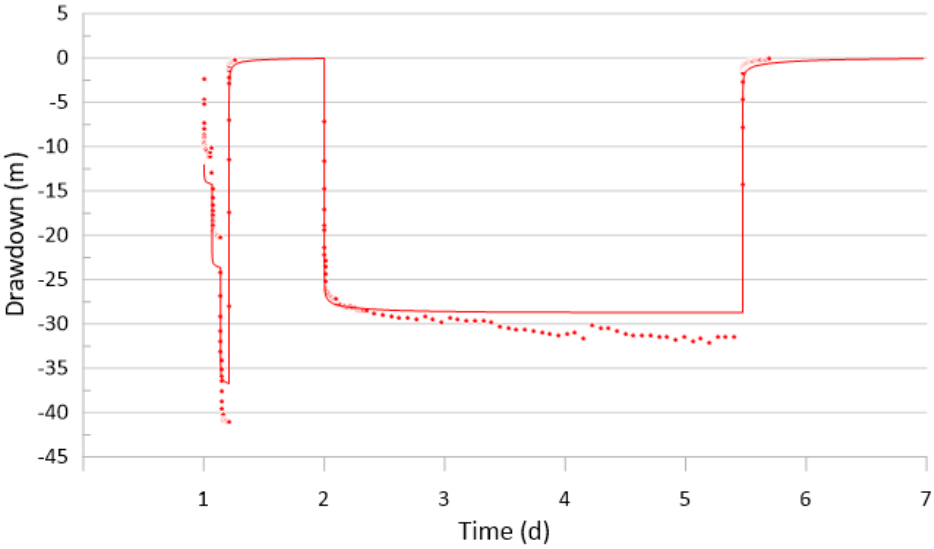

Figure A1.12. Observed drawdown for pumping bore RN 19386 at Site 2, together with drawdown simulated by six-layer model. Note that time is offset by 1 day.

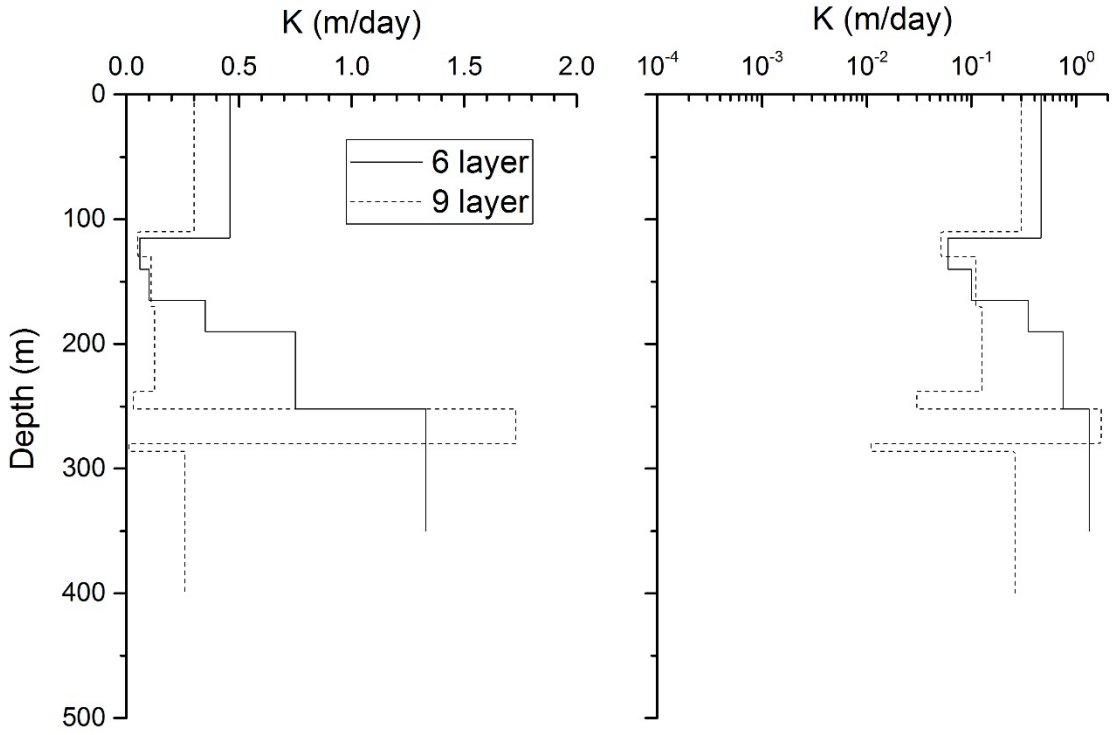

Figure A1.13. Hydraulic conductivity versus depth from numerical modelling of pumping test at Site 2. Results of 9-layer and 6-layer model are compared.

APPENDIX 2. WATER LEVEL DATA

Table A2.1. Water level data used to construct potentiometric surface map.

		2000 Data		2017-2019 Data	
Obs Well	MP	Date	SWL (m)	Date	SWL (m)
RN 3602	544.14	15/06/2000	88.75	10/08/2018	93.48
RN 3609	540.74	15/06/2000	106.73	10/08/2018	117.4
RN 4458	534.17	15/06/2000	48.70		
RN 4461	532.05	15/06/2000	49.88		
RN 4462	536.23	9/12/1997	78.00		
RN 4463	527.87	18/03/1999	70.30	5/12/2016	75.36
RN 4464	530.14	15/06/2000	51.65	10/08/2018	50.42
RN 4467	527.32	22/10/1997	82.80		
RN 4480	524.57	15/06/2000	76.22	9/08/2018	81.23
RN 4481	533.26	15/06/2000	55.24	10/08/2018	53.84
RN 4482	535.5	15/06/2000	95.66	10/08/2018	104.54
RN 4484	526.11	15/06/2000	81.38	9/08/2018	92.15
RN 4502	523.54	23/07/1996	78.04		
RN 4503	514.46	8/05/2000	61.65	9/08/2018	64.35
RN 4504	515.28	8/05/2000	62.05	9/08/2018	64.65
RN 4687	531.94	15/06/2000	91.83	10/08/2018	99.95
RN 4688	532.98	15/06/2000	93.30	10/08/2018	101.37
RN 4690	526.83	15/06/2000	78.48	2/12/2016	82.20
RN 4693	514.23	15/06/2000	62.68	30/03/2017	65.52
RN 4748	518.21	8/05/2000	61.32	8/08/2018	64.13
RN 6504	491.33	9/05/2000	43.03	11/04/2019	44.00
RN 10216	529.16	15/06/2000	78.07	16/03/2017	80.55
RN 10405	516.06	8/05/2000	60.94	9/08/2018	63.13
RN 10720	504.99	8/05/2000	52.08	7/08/2018	53.83
RN 10722	477.83	9/05/2000	29.08		
RN 10728	481.37	9/05/2000	31.73		
RN 10729	481.05	9/05/2000	31.44		
RN 10755	512.29	8/05/2000	58.32	9/08/2018	60.79
RN 10919	506.88	8/05/2000	54.20	9/08/2018	56.67
RN 10922	506.62	8/05/2000	53.64	16/02/2017	55.49
RN 11113	506.63	8/05/2000	51.91	17/02/2017	53.3
RN 11152	506.59	8/05/2000	53.74	8/08/2018	56.01
RN 11169	508.13	8/05/2000	55.46	9/08/2018	57.92
RN 11177	515.97	8/05/2000	61.17	9/08/2018	63.65
RN 11184	513.05	8/05/2000	60.39	9/08/2018	62.90
RN 11320	521.52	15/06/2000	70.31	9/08/2018	74.29
RN 11324	519.4	15/06/2000	71.70	9/08/2018	76.68
RN 11325	522.24	15/06/2000	76.10	9/08/2018	81.96
RN 11336	519.64	15/06/2000	72.04	9/08/2018	76.70
RN 11340	515.93	8/05/2000	63.07	9/08/2018	65.40

RN 11460	510.99	8/05/2000	58.39	9/08/2018	60.88
RN 11461	503.74	8/05/2000	50.99	9/08/2018	53.44
RN 11462	511.77	21/01/2000	58.78	8/08/2018	60.90
RN 11487	515.27	15/06/2000	62.88	9/08/2018	65.68
RN 11488	518.03	15/06/2000	66.93	9/08/2018	70.31
RN 11489	523.419	15/06/2000	79.03	9/08/2018	85.24
RN 11491	530.92	15/06/2000	85.94		
RN 11531	506.39	8/05/2000	53.59	9/08/2018	55.90
RN 11532	514.09	8/05/2000	61.68	9/08/2018	64.26
RN 11832	526.14	2/12/1999	72.51		
RN 11833	470.27	2/12/1999	41.86		
RN 11836	421.27	2/12/1999	26.19		
RN 11844	438.39	2/12/1999	34.47		
RN 11845	428	2/12/1999	24.14		
RN 11847	421.74	2/12/1999	21.66		
RN 11849	438.39	30/11/1998	34.97		
RN 11852	576.81	3/12/1999	123.97		
RN 14869	493.6	3/12/1999	90.54		
RN 17229	571.69	8/05/2000	117.63	8/08/2018	118.87
RN 17234	509.49	8/05/2000	56.34	7/08/2018	58.28
RN 17235	508.33	3/04/1998	54.81	7/08/2018	57.95
RN 17236	525.9	8/05/2000	72.48	7/08/2018	74.01
RN 17243	529.32	9/05/2000	78.94	7/08/2018	79.35
RN 17244	505.02	8/05/2000	52.09	8/08/2018	54.09
RN 17245	505.22	8/05/2000	52.40	8/08/2018	54.34
RN 17246	524.2	8/05/2000	70.86	8/08/2018	72.15
RN 17329	499.58	9/05/2000	49.47	7/08/2018	50.45
RN 17331	526.15	8/05/2000	72.43	8/08/2018	73.77
RN 17332	539.03	8/05/2000	84.84		
RN 17333	515.09	8/05/2000	62.47	9/08/2018	64.92
RN 17334	515.55	8/05/2000	62.23	9/08/2018	64.28
RN 17335	513.15	8/05/2000	60.39	8/08/2018	62.68
RN 17336	498.64	9/05/2000	45.33	7/08/2018	47.78
RN 17337	499.59	9/05/2000	46.63	7/08/2018	48.75
RN 17338	502.28	24/01/2000	49.35	7/08/2018	51.61
RN 17339	505.82	8/05/2000	41.67	9/08/2018	41.61
RN 17391	503.92	8/05/2000	51.19	7/08/2018	53.15
RN 17392	505.54	8/05/2000	52.70	8/08/2018	54.83
RN 17393	489.65	9/05/2000	37.31	7/08/2018	38.81
RN 17394	459.39	9/05/2000	24.37	7/08/2018	25.71
RN 17436	509.86	9/05/2000	56.89	7/08/2018	58.96
RN 17437	518.52	8/05/2000	65.42	7/08/2018	67.32
RN 17438	498.08	9/05/2000	45.16	7/08/2018	47.25
RN 17536	525.51			10/05/2017	77.56
RN 17537	506.86			10/05/2017	57.04
RN 17538	517.26			11/04/2019	67.10

APPENDIX 3. SALINITY DATA

Table A3.1. Bore data used to construct groundwater TDS map. Data used for TDS maps of Read and Paul (2002) and Cozens (2017) are shown, together with data used to construct Figure 28 of this report.

Obs Well	Depth (m)	Read and Paul (2002)	Cozens (2017)	This Report	
				TDS (mg/L)	Date Sampled
RN 2465	111.3	860	800	800	1/12/1985
RN 2692	60.3			1518	7/05/1952
RN 3171	114.3			2243	8/01/1964
RN 3410	91.5	616		616	24/08/1995
RN 3877	80.8			1150	26/03/1997
RN 4017	98.5	603		603	
RN 4461	121.3			560	22/09/1964
RN 4462	222.8			898	22/07/1964
RN 4463	173.7			603	14/07/1964
RN 4464	133.5			749	13/07/1964
RN 4467	149		804	804	19/08/1964
RN 4480	137.2	747	747	747	28/08/1964
RN 4481	182.9			1190	24/07/1964
RN 4482	119.5	450	450	450	08/02/1965
RN 4484	106.4	637	637	637	02/09/1964
RN 4502	81.7	661	661	661	09/12/1964
RN 4503	140.9		948	948	22/09/1964
RN 4504	93.1	648	648	648	22/09/1964
RN 4687	111.3	873	893	893	21/11/1964
RN 4688	130.5	650	650	650	01/12/1975
RN 4690	108.8	584	584	584	08/02/1965
RN 4693	140.5		732	732	22/09/1964
RN 4706	106.7			850	23/03/1965
RN 4712	167.6			850	23/03/1965
RN 4748	168.2	605	605	605	15/02/1965
RN 6504	360	1240		1240	2/11/1973
RN 6989	123.4	590	590	590	15/04/1977
RN 10328	125	674	610	610	30/12/1977
RN 10405	181.4			814	7/10/1964
RN 10669	94.2	580	582	570	17/09/2015
RN 10720	157	1040	922	922	30/11/2016
RN 10722	119	2030		2030	3/05/1974
RN 10729	108	780	780	780	12/12/1973
RN 10743	54.5	765		765	3/04/1989
RN 10752	216	740	740	740	23/03/1974

RN 10755	228	530	490	490	30/03/2017
RN 10919	219	470	456	456	30/03/2017
RN 10922	260	540	540	540	25/11/1975
RN 11113	170	750	750	750	8/10/1975
RN 11152	234.3	390	333	333	28/11/2016
RN 11169	176.2	500	452	452	28/03/2017
RN 11177	167	520	520	520	15/09/1976
RN 11184	223		563	563	29/03/2017
RN 11192	160.3	520	520	520	21/11/1975
RN 11324	229.9	460	425	425	21/03/2017
RN 11325	176.6	630	545	545	6/12/2016
RN 11336	225.2	480	429	429	21/03/2017
RN 11340	222.4	380	275	275	29/03/2017
RN 11408	98.9	610	610	610	20/07/1976
RN 11459	140.4	490	490	490	15/10/1976
RN 11460	207.7	500	479	479	28/03/2017
RN 11461	218.5	450	389	389	28/11/2016
RN 11462	150.5	460	460	460	29/10/1976
RN 11487	144.7	540	497	497	31/03/2017
RN 11488	227.5	490	410	410	31/03/2017
RN 11489	185.9	540	464	464	6/12/2016
RN 11491	300.4	500	428	428	5/12/2016
RN 11531	263.7	440	370	370	27/03/2017
RN 11532	240.8	560	502	502	7/06/2007
RN 11589	36.6			4170	3/08/1973
RN 11729	193	1220	1220	1220	19/10/1977
RN 11980	116	1290	1290	1290	25/08/1995
RN 12045	109	1770	1400	1400	30/11/2016
RN 12958	120	410	504	504	2/12/2016
RN 13021	81	590	473	473	25/11/2016
RN 13298	104	685		685	25/08/1995
RN 14566	189	667	667	667	23/03/1997
RN 15101	392.5			635	26/09/1992
RN 17035	173			570	17/09/2015
RN 17229	333.2	887	887	887	17/07/1997
RN 17234	200	631	631	631	31/03/1998
RN 17235	201.6	653	672	672	24/03/2017
RN 17236	301.4	767	438	438	23/03/2017
RN 17243	304.5	668		668	21/07/1998
RN 17244	330.9	540	605	605	19/05/1999
RN 17246	251.4	628	584	584	13/10/1999
RN 17329	200	1080	1075	1075	16/06/1998
RN 17330	163.9	991	991	991	20/06/1998

RN 17332	84	1500	1500	1500	1/07/1998
RN 17334	71.3		270	270	5/10/1999
RN 17335	71.2		343	343	26/11/2016
RN 17336	54.3			601	7/10/1999
RN 17337	52.6		599	599	1/10/1999
RN 17338	55	581	504	504	6/10/1999
RN 17339	50		866	866	5/10/1999
RN 17354	503			913	22-24/06/2000
RN 17391	192.3	600	510	510	1/12/2016
RN 17392	269.8	457	400	400	1/12/2016
RN 17393	66.8	559	559	559	21/05/1999
RN 17394	144.6	6000		7650	26/05/1999
RN 17436	61.5	479	479	479	11/03/1999
RN 17437	193.5	844	716	716	23/03/2017
RN 17536	351	1060	823	823	30/11/2016
RN 17537	142.6	486	486	486	14/06/2000
RN 17538	103.7	557		557	20/06/2000
RN 17553	79	600			
RN 17817	170			480	17/09/2015
RN 19677	200			505	[1]08-09/2018
RN 19678	218.9			435	[2]09/2018

[1] Average of values measured on 07/08/2018 and 28/09/2018

[2] Average of values measured on 03/09/2018 and 19/09/2018

Table A3.2. Additional bores with groundwater electrical conductivity data, used to inform contouring of TDS. In both cases, EC was measured in the field, during drilling.

Obs Well	Depth (m)	EC (μS/cm)	Date Measured
RN 3011	61	3238	22/08/1962
RN 19753	156	789	2/08/2018

APPENDIX 4. GROUNDWATER ISOTOPE DATA

Table A4.1. Groundwater isotope data for bores from the eastern Amadeus Basin. Data compiled from Calf (1978), Jacobsen et al. (1989), Cresswell et al. (1999), Hostetler (2000) and Kulongoski et al. (2007)

Obs Well	Date Sampled	^{14}C (pmC)	^{13}C (‰)	^{2}H (‰)	^{18}O (‰)	$^{36}Cl/Cl$ (x 10^{-15})	^{3}H (TU)	Source
RN 52	25/09/1986	20	-9.94	-47.7	-7			2
RN 2830	09/1986	16	-10.04	-52.5	-6.71			2
RN 3410	12/09/1999	38.4	-11.3	-55.2	-8.48		< 0.3	5
RN 3617		26.2	-9.8	-56.8	-8.8			1
RN 3738	25/11/1975	36.9	-11.2	-59.6	-8.2			1
RN 3738	21/09/1999	33.7	-11	-57.1	-8.7	133		4,5
RN 4437	28/11/1975	44.4	-10.7	-60.8	-9.1			1
RN 4437	29/09/1999	35.7	-11	-58	-8.75	157		4,5
RN 4688	1/12/1975	43.3	-10.6	-58.7	-9.2			1
RN 4969	02/12/1975	52.5	-12.1	-61.2	-8.1			1
RN 5003	02/12/1975	44.2	-11	-61.1	-9.2			1
RN 5728	25/11/1975	53.9	-10.5	-62.6	-9.4			1
RN 5741		63.4	-11.5	-55	-8.04			2
RN 5758	03/05/1974	26.7	-9.7	-58.5				1
RN 5797	28/11/1975	23.2	-9.8	-59.4	-7.7			1
RN 6098	28/11/1975	22.7	-9.9	-60	-8.8			1
RN 6519	25/11/1975	36.3	-10.7	-60.7	-9.6			1
RN 6740		2.9	-5.22	-51.3	-7.27			2
RN 6824		14.1	-10.29	-56	-8.07			2
RN 6949		87.1	-11.25	-52.2	-7.94			2
RN 6985	27/11/1975	32.4	-10.8	-58.9	-9.2			1
RN 6986	25/11/1975	46.8	-11.5	-61.8	-9.1			1
RN 6989	03/05/1974	46.7	-10.1	-59.1				1
RN 7033	27/11/1975	34.4	-10.5	-59.9	-8.3			1
RN 7033	22/09/1999	36.8	-11.9	-61.1	-9.14	158	< 0.3	4,5
RN 10209		4.6	-7.91	-44.1	-6.39			2
RN 10381	03/05/1974	6.1	-9.2	-61.7				1
RN 10499	26/11/1975	45	-10.4	-63	-9.3			1
RN 10499	23/03/2000	47.3	-15.2	-59.3	-8.91	175	< 0.3	5
RN 10500	26/11/1975	57.9	-11	-63.3	-9.6			1
RN 10500	22/03/2000	46.5	-11.9	-59.9	-8.98	200	< 0.3	5
RN 10501		47.4	-10.6	-62.7	-8.6			1
RN 10501	17/09/1999	47.2	-12.1	-60.4	-9.05	149		4,5
RN 10722	03/05/1974	63.4	-9.9	-56.5				1
RN 10724	09/10/1999	50.4	-11.9	-57.1	-8.65	144	< 0.3	4,5
RN 10898		31.4	-11.8	-59.3	-9.1			2
RN 10900	26/11/1975	39.6	-10.8	-61.5	-8.4			1
RN 10902	03/12/1975	39.2	-10.9					1
RN 10919	25/11/1975	46.7	-11.5	-66.3	-9.5			1

RN 10922	25/11/1975	58.2	-11.5	-70.6	-10.4			1
RN 10922	08/10/1999	64.9	-11.6	-69	-10.19	118	< 0.3	4,5
RN 10943	27/11/1975	16.7	-9.3	-50.7	-7.7			1
RN 10943	27/09/1999	18.9	-9.4	-50.9	-7.55	93		4,5
RN 10946	23/09/1999	33.9	-10	-61	-8.76	126		4,5
RN 11009	02/12/1975	5.1	-9.5	-51.2	-7.5			1
RN 11168	05/10/1999			-58.8	-8.86	143		4
RN 11182	2/12/1975	39.7	-10.9	-61.8	-9.9			1
RN 11194	2/12/1975	33.7	-9.9	-60.1	-9.3			1
RN 11195	12/1975	36.4	-11	-61.7	-8.7			1
RN 11321		61.4	-11.5	-51.2	-8.12			2
RN 11321	28/09/1999	39.6	-10.8	-50.7	-7.82	150		4,5
RN 11334	17/09/1999	37.7	-11.5	-60	-8.72			5
RN 11489	10/10/1999	35.7	-10.3	-62.2	-9.2	129	< 0.3	5
RN 11589	31/03/2000	76.1	-10			43	0.4	5
RN 11768	24/09/1999	35	-10.7	-61.7	-8.55	116		4,5
RN 11831		7.4	-6.9	-52	-7.48			2
RN 11843		7.8	-7.34	-54.6	-7.46	107		2, 3
RN 11843	27/03/2000	11.1	-7.3	-53.9	-7.74	121	< 0.3	5
RN 11855		41.6	-16	-60.6	-9.22			2
RN 11980	29/03/2000	7.4	-7.7	-54	-8.01	142	< 0.3	5
RN 12127		16.5	-10.3	-49.3	-7.64			2
RN 12309	28/03/2000			-59.3	-8.78	164	< 0.3	5
RN 12650		19.2	-9.17	-54.3	-7.8			2
RN 12681		6.7	-7.1	-54.2	-7.68	166		2, 3
RN 13298	29/03/2000	16	-9.2	-53.9	-8.16	164	< 0.3	5
RN 13407	21/09/1999	47	-11.9	-63.2	-8.99	145	< 0.3	4,5
RN 13408	23/09/1999	17.7	-9.8	-52.4	-7.67	115		4,5
RN 13652		17.6	-7.95	-53.3	-7.32	158		2, 3
RN 13653		15.9	-7.31	-52.1	-7.42	190		2, 3
RN 13669		39.1	-9.07	-58.2	-8.18	158		2, 3
RN 14166		20	-8.74	-48	-7.24			2
RN 14520	05/10/1999	22.1	-9.7	-57.3	-8.46	115		4,5
RN 14522	05/10/1999	22.4	-9.8	-57.1	-8.42	114		4,5
RN 14566		6	-8.01	-55.1	-7.5			2
RN 14566		6				183		3
RN 14566	02/04/2000	9.9	-6.8	-52.7	-7.81	155	< 0.3	5
RN 14618		13.5	-9.92	-44.3	-6.1			2
RN 14864	20/09/1999	36.7	-11.3	-59.6	-8.86	129		4,5
RN 14869						180		3
RN 14998	02/04/2000	77.8	-12.6	-61.2	-9.3	151	< 0.3	5
RN 15097	23/03/2000	17.4	-8.7	-51.6	-7.77	108	< 0.3	5
RN 15099	14/09/1999	112.4	-12	-37.5	-6.23		2.5	5
RN 15760	15/09/1999	102	-11.6	-42.7	-6.86		< 0.3	5
RN 17246	11/10/1999	48.6	-12.2	-53.2	-7.94	129	3.3	4
RN 17334	04/10/1999	36.2	-11.3	-73.5	-10.88	101		5
RN 17335	01/10/1999	41.2	-12	-63.7	-9.71	124	0.4	4,5
RN 17336	07/10/1999	54.5	-11.8	-59.9	-8.94	131	< 0.3	5
RN 17337	06/10/1999	52.3	-11.7	-61.1	-9.06	117	< 0.3	4

RN 17338	06/10/1999	47.1	-12.2	-63.4	-9.35	133	< 0.3	4,5
RN 17339	05/10/1999	12.5	-10.4	-51	-7.77	113	< 0.3	4,5

[1] Calf GE (1978) The isotope hydrology of the Mereenie Sandstone aquifer, Alice Springs, Northern Territory, Australia. Journal of Hydrology, 38: 343-355.

[2] Jacobson G, Calf GE, Jankowski J and McDonald PS (1989) Groundwater chemistry and palaeorecharge in the Amadeus Basin, central Australia. Journal of Hydrology, 109: 237-266.

[3] Cresswell RG, Jacobson G, Wischusen J and Fifield LK (1999) Ancient groundwater in the Amadeus Basin, Central Australia: evidence from the radio-isotope ^{36}Cl. Journal of Hydrology, 223:212-220.

[4] Kulongoski JT, Hilton DR, Cresswell RG, Hostetler S and Jacobson G (2007) Helium-4 characteristics of groundwaters from Central Australia: Comparative chronology with chlorine-36 and carbon-14 dating techniques. Journal of Hydrology, 348: 176-194.

[5] Hostetler (2000) Age of Groundwater, Alice Springs, NT. Bureau of Rural Sciences, November 2000. NT Water resources Branch external report number A1186.

Table A4.2. Groundwater isotope data for bores located at Site 1 and Site 2, within NT Portion 4704. Ion chemistry for RN 19383-2 and RN 19383-1 show contamination by drilling fluids (see Table 2), and this has noticeably affected $^{36}Cl/Cl$ results. Isotope results for these bores are included in parentheses below but are not discussed in this report.

Obs Well	^{14}C (pmC)	^{13}C (‰)	^{2}H (‰)	^{18}O (‰)	$^{36}Cl/Cl$ (x 10^{-15})
RN 19383-2	52.7	-9.83	-69.4	-10.19	(103.1)
RN 19383-1	52.9	-3.03	-62.4	-9.24	(58.6)
RN 19381-2	18.1	-9.08	-60.3	-8.87	191.0
RN 19381-1	30.6	-8.39	-62.7	-9.33	195.7
RN 19382					
RN 19380	11.9	-8.57	-53.6	-8.15	168.7
RN 19388					
RN 19387	33.4	-10.34	-60.9	-8.89	172.4
RN 19384-2	37.5	-9.16	-62.5	-9.09	183.9
RN 19384-1	34.0	-9.47	-62.3	-8.96	174.9
RN 19386	47.9	-9.99	-66.9	-9.62	175.9